UNIVERSIDADE DO ALGARVE

Geomorphology and Morphodynamics of Embayed Beaches in Contrasting Environments



Carlos Manuel Silva Loureiro Alves Ferreira

Doutoramento em Ciências do Mar, da Terra e do Ambiente,
Ramo de Geociências, Especialidade em Geomorfologia

2012

UNIVERSIDADE DO ALGARVE

Geomorphology and Morphodynamics of Embayed Beaches in Contrasting Environments

Carlos Manuel Silva Loureiro Alves Ferreira

Doutoramento em Ciências do Mar, da Terra e do Ambiente,
Ramo de Geociências, Especialidade em Geomorfologia

Tese orientada por:

Doutor Óscar Ferreira (Universidade do Algarve)
Doutor Andrew Cooper (University of Ulster)

2012









Dedicado às matriarcas, Irene e Felícia,
que serão sempre a força que tudo agrega…

Aos meus pais, Manuel e Amélia,
Aos meus irmãos, Eduardo e João,
À minha irmã, Violeta,
por me apoiarem incondicionalmente, mesmo quando o meu trabalho me leva cada vez para mais longe…

Quando avistei
Ao longe o mar
Ali fiquei
Parado a olhar

Quando avistei
Ao longe o mar
Sem querer deixei-me
Ali ficar

(Pedro Ayres de Magalhães)

It's true Hobbes…

… once you know things, you start seeing problems everywhere…

… and once you see problems, you feel like you ought to try to fix them…

… and fixing problems always seems to require personal change…

… and change means doing things that aren't (always) fun.

From The Daily Calvin & Hobbes of 20/05/2012

by Bill Watterson

ACKNOWLEDGEMENTS

Exactly five years have passed since I started to work for this thesis in May 2007. By that time I started to work in Olhão, eventually moved back to Faro, and in between I end up spending almost a year in Northern Ireland. During all this moving around I was privileged to have meet many people, and receive a lot of help, assistance, collaboration and so many other words that would emphasize that they all have somehow contributed to make this thesis possible.

First, I would like to express my sincere appreciation to my supervisors, Óscar Ferreira and Andrew Cooper, for their continuous guidance and unwavering support. So many of the ideas for this thesis that we have discussed along this journey have changed, some end up being abandoned, but I could always count on your help to guide me but also to let me explore my own ideas and directions. Óscar's enthusiasm, insight and willingness to help me in all possible ways, gave me the reassurance that I could always count on him for good or bad times. By now, I hope I may have got some of his attention to detail and focused analysis. Andrew accepted to be my supervisor even before we meet, but even then I could count with his invaluable help. As I started my visits to Northern Ireland, roughly around halfway of the thesis, Andrew was there to warmly welcome me and always willing to share his extensive knowledge. His ability to look at the big picture and ask me what was the story I wanted to tell helped me to direct my research. Thank you so much to both for everything.

The fieldwork on which this thesis is founded was developed during two rough winters and two not so bad summers. Almost everyone on the Coastal Processes group was dragged to the field, frequently before sunrise, and often pushed into the cold and stormy water for getting some more GPS points. Thank you all: Ana Matias, André Pacheco, Bruna Rodrigues, Erwan Garel, Francisca Rosa, Isabel Mendes, Júlio Cunha,

Mara Nunes, Margarida Ramires, Maria Bezerra, Michalis Vousdoukas, Pedro Almeida, Rita Carrasco. Special thanks to Mara, for being always available to go to the field and for being so dedicated, André for teaching me the fundamentals of the fieldwork equipment, Margarida and Sr. Cunha for the hundreds of samples processed, Pedro and Michalis for helping me sorting several Matlab doubts. A lot of people at CIMA have also helped, encouraged or otherwise gave support to my work during the course of the years, and to all I express my gratitude.

Over the course of these five years I was fortunate enough to have spent almost a year in Northern Ireland, an amazing and enriching experience. I was so very warmly welcome by everyone in the Centre for Coastal and Marine Research that it didn't take long to feel like I was part of the group. The atmosphere in the Coastal Systems group was great and I would like to thank everyone that made it so: Derek Jackson, Irene Delgado-Fernandez, Jeremy Pile, Jiandong Huang, Lluís Gómez-Pujol, Marianne O'Connor, Rowena Moore and Thomas Smyth. A very special thanks to my dearest Irene, can wait to have a pint with you and start changing the world, and to my mate Thom, it wouldn't have been nearly as great without you man! I received a lot of encouragement and sympathy from everyone while I was in Northern Ireland, but special thanks is reserved to Sarah Coulthard, for being such an enjoyable person to live with, and to Julie Campbell, for the enthusiastic and relentless energy.

All through these years the strong support received from my family and friends has been fundamental. In particular, Daniela and Tiago thanks for letting me use the Mt. Clérigo house every once in a while, and Marta and Sérgio thank you for coming here every once in a while. To my parents, Manuel e Amélia, and siblings, Eduardo, Violeta e João, thanks for your constant support, encouragement, kindness, love, and basically everything that I am. Going back home is always so good, even when it is just for a few

days. To my sweet Violeta, thanks for taking care of the base station for those long, long hours. Eduardo thanks for getting me to think about Bayesian stats amongst many other things, and thanks João, for being always so enthusiastic about everything. To my new sister Jaqueline and to my adorable nephew David thanks for being such a bright source of happiness in the past three years.

Lastly, I have to give special mention to the person that has accompanied me from the very start to the very end of this project, Mara. You are my best friend and I couldn't have done it without you to share the joys and frustrations. Nearly everything on this thesis was chattered and discussed with you, and your patience, dedication and attentive look in the final stretch kept me on track. Thank you for being here for me.

This research was possible through the financial support of:

- Ph.D grant by Fundação para a Ciência e Tecnologia (SFRH/BD/27878/2006)
- Research grant by Centro de Investigação Marinha e Ambiental

Data collection was funded by:

- BAYBEACH Project – Evolution and Management of Embayed Beaches in Contrasting Environments, funded by Fundação para a Ciência e Tecnologia (PTDC/CTE-GEX/66893/2006)

Additional support by:

- Hydrodynamic data provided by Instituto Hidrográfico
- Hydrodynamic data provided by Puertos del Estado

ABSTRACT

This study investigates the medium-term (months to years) morphodynamic variability of embayed beaches in contrasting geomorphological settings, combining two years of topographic and sedimentary monitoring in six embayments on the southwestern Portuguese coastline (three on the west coast and three on the south coast) with hydrodynamic forcing data explored using statistical and modelling techniques. From a broader, embayment-wide scale, towards a focused, process-oriented scale, the thesis addresses the following points: (*i*) the classification of morphodynamic state in embayed beaches, (*ii*) assessment of geological boundaries as constraints on the morphological variability of embayed beaches, (*iii*) the identification of morphodynamic mechanisms responsible for non-uniform alongshore behaviour in high-energy embayed beaches, and (*iv*) the development of megarips and their role in enhancing erosion during storm groups.

This study demonstrates that: (*i*) geological control significantly influences embayed beach morphodynamic behaviour; (*ii*) beach morphodynamic parameters have limited ability to adequately differentiate beach types, particularly within the intermediate domain; (iii) geological boundaries constrain morphological change and promote conspicuous alongshore variability in embayed beaches; (*iv*) beach rotation processes in south coast embayments and topographically-controlled rip circulation in the west coast embayments are the primary drivers of alongshore non-uniform variability; (*v*) under high-energy conditions topographically-controlled rips evolve to megarips, which promote significant beach erosion; (*vi*) the persistence of megarips during storm groups leads to extreme beach erosion, and maintenance of megarip circulation following storms inhibits post-storm beach recovery. Further research is still necessary to improve the present understating of embayed beach morphodynamics,

particularly involving detailed field studies of nearshore circulation and morphologic change. Embayed beaches frequently present site-specific behaviour and knowledge of their dynamics is fundamental to improve both beach safety and management.

KEYWORDS: embayed beaches; beach morphodynamics; morphological variability; geological control; storm impacts; megarips.

RESUMO

Este estudo tem como objetivo a definição da variabilidade morfodinâmica de médio-termo (meses a anos) em praias encastradas expostas a ambientes contrastantes. Para tal combina a monitorização topográfica e sedimentar com dados de forçamento hidrodinâmico obtidos para seis praias encastradas na costa sudoeste de Portugal (três no sector oeste e três no sector sul), recorrendo a técnicas de modelação e análise estatística. Partindo de uma escala abrangente, ao nível da praia no seu conjunto, para uma escala de detalhe, relativa aos mecanismos morfodinâmicos, esta tese aborda os seguintes temas: (*i*) aplicabilidade da classificação do estado morfodinâmico em praias encastradas; (*ii*) avaliação do controlo geológico no constrangimento da variabilidade morfológica; (*iii*) identificação dos mecanismos morfodinâmicos que determinam comportamentos heterogéneos ao longo de praias encastradas expostas a condições de elevada energia; (*iv*) análise do desenvolvimento de "megarips" e seu papel na erosão sedimentar de praias encastradas durante grupos de tempestades.

Este estudo demostra que: (*i*) o controlo geológico influencia significativamente o comportamento morfodinâmico de praias encastradas; (*ii*) as classificações paramétricas do estado morfodinâmico apresentam capacidades limitadas para diferenciar o estado morfodinâmico de praias encastradas, particularmente entre diferentes estados de comportamento intermédio; (*iii*) a existência de limites geológicos constringe a variabilidade morfológica, promovendo notáveis diferenças longitudinais; (*iv*) os principais mecanismos de variabilidade longitudinal são o desenvolvimento de processos de rotação nas praias da costa sul e o estabelecimento de correntes de fuga controladas topograficamente nas praias da costa oeste; (*v*) durante condições de elevada energia as correntes de fuga controladas topograficamente evoluem para "megarips", promovendo erosão sedimentar significativa; (*vi*) a persistência de

"megarips" durante grupos de tempestades desencadeia situações de erosão extrema e a sua manutenção pós-tempestades inibe a recuperação sedimentar. São necessários mais estudos para aperfeiçoar o conhecimento sobre a morfodinâmica de praias encastradas e, consequentemente, melhorar a gestão costeira e a segurança no seu uso balnear.

PALAVRAS-CHAVE: praias encastradas; morfodinâmica de praias; variabilidade morfológica; controlo geológico; impacto de temporais; correntes de fuga.

RESUMO ALARGADO

Praias encastradas são acumulações sedimentares limitadas por promontórios ou afloramentos rochosos. Este tipo de praia é particularmente frequente em litorais oceânicos, apesar de ocorrer também em zonas estuarinas ou mesmo lagunares. A morfologia de praias encastradas, tal como da generalidade das praias, modifica-se em função de alterações nas condições de agitação marítima e da maré que variam tanto cíclica como episodicamente. O efeito limitador de promontórios ou afloramentos rochosos influencia significativamente a configuração da linha de costa em praias encastradas, o transporte sedimentar e o ajustamento morfológico às variações nos elementos forçadores. O comportamento morfodinâmico de praias encastradas apresenta, assim, diferenças significativas em relação a praias abertas, sendo restringido pelo controlo geomorfológico. Este controlo determina o comportamento de variáveis como a geometria e extensão da praia, distância entre promontórios, razão de indentação, características granulométricas do sedimento, declividade da praia submersa, presença de correntes de fuga e localização de barras submersas. O controlo geomorfológico na morfodinâmica de praias encastradas expressa-se não apenas no constrangimento da variabilidade morfológica, mas também na promoção de mecanismos morfodinâmicos característicos de praias encastradas, nomeadamente no estabelecimento de correntes de fuga controladas topograficamente ou no desenvolvimento de processos de rotação de praia. Apesar da franca distribuição de praias encastradas por todo o globo, os estudos que incidem sobre a variabilidade morfológica e mecanismos morfodinâmicos específicos deste tipo de praias são relativamente escassos, em contraponto com a extensa investigação realizada sobre morfodinâmica de praias abertas. Torna-se então fundamental desenvolver estudos dedicados à análise do comportamento morfodinâmico de praias encastradas, com vista

a melhorias na compreensão da sua variabilidade e respetiva integração em procedimentos de gestão do litoral.

A presente tese, tendo como objetivo principal a definição da variabilidade morfodinâmica de médio-termo (meses a anos) em praias encastradas expostas a ambientes geomorfologicamente contrastantes, analisa as variações morfológicas em função das condições hidrodinâmicas e sedimentares em seis praias encastradas na costa sudoeste de Portugal. As seis praias: Amoreira, Monte Clérigo e Arrifana, localizadas no sector oeste, e Salema, Boca do Rio e Cabanas Velhas, localizadas no sector sul, encontram-se expostas a condições marcadamente distintas, não só em termos de enquadramento geomorfológico mas também no que diz respeito às condições de forçamento ambiental. No sector oeste, as praias apresentam dimensão considerável e significativo volume sedimentar e, encontrando-se expostas a condições de agitação de elevada energia, apresentam tipologias morfodinâmicas intermédias a dissipativas. Já no sector sul, as praias encontram-se sujeitas a um regime de agitação de energia baixa a moderada, apresentando genericamente menores dimensões, reduzido volume sedimentar e tipologia morfodinâmica intermédia a refletiva.

Partindo de uma escala abrangente, ao nível praia, para uma escala de detalhe, ao nível dos mecanismos morfodinâmicos, esta tese aborda os seguintes objetivos específicos: (*i*) aplicabilidade da classificação paramétrica do estado morfodinâmico em praias encastradas; (*ii*) avaliação do impacto do controlo geomorfológico no constrangimento da variabilidade morfológica de praias encastradas; (*iii*) identificação dos mecanismos morfodinâmicos que determinam comportamentos longitudinalmente heterogéneos em praias encastradas expostas a condições de elevada energia; (*iv*) definição das condições para o desenvolvimento de "megarips" e o seu papel no aumento da erosão sedimentar de praias encastradas durante grupos de tempestades. A

hipótese fundamental deste trabalho, transversal às escalas de análise e objetivos específicos, pressupõe que o controlo geomorfológico influencia de forma expressiva o comportamento morfodinâmico de praias encastradas. Esta hipótese foi testada e confirmada através da exploração de dados morfológicos, sedimentares e hidrodinâmicos com recurso a diversas técnicas estatísticas e de modelação numérica e conceptual.

As abordagens paramétricas para classificação do estado morfodinâmico de praias revelaram reduzida aplicabilidade na determinação do estado morfodinâmico de praias encastradas. Esta situação deve-se, principalmente, à ausência de variáveis que incorporem o papel fundamental do controlo geológico nas formulações regularmente utilizadas para classificação paramétrica do estado morfodinâmico de praias. A determinação paramétrica do estado morfodinâmico, com recurso a valores médios das condições de agitação, maré e granulometria observados para cada praia, foi avaliada em conjunto com uma abordagem probabilística, implementada através de um modelo de rede bayesiana, em que se considerou a totalidade das distribuições para as mesmas variáveis. As duas abordagens revelaram inconsistências com o estado morfodinâmico observado nas praias, determinado com base numa classificação hierárquica para identificação do estado morfodinâmico. Esta classificação foi desenvolvida e aplicada neste estudo recorrendo a observações de campo, assentando na diferenciação entre a presença e tipologia de barra submersa interna, na geometria do perfil de praia e na existência de variabilidade morfológica longitudinal. As inconsistências identificadas entre os estados determinados parametricamente e observados resultam fundamentalmente da inadequação das tipologias de praia consagradas nos modelos de comportamento morfodinâmico existentes. Estas revelaram-se insuficientes para diferenciar as tipologias existentes em praias encastradas. A inadequação entre

tipologias é particularmente evidente para caracterização de diferentes comportamentos intermédios. Neste sentido, será importante desenvolver esforços com vista a uma identificação detalhada de tipologias morfodinâmicas de praias encastradas, já que tal será fundamental para que se consiga uma melhor representação dos efeitos do controlo geológico no comportamento morfodinâmico de praias. Os resultados obtidos permitem ainda afirmar que a classificação paramétrica baseada na velocidade de sedimentação adimensional revelou-se útil na diferenciação das tipologias refletiva e dissipativa, mesmo para condições mesotidais e em ambientes sujeitos a significativo controlo geológico. Quando considerado todo o espectro de classificação morfodinâmica, a velocidade de sedimentação adimensional não permitiu, contudo, diferenciar de forma consistente as tipologias intermédias. Conclui-se que parâmetros adimensionais possuem relativa utilidade, mas apenas como descritores elementares da tipologia morfodinâmica de praias encastradas. O seu uso deverá ser restrito à diferenciação entre as três principais tipologias (refletiva-intermédia-dissipativa). A diferenciação de tipologias morfodinâmicas mais pormenorizadas para praias encastradas deverá ser desenvolvida a uma escala regional, não global, e com base em observações do comportamento morfológico. Analisar a classificação morfodinâmica de praias no quadro de abordagens probabilísticas, como proposto no presente trabalho, apresenta-se como uma alternativa com particular potencialidade para integração de variáveis adicionais, não necessariamente paramétricas. Para tal, o recurso a redes bayesianas apresenta grande potencialidade. Contudo, é necessária mais investigação para avaliar esta hipótese e tal investigação deverá estar sempre assente no pressuposto de que valores paramétricos são somente descritores elementares do comportamento morfodinâmico e que, em praias encastradas, o controlo geológico altera

significativamente a variabilidade morfológica e, consequentemente, o comportamento morfodinâmico.

A análise da variabilidade morfológica nas seis praias em que incidiu este estudo, permitiu verificar que a mesma se encontra significativamente constrangida pela presença de limites geológicos sob a forma de promontórios e afloramentos rochosos. Verificou-se que estes limites geológicos são responsáveis pela determinação de padrões de variabilidade espacial e temporal diversos nas seis praias analisadas. A distinção dos padrões de variabilidade morfológica com recurso a funções ortogonais empíricas e análise de correlação estatística permitiu demonstrar a presença de respostas localizadas nas praias em estudo. Estas respostas são promovidas pela interferência dos limites geológicos verticais e laterais no comportamento morfodinâmico das praias e incluem o desenvolvimento de processos de rotação de praia, o estabelecimento de correntes de fuga controladas topograficamente e a constrição da mobilidade do perfil de praia. Apesar da importância destes mecanismos morfodinâmicos na determinação de respostas morfológicas longitudinalmente heterogéneas, verificou-se que o principal modo de variabilidade morfológica possui componente transversal (*i.e.* perpendicular à linha de costa), representando entre 67% a 94 % da variância do volume sedimentar para as seis praias analisadas. Esta componente transversal encontra-se significativamente correlacionada com o fluxo de energia das ondas normalizado pela amplitude de maré, sendo esta correlação estatisticamente significativa para valores de $p = 0.01$ na maioria das praias analisadas. A identificação desta relação permite destacar a importância de parâmetros que combinem o forçamento conjunto das ondas e marés para analisar relações de processo-resposta entre a hidrodinâmica e a variação morfológica em ambientes costeiros mesotidais. É, no entanto, necessária mais investigação para avaliar o potencial de aplicabilidade do fluxo de energia das ondas

normalizado pela amplitude de maré num contexto mais abrangente ao nível da análise morfodinâmica de praias. Para além da dissociação espacial entre respostas transversais e longitudinais, foi ainda possível identificar uma variação em termos de tempo de resposta das praias, caracterizada por um aumento dos tempos de resposta para situações de maior constrangimento das praias (de 1 dia em praias mais expostas para 1 semana ou mais em praias mais protegidas). Uma maior frequência de monitorização, eventualmente com recurso a técnicas de monitorização com vídeo, poderá permitir uma definição mais detalhada das relações de processo-resposta, bem como aperfeiçoar a determinação dos tempos de resposta das praias. Com base nos resultados obtidos é apresentado um quadro conceptual para descrição dos efeitos dos limites geológicos em praias encastradas. Sugere-se que a redução no volume sedimentar e/ou diminuição da profundidade relativa a que se encontra o substrato rochoso intensificam os efeitos dos limites geológicos verticais, enquanto o aumento no grau de indentação e/ou a maior obliquidade da agitação incidente reforçam o efeito dos limites geológicos laterais. São, no entanto, necessários mais esforços de investigação para avaliar o quadro conceptual proposto e contextualizá-lo quantitativamente. Neste sentido, a determinação da espessura de sedimento necessária para a variação livre do perfil de praia é um tópico de especial importância para futura exploração, particularmente em ambientes controlados geologicamente.

Os resultados obtidos demonstram claramente que o controlo geológico influencia significativamente a variabilidade morfológica nas seis praias estudadas. Contudo, para as praias da costa oeste, expostas a condições de agitação de elevada energia e possuindo maior volume sedimentar, verificou-se uma maior variabilidade temporal e espacial. Estando localizadas num ambiente dominado por ondulação de geração distante, com marcada sazonalidade, as alterações morfológicas nas praias

apresentaram um padrão genérico de variabilidade igualmente sazonal. Este padrão sazonal foi, contudo, suplantado por uma componente episódica promovida pela ocorrência de um grupo de tempestades, composto por 5 eventos individuais, e que levaram a uma perturbação significativa da variabilidade sazonal. Este grupo de tempestades promoveu erosão sedimentar muito expressiva nas praias da costa oeste, apesar de restrita à praia emersa e submersa, não tendo alcançado o cordão dunar (existente apenas nas praias da Amoreira e Monte Clérigo). Esta situação tem implicações para o comportamento de longo-termo de praias encastradas expostas a condições de elevada energia, indicando que mesmo os eventos extremos poderão não ter impactos duradouros na evolução geral das praias. É necessário, contudo, aprofundar os estudos sobre a resposta morfológica a temporais, já que as praias encastradas possuem elevada especificidade local em termos de resposta a condições de elevada energia. Para além da especificidade nas variações morfológicas verificadas entre praias, foi possível identificar diferenças longitudinais significativas dentro de cada praia. Da análise efetuada à heterogeneidade da variação morfológica longitudinal concluiu-se que esta se encontra relacionada com o desenvolvimento de "megarips" (*i.e.* correntes de fuga controladas topograficamente que adquirem extensão e intensidade muito significativa em condições de elevada energia), uma vez que a localização de megarips é consistente com os sectores de maior variabilidade observados em cada praia.

Para definir o papel das "megarips" na determinação do comportamento morfodinâmico das três praias encastradas da costa oeste, foram analisadas detalhadamente as condições do desenvolvimento de "megarips" em situações de tempestade e a avaliação do seu impacto na erosão ao longo das praias em estudo. De forma a relacionar a influência das "megarips" com a variação morfológica das praias,

desenvolveu-se uma classificação para discriminar a presença de correntes de retorno e sua influência no perfil de praia. Esta classificação baseou-se em evidências morfológicas e visuais características dos canais principais e de alimentação de correntes de fuga. Os resultados obtidos indicam que, para tempestades individuais, as praias respondem com erosão moderada dos perfis de praia influenciados pelo desenvolvimento de canais principais e de alimentação de "megarips". No entanto, ocorreu erosão extrema das praias quando as "megarips" se tornaram persistentes, promovendo erosão continuada e exportação sedimentar para a praia submersa. Esta situação foi observada durante a incidência de um grupo de 5 tempestades que teve lugar ao longo de 22 dias entre Janeiro e Fevereiro de 2009. Verificou-se que os canais das "megarips" se mantiveram estáveis por vários meses, continuando a funcionar como mecanismos de exportação sedimentar para a zona submersa da praia, mesmo em condições de agitação de moderada energia. Esta situação reduziu significativamente a capacidade de recuperação pós-temporal das praias em análise. Para análise das condições que levam ao desenvolvimento das "megarips", cuja localização é controlada topograficamente, recorreu-se à análise visual e modelação numérica da agitação na rebentação. De acordo com os resultados obtidos, concluiu-se que o desenvolvimento e localização das "megarips" são determinados por variações longitudinais na altura e obliquidade das ondas na rebentação e, ainda, pela interação de padrões de circulação promovidos pela agitação com a topografia da zona submersa adjacente à praia. As "megarips" são um mecanismo de resposta morfodinâmica de praias encastradas pouco estudado e apesar dos avanços apresentados neste trabalho sobre as condições de desenvolvimento de "megarips" e do seu papel na intensificação da erosão e redução da capacidade de recuperação de praias encastradas, é ainda necessário efetuar um significativo esforço de investigação. São particularmente necessários estudos que

incidam na monitorização morfológica de praias encastradas e zonas submersas adjacentes para condições de temporal, assim como medições do forçamento hidrodinâmico para condições de elevada energia. A circulação hidrodinâmica em praias encastradas é complexa, mas um melhor conhecimento é necessário para que se compreenda o funcionamento morfodinâmico de praias encastradas.

Apesar dos objetivos desta tese se relacionarem fundamentalmente com uma melhoria do conhecimento científico sobre a geomorfologia e morfodinâmica de praias encastradas, existem implicações para a gestão e ordenamento de praias encastradas nos resultados apresentados. Estudar praias encastradas em ambientes geomorfologicamente contrastantes permitiu, desde logo, identificar uma elevada variabilidade de comportamentos e mecanismos morfodinâmicos. Se mais praias encastradas, com diferentes características, tivessem sido incluídas na análise seria provável que uma ainda maior diversidade morfodinâmica fosse identificada. Este potencial de variabilidade para praias encastradas implica que qualquer intervenção de gestão realizada nestes ambientes seja efetuada com particular cautela, caso não seja precedida de uma monitorização prolongada para determinar os principais mecanismos de variabilidade morfológica. Identificar se numa praia encastrada se verifica a ocorrência de fenómenos de rotação de praia, ou mesmo o desenvolvimento de "megarips", tem importantes implicações para o correto planeamento e configuração de intervenções de gestão costeira. No mesmo sentido, a minuciosa definição dos padrões de circulação hidrodinâmica de uma praia encastrada é extremamente importante para melhorar a segurança no uso balnear deste tipo de praias. A circulação hidrodinâmica em praias encastradas é frequentemente determinada por células de circulação complexas, com elevado controlo geológico. A sua identificação e conhecimento podem representar um claro avanço para salvaguardar a segurança das populações.

TABLE OF CONTENTS

Dedication i
Acknowledgements iii
Abstract vii
Resumo ix
Resumo alargado xi
Table of contents xxi
List of figures xxv
List of tables xxx

1 Introduction 1
1.1 Motivation 2
1.2 Study area 5
1.2.1 The southwestern Portuguese coastline 5
1.2.2 Study embayments 8
1.3 Thesis objectives and outline 14
1.4 References 17

2 Applicability of parametric beach morphodynamic state classification in embayed beaches 23
2.1 Introduction 26
2.2 Study sites 30
2.3 Bayesian probabilistic model 32
2.3.1 Model implementation 33
2.3.2 Data set 35
2.3.2.1 Wave forcing 35
2.3.2.2 Tidal range 37
2.3.2.3 Sediment fall velocity 38
2.4 Field classification of beach state 38
2.5 Results 41

2.6 Discussion 48

2.6.1 Modal values and probabilistic distributions in parametric beach state classifications 48

2.6.2 Parametric values and beach morphodynamic states 50

2.6.3 Embayed configuration and geological influence on beach state 53

2.7 Conclusion 55

2.8 Acknowledgements 57

2.9 References 57

3 Geologically constrained morphological variability and boundary effects on embayed beaches 63

3.1 Introduction 66

3.2 Field site description 69

3.3 Data and methods 73

3.3.1 Topographic data 73

3.3.2 Empirical orthogonal function analysis 74

3.3.3 Comparison with forcing parameters 75

3.3.3.1 Offshore waves and tides 76

3.3.3.2 Forcing parameters 77

3.3.3.3 Correlation analysis 80

3.4 Results 82

3.4.1 Amoreira 82

3.4.2 Mt. Clérigo 85

3.4.3 Arrifana 87

3.4.4 Salema 88

3.4.5 Boca do Rio 90

3.4.6 Cabanas Velhas 91

3.5 Discussion 92

3.5.1 Forcing parameters and response times 92

3.5.2 Mechanisms for alongshore variability 94

3.5.3 Boundary effects 96
3.6 Conclusions 101
3.7 Acknowledgements 102
3.8 References 102

4 Morphologic change and morphodynamics at high-energy embayed beaches in southwestern Portugal 111
4.1 Introduction 113
4.2 Study area 115
4.3 Methods 117
4.4 Results 119
4.4.1 Wave forcing 119
4.4.2 Seasonal and storm induced beach change 121
4.4.3 Alongshore non-uniform beach change 123
4.5 Discussion and conclusion 126
4.6 Acknowledgements 129
4.7 References 130

5 Extreme erosion in high-energy embayed beaches: influence of megarips and storm grouping 133
5.1 Introduction 135
5.2 Environmental setting 137
5.3 Methods 140
5.3.1 Beach and nearshore morphology 140
5.3.2 Rip and feeder configuration 141
5.3.3 Offshore wave data 144
5.3.4 Nearshore wave propagation 146
5.3.5 Embayment scaling parameter (δ') 148
5.4 Results 149
5.4.1 Wave conditions 149

5.4.2 Morphological change 151
5.4.2.1 Arrifana 151
5.4.2.2 Mt. Clérigo 153
5.4.2.3 Amoreira 155
5.4.3 Nearshore wave modelling 156
5.4.4 Embayment circulation 161
5.5 Discussion 162
5.5.1 Megarips of large rips? 162
5.5.2 Megarip development 165
5.5.3 Enhanced erosion by megarips and storm grouping 169
5.5.4 Implications for beach recovery 171
5.6 Conclusion 173
5.7 Acknowledgements 175
5.8 References 175

6 General conclusions 183

LIST OF FIGURES

1.1 Geographical location and aerial view of the study embayments within the southwestern Portuguese coastline 6

1.2 Wave rose for western (left) and southern (right) sectors of southwestern Portugal based on directional wave data collected respectively at Sines and Faro waverider buoys between 2007 and 2009 8

1.3 Amoreira embayment: aerial view (left) and oblique photograph taken in July 2009 from the southern headland (right) 9

1.4 Mt. Clérigo embayment: aerial view (left) and oblique photograph taken in June 2008 from the southern headland (right) 10

1.5 Arrifana embayment: aerial view (left) and oblique photograph taken in June 2008 from the northern headland (right) 11

1.6 Salema embayment: aerial view (left) and oblique photograph taken in April 2009 from the eastern headland (right) 12

1.7 Boca do Rio embayment: aerial view (left) and oblique photograph taken in April 2009 from the eastern cliff (right) 13

1.8 Cabanas Velhas embayment: aerial view (left) and oblique photograph taken in May 2009 from the western cliff (right) 13

2.1 Yearly citations for Wright and Short (1984) (dark grey) and Masselink and Short (1993) (light grey) morphodynamic beach classification models based on Thomson Reuters ISI Web of Knowledge (V 5.5) checked on 23/02/2012 27

2.2 Geographic location and aerial view of the study sites (indicated by black circles in the map). Location of directional wave buoys, modelled WANA wave grid points and tide gauges indicated by asterisks, stars and doted circles, respectively. Wave roses for Sines and Faro computed from wave buoy data (asterisks in location image), from 2007 to 2009. 31

2.3 Schematic diagram of a Bayesian network for parametric beach morphodynamic classification 34

2.4 Hierarchical frameworks for field based classification of beach states according to a) Wright and Short (1984); and b) Masselink and Short (1993) models of beach morphodynamic state 40

2.5 Prior probability distributions for the variables in the Bayesian networks for west coast embayments. Beach states as defined by Wright and Short (1984): R - reflective; LTT – low-tide terrace; TBR – transverse bar and rip; RBB – rhythmic bar and beach; LBT – longshore bar-trough; D - dissipative.. 42

2.6 Prior probability distributions for the variables in the Bayesian networks for south coast embayments. Beach states as defined by Wright and Short (1984): R - reflective; LTT – low-tide terrace; TBR – transverse bar and rip; RBB – rhythmic bar and beach; LBT – longshore bar-trough; D - dissipative.. 43

2.7 Prior probability distributions of Ω (light grey) and observed beach state histograms (black) according to Wright and Short (1984) beach states. Stars indicate the beach state determined by Ω single averaged value calculation and circles the beach state determined by the mean probabilistic weighted value... 45

2.8 Beach state classification within the dimensionless Ω - RTR space according to Masselink and Short (1993). Observed beach states and frequency (grey rectangles) with modal state indicated by darker shading. Stars indicate the beach state determined by single averaged value calculation and circles the beach state determined by the mean probabilistic weighted value. Beach types as defined by Masselink and Short (1993): R - reflective; B - barred; BD - barred dissipative; LTT+R – low-tide terrace + rip; LTB/R – low-tide bar/rip; NBD – non-barred dissipative; LTT – low-tide terrace; UD – ultra-dissipative; TT – transition to tidal flats.... 47

3.1 Geographic location and aerial view of the study sites (indicated by black circles in the map). Location of beach profiles, directional wave buoys, modelled wave points and tide gauges indicated by black lines, asterisks, stars and doted circles, respectively. Wave roses for Sines and Faro were computed from wave buoy data (asterisks in location image), from 2007 to 2009.. 72

3.2 Linear correlation (R) between forcing parameters Ω (black line) and Pn_o (grey dotted line) and the first temporal eigenfunction ($c_1(t)$) for Arrifana beach. Results are presented for the averaging windows of 1 to 30 days prior to each survey. Averaging days (D) for the first peak in correlation above the $R_{crit\ 95\%}$ level are indicated for each forcing parameter..... 81

3.3 Normalized spatial ($e_n(s)$) and temporal ($c_n(t)$) eigenfunctions for Amoreira beach dataset (upper panels). Reconstruction of the first two EOF modes, based on the combined analysis of the spatial and temporal eigenfunctions (lower panels). North, Centre and South are relative to the profiles location at the beach.... 85

3.4 Normalized spatial ($e_n(s)$) and temporal ($c_n(t)$) eigenfunctions for Mt. Clérigo beach dataset (upper panels). Reconstruction of the first two EOF modes, based on the combined analysis of the spatial and temporal eigenfunctions (lower panels). North, Centre and South are relative to the profiles location at the beach.... 86

3.5 Normalized spatial ($e_n(s)$) and temporal ($c_n(t)$) eigenfunctions for Arrifana beach dataset (upper panels). Reconstruction of the first two EOF modes, based on the combined analysis of the spatial and temporal eigenfunctions (lower panels). North, Centre and South are relative to the profiles location at the beach.... 88

3.6 Normalized spatial ($e_n(s)$) and temporal ($c_n(t)$) eigenfunctions for Salema beach dataset (upper panels). Reconstruction of the first two EOF modes, based on the combined

analysis of the spatial and temporal eigenfunctions (lower panels). West, Centre and East are relative to the profiles location at the beach.... 89

3.7 Normalized spatial ($e_n(s)$) and temporal ($c_n(t)$) eigenfunctions for Boca do Rio beach dataset (upper panels). Reconstruction of the first two EOF modes, based on the combined analysis of the spatial and temporal eigenfunctions (lower panels). West, Centre and East are relative to the profiles location at the beach.... 90

3.8 Normalized spatial ($e_n(s)$) and temporal ($c_n(t)$) eigenfunctions for Cabanas Velhas beach dataset (upper panels). Reconstruction of the first two EOF modes, based on the combined analysis of the spatial and temporal eigenfunctions (lower panels). West, Centre and East are relative to the profiles location at the beach.... 92

3.9 Conceptual framework describing boundary effects in embayed beaches 100

4.1 Location of the study area in the southwestern coast of Portugal (A). Amoreira (B), Mt. Clérigo (C) and Arrifana (D) embayments with profile identification (black lines)..... 116

4.2 Daily averages of offshore wave conditions at Sines between September 2007 and September 2009. Thick black line depicts smoothed values using a 3-month running average..... 120

4.3 Offshore significant wave height, water level and surge level during the January-February 2009 storm group. Numbers indicate individual storm events..... 121

4.4 Cumulative beach change for each profile and averaged per beach. Left panels represent the beach volume (m^3/m) and beach width (m) is shown in the right panels..... 123

4.5 Profile volumetric mobility and envelope..... 124

5.1 Geographical location of the study sites. Aerial view of Amoreira (A), Monte Clérigo (B) and Arrifana (C) embayments with indication of beach profiles location (black lines) and positions for image acquisition (stars). Bathymetry is given in metres below mean sea level (MSL). The wave rose was computed from Sines wave buoy data (black star in inset of location image), from September 2007 to September 2009..... 139

5.2 Synthesis of morphological features and graphical signatures used for classification of beach profiles and rip systems interaction. Flow arrows in the boundary diagram are not scaled to velocity..... 144

5.3 Location of Sines directional wave buoy (asterisk) and WANA grid points (crossed circles). Study sites are indicated by black dots and bathymetry is given in metres below MSL..... 145

5.4 Nested grids used in SWAN runs. The small grids for each run are nested into a medium resolution grid encompassing the entire nearshore area of the study sites, which is then nested into a larger grid of the southwestern coast of Portugal (entire area of this figure), for which water depths below MSL are provided..... 147

5.5 Time series of offshore significant wave height (H_{so}), peak period (T_p) and peak wave direction (θ) from September 2007 to September 2009. Circles in the top panel indicate timing of beach surveys. Shading highlights high-energy events (light grey) and extreme events (dark grey) during the monitoring period..... 150

5.6 Time series of offshore significant wave height (H_{so}) (top panel) and cumulative volume changes for Arrifana beach profiles (black solid line in lower panels). Circles represent profile and rip interaction, with black, grey and hollow circles indicating the influence of rip-neck, feeder channel and no rip influence, respectively. Shaded bars highlight high-energy events..... 152

5.7 Time series of offshore significant wave height (H_{so}) (top panel) and cumulative volume changes for Mt. Clérigo beach profiles (black solid line in lower panels). Refer to Fig. 5.6 caption for description of symbols..... 154

5.8 Time series of offshore significant wave height (H_{so}) (top panel) and cumulative volume changes for Amoreira beach profiles (black solid line in lower panels). Refer to Fig. 5.6 caption for description of symbols..... 156

5.9 Alongshore variation in breaking wave height (H_b) for each embayment. Wave conditions were modelled for the storms identified in Table 5.2 (left panel) and for synthetic storms (right panel). Synthetic storms have constant offshore wave height (5 m) and peak period (15 s), but variable offshore wave directions of 315º (NW), 270º (W) and 225º (SW). Profile location is represented by grey lines..... 159

5.10 Modelled significant wave height (H_s) for the average conditions recorded during the January-February 2009 storm group (offshore boundary conditions: Hso – 4.5 m; Tp – 14.5 s; θ – 300º) at Arrifana (top panel), Mt. Clérigo (centre panel) and Amoreira (bottom panel). Depth contours (dotted lines) are in metres below MSL, and black lines indicate profile location..... 160

5.11 Embayment scaling parameter (δ') for different alongshore averaged breaking wave heights ($H_{b\bar{y}}$) in each embayment (refer to Table 5.1). Shading highlights modal conditions at each embayment..... 162

5.12 Panoramic mosaics of megarip circulation during storm and post-storm wave conditions for Arrifana. The upper panel presents the embayment under storm conditions, recorded on 05/02/2009 under 5.5 m WNW offshore waves. Arrows provide flow-behaviour indications of the megarips, and dashed lines indicate rip-head plumes. The intense wave breaking across the entire surf zone is reduced within the rip-neck channel due to wave–current interaction. Post-storm conditions, recorded on 09/02/2009, are shown in the lower panel. Dark patches and the absence of wave breaking on both beach extremities indicate the position of the feeder channels and deep rip-neck channels..... 164

5.13 Schematic mapping of megarip circulations during storm (left panel) and post-storm conditions (right panel) for Arrifana embayment. Rip-neck channels (limited by solid black lines) are indicated for both storm and post storm conditions; while feeder channels (limited by dashed black line) are only clearly identifiable during post-storm

conditions (refer to Fig. 5.12 for snapshot view). Arrows indicate flow direction only and are not scaled to velocity, and bathymetry is in metres below MSL..... 166

5.14 Schematic mapping of megarip circulations during storm (left panel) and post-storm conditions (right panel) for Mt. Clérigo embayment. Refer to Fig. 5.13 caption for description of symbols..... 168

5.15 Schematic mapping of megarip circulations during storm (left panel) and post-storm conditions (right panel) for Amoreira embayment. Refer to Fig. 5.13 caption for description of symbols..... 168

LIST OF TABLES

2.1 Specifications of SWAN implementation 36

2.2 Mean beach hydrodynamic and sediment characteristics and parametric classifications (single averaged value – *sv* – and probabilistic weighted mean – μ) 46

3.1 Summary of the relevant characteristics of monitoring sites and correlation criteria 74

3.2 Percentage of variance explained by the first two eigenfunctions at each site..... 82

3.3 Pearson's product moment correlation coefficient's between the temporal eigenfunctions (cn(t)) for the peak D days averages of the hydrodynamic forcing parameters preceding each survey (only correlations at the 95% or higher confidence levels are presented) 83

4.1 Correlation coefficients for beach profile volume and width variation..... 125

5.1 Mean offshore wave conditions used in model runs and corresponding alongshore averaged breaking wave heights ($H_{b\bar{y}}$) and standard deviation ($H_{b\sigma}$) for Arrifana, Mt. Clérigo and Amoreira embayments. Grey shading highlights modal conditions.. 157

5.2 Characteristics of observed storms from different directions used for model runs. Values of H_{so}, T_p and θ are time averages for the duration of each event. 159

5.3 Geometric and morphodynamic characteristics of the embayments 161

CHAPTER 1

Introduction

1.1 MOTIVATION

Beaches are the most unlikely of landforms to be found facing the open sea (Pethick, 1984), and when coastlines are rocky and rugged it seems even less likely that a pile of unconsolidated sediment confined by headlands and cliffs would be able to withstand the relentless pounding of waves. Yet, it is exactly the lack of cohesion that enables beaches to adapt to the wide variations in waves and currents, while neighbouring cliffs are irremediably lost to the sea. By constant morphodynamic adjustment between morphology and hydrodynamic forcing through sediment transport mechanisms (Wright and Thom, 1977), beaches and their nearshore act as adaptable buffers, dissipating the energy of waves that reach the shore (Carter, 1988). Within an embayed coastline, however, the presence of rocky headlands or outcrops can have a major influence on such morphodynamic adjustment (Short and Masselink, 1999).

By definition, embayed beaches are sandy coastlines bounded by rocky headlands or outcrops, natural or artificial, where the shoreline generally assumes some degree of curvature (Klein and Menezes, 2001). These beaches are ubiquitous (Silvester and Hsu, 1997), being common on most oceanic shorelines (LeBlond, 1979; Finkelstein, 1982; Phillips, 1985), but also on estuarine coasts, enclosed seas and lakes (Silvester and Hsu, 1997). The morphology of embayed beaches, like all beaches,

responds mainly to the changing wave and tide conditions, which vary cyclically, seasonally and episodically. However, the restraining and protective effect of rocky headlands and outcrops significantly influences how the planform, sediment transport and profile morphology adjust to forcing in embayed beaches (Short and Masselink, 1999). Such influence is evidenced by changes induced in sediment transport processes and morphological responses in embayed beaches, which are different from processes and responses in unconstrained sandy shores (Short, 2002).

It has been recognized that morphological behaviour in embayed beaches is mainly determined by beach planform and indentation ratio, beach length, presence of rip currents and submerged bars, beach type, longshore grain size distribution and nearshore slope (Klein and Menezes, 2001; Klein *et al.*, 2002). Furthermore, in such bedrock-framed beach systems, geological control was found to exert substantial influence not only in beach planform, but also on beach morphology, limiting the extent to which contemporary dynamics were expressed (Jackson *et al.*, 2005). Morphological responses to environmental forcing in embayed beaches are, therefore, affected by boundary effects, including wave diffraction and attenuation, constraining of longshore currents and modification of rip current systems (Short and Masselink, 1999). These lead to morphodynamic mechanisms specific to embayed beaches, particularly the development of topographically-controlled rips, formed during moderate to low wave conditions, and megarips developed under high wave conditions (Short, 1985), beach rotation phenomena in embayed beaches exposed to variable wave climate (Short and Masselink, 1999; Klein *et al.*, 2002), and headland bypassing of subaqueous sand (Short and Masselink, 1999).

Although rocky coasts are the dominant element around the world's coastlines (Inman and Nordstrom, 1971; Emery and Kuhn, 1982; Trenhaile, 1987), which implies

a worldwide prevalence of embayed beaches (Short and Masselink, 1999), most geomorphological research about beaches has been directed to low-lying sandy shores of coastal plains and deltas (Psuty *et al.*, 2004). In recent decades, however, embayed beaches have received more attention, being recognized as morphologically distinct from open coast beaches (Stephenson and Brander, 2003), and recent coastal geomorphology research has further focused towards embayed coastlines (Hsu *et al.*, 2010). Nevertheless, significant knowledge gaps still exist on beach morphodynamics in general, and particularly in embayed beaches, as most beach morphodynamic reasoning has been conducted considering unconstrained beach environments (Short and Jackson, *in press*). The role of geological control in embayed beach morphodynamics has yet to be fully explored (Jackson and Cooper, 2009), and investigations of waves, currents, sediment transport and morphologic adjustment process in such constrained coastal environments are particularly required (Klein *et al.*, 2010) as a matter of urgency, since beaches have become threatened environments (Pilkey *et al.*, 2011).

To date, research on the geomorphology and morphodynamics of embayed beaches along the Portuguese coastline has been limited considering the proportion of the country's coastline that is rocky. Significant contributions have, however, been presented in the last decade, detailing embayed beach morphologic behaviour (Gama, 2005; Pinto *et al.*, 2009; Trindade, 2010; Gama *et al.*, 2011a; 2011b), sediment distribution (Trindade and Pereira, 2009), longshore sediment transport (Laranjeiro *et al.*, 2003) and also planform stability (Oliveira and Barreiro, 2010). There is, nonetheless, a scarcity of datasets detailing the three-dimensional morphological variability of Portuguese embayed beaches, particularly with sufficient resolution to resolve response to storm events, as well as detailing the morphodynamic mechanisms

that determine morphological change for geologically constrained settings and under contrasting environmental conditions.

Considering the relative scarcity of national and even international studies dedicated to embayed beach morphodynamics and, consequently, a reduced understating of their variability and behaviour, this investigation was designed in order to include embayed beaches with diverse characteristics, exposed to contrasting energetic conditions and with potential for variable responses to environmental forcing.

1.2 STUDY AREA

1.2.1 The southwestern Portuguese coastline

The rocky coastline of southwestern Portugal (Fig. 1.1), a protected heritage coast since 1995, presents striking geomorphological contrasts, reflecting major differences in geological composition, morphostructural setting, paleogeographic evolution and environmental conditions between the western and southern segments (Feio, 1951; Pereira, 1990). The littoral platform, where generally short and narrow embayed beaches can be found in coastal re-entrants fronting the cliff or in association with small estuaries, has a complex genesis, involving both fluvial and marine influences, coupled with faulting, uplift and downlift since the Pliocene (Pereira, 2006). The coastline that limits the littoral platform is composed of slowly retreating cliffs (Marques, 1997), developed on Carboniferous shale and greywacke cliffs along the majority of the western coastline, while Jurassic to Miocene calcareous cliffs frame the southern segment. This coastline faces a relatively narrow continental shelf (10-30 km), dipping moderately towards the continental slope and with reduced sediment coverage

in the western section, while in the south considerable sediment accumulations, although heterogeneously distributed, cover a gently sloping shelf (Pereira, 1992).

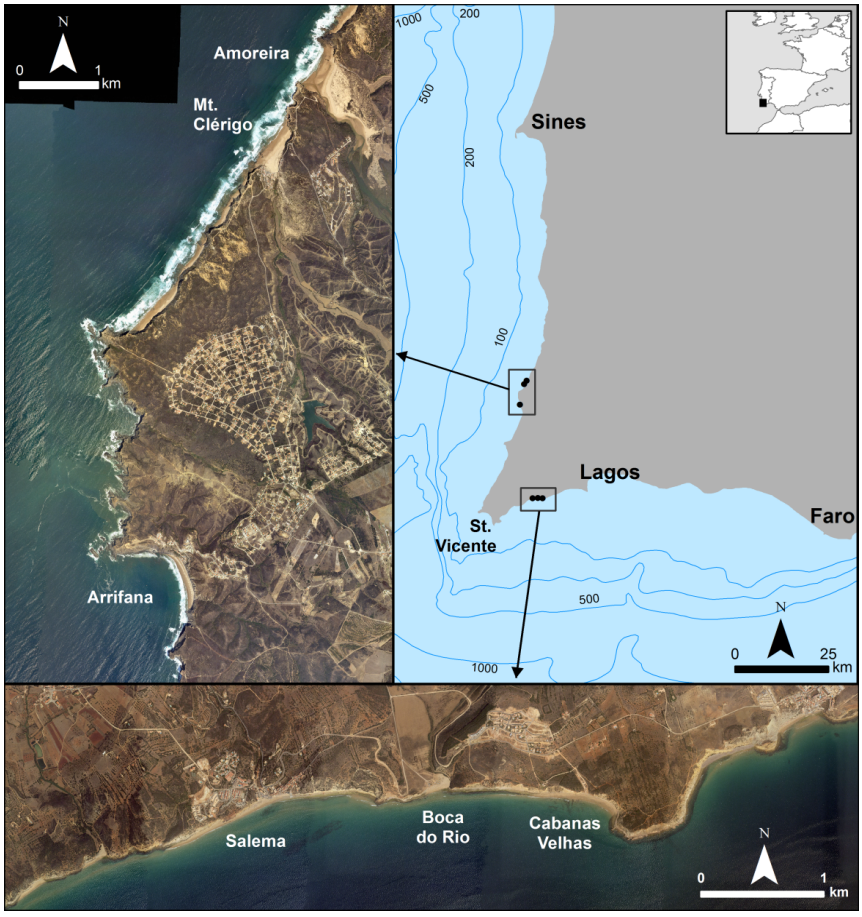

Figure 1.1 Geographical location and aerial view of the study embayments within the southwestern Portuguese coastline.

The indented and intricate outline of the southwestern Portuguese coastline reflects, besides noticeable lithological variations, a combination of cycles of coastline progradation, stabilization and recession that have shaped the Portuguese margin during the Quaternary. Sea-level stabilized at its present level around 3500 years BP on the Portuguese coast (Dias *et al.*, 2002), yet, despite evidence of sediment reworking across the Portuguese continental shelf during the Holocene transgression (Dias *et al.*, 2002) and, particularly, evidences of abundant aeolian deposits along the southwestern margin (Pereira, 1987), the present day coastline of southwestern Portugal is sediment-starved,

presenting negligible continental sediment supply. Such conditions imply that contemporary beach dynamics in southwestern Portugal are mostly constrained to the relatively small amounts of sediment contained within embayments and the reworking of adjacent nearshore sands.

The contrasts in geomorphological setting between the western and southern sectors of the southwestern Portuguese coastline are also noticeable in terms of oceanographic conditions, particularly wave climate. Tide conditions are identical and characterized by a semidiurnal regime, with a tidal cycle of approximately 12h25m, and mesotidal amplitudes that can range from barely 1 m during neap tides, to more than 3.5 m in spring tides (Instituto Hidrográfico, 2008). Belonging to the same anticlockwise tidal wave, with south-north propagation along the western sector and west-east propagation along the southern sector, tide conditions are nearly synchronous for both sectors of the coastline. Storm surge has been shown to increase water levels up 0.75 m, but only under extreme conditions, as on 99% of occurrences storm surge values are below 0.5 m for both coastline sectors (Gama *et al.*, 1994). As stated, wave regimes differ markedly between western and southern sectors (Fig. 1.2). Being directly exposed to the North Atlantic swell and storms, offshore wave conditions in the western sector are characterized by high-energy conditions throughout the entire year. Mean offshore significant wave height is between 1.5 and 2 m and peak wave period is between 9 and 13 s for summer and winter periods, respectively, indicating a marked seasonality in wave climate (Costa and Esteves, 2010). There is, however, no seasonality in wave direction, as waves approach from north-westerly to westerly directions throughout the year (Costa and Esteves, 2010).

The southern facing section, being relatively sheltered from the North Atlantic swell, experiences moderate wave conditions, with mean significant wave height around

0.9 m and mean peak period of 8 s (Costa *et al.*, 2001). Slight variations occur between summer and winter conditions, but not as markedly as on the western sector. Dominant waves reach the southern coastline from a westerly to south-westerly direction, yet shorter period SE wave generated within the Gulf of Cadiz account for roughly a quarter of occurrences (Costa *et al.*, 2001), creating a noticeably bimodal wave distribution (Fig. 1.2). Differences in wave climate for both sectors are also manifest in how storm events are defined. For the higher-energy western coastline offshore significant wave heights over 5 m are defined as storms (Pita and Santos, 1989), while on the moderate-energy southern coastline the threshold is lowered to 3 m (Pessanha and Pires, 1981).

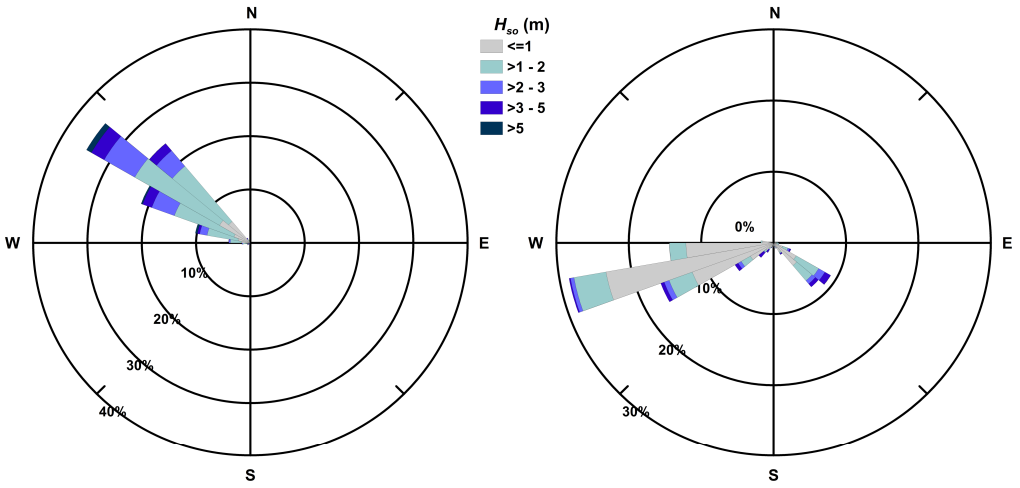

Figure 1.2 Wave roses for western (left) and southern (right) sectors of southwestern Portugal based on directional wave data collected respectively at Sines and Faro waverider buoys between 2007 and 2009.

1.2.2 Study embayments

Six embayments located in two clusters, each composed of three closely located beaches (Fig 1.1), were selected as study sites based on their general orientation in relation to the dominant wave directions. The western coast cluster included Amoreira, Mt. Clérigo and Arrifana embayments, while the southern cluster included Salema, Boca do Rio and Cabanas Velhas embayments.

Amoreira is a 600 m-long northwest facing embayment (Fig. 1.3), bounded at the northern end by a 50 m-high shale and greywacke headland and at the southern end by a 20 m-high sandstone cliff, which is part of an extensive cemented sand dune system (Pereira, 1987). This embayment contains a bay-barrier estuary, with a small tidal stream that runs through a highly variable shallow channel adjacent to the southern headland (Oliveira *et al.*, 2010, Freire *et al.*, 2011). The beach has a persistent low-tide terrace, occasionally crossed by a northward-directed secondary channel of the stream, creating a ridge and runnel-like morphology. Within the northern part of Amoreira, a rocky shore platform and remnants of dune sandstone outcrop frequently, indicating the presence of only a thin sand veneer covering this section of the embayment. An extensive dune field exists along the central part of the embayment. In the last decades a retreat of the frontal dune has been observed, while the inner dunes have been showing some signs of expansion (Gama, 2005). The beach sediment is typically fine to medium sand ($D_{50} \approx 0.30$ mm), with approximately 32% carbonate fraction in the beach face, increasing to more than 35% on the intertidal terrace (Gama, 2005). Typical gradients for the intertidal and nearshore zones are 0.02 and 0.03, respectively.



Figure 1.3 Amoreira embayment: aerial view (left) and oblique photograph taken in July 2009 from the southern headland (right)

Mt. Clérigo embayment, located approximately 400 m southwards of Amoreira embayment, and separated from it by sandstone cliffs that are part of the cemented dune system (Pereira, 1987), also faces directly the dominant NW waves (Fig. 1.4). The beach, approximately 550 m-long, is narrow and backed by 50 m-high shale and greywacke cliffs in the northern part, while the central and southern sections are wide and backed by partly vegetated dunes. The dune field develops against mildly inclined slopes, extending south-eastwardly along a wide creek were a temporary stream occasionally reaches the beach. Within the southern section of the beach, sediment cover is generally thin and rocky outcrops and shore platforms are often visible in the intertidal area. At Mt. Clérigo beach sediment is also typically composed of fine to medium sand ($D_{50} \approx 0.30$ mm). Carbonate fractions range from approximately 28% on the beach face to around 35% on the intertidal terrace (Gama, 2005). Typical gradients for the intertidal and nearshore zones are identical and around 0.03.



Figure 1.4 Mt. Clérigo embayment: aerial view (left) and oblique photograph taken in June 2008 from the southern headland (right)

Arrifana is a swash-aligned 650 m-long beach (Fig. 1.5), completely enclosed by up to 100 m-high shale and greywacke cliffs. The embayment is partially protected from the dominant north-westerly waves by a prominent northern headland, being particularly exposed to westerly and south-westerly waves (Gama, 2005). A lag deposit,

composed of coarse gravel and boulders, separates the narrow subaerial beach, composed of typically medium to fine sand ($D_{50} \approx 0.27$ mm), from the steeply sloping cliffs. Carbonate contents of beach sediment are around 30 % (Gama, 2005) and intertidal and nearshore gradients are around 0.04 and 0.02, respectively.



Figure 1.5 Arrifana embayment: aerial view (left) and oblique photograph taken in June 2008 from the northern headland (right)

Located approximately 15 km eastward of St. Vicente cape, the southern embayments cluster comprises the beaches of Salema, Boca do Rio and Cabanas Velhas (Fig. 1.1). These are mostly low-volume sandy beaches, with frequent coarse-grained lower layers (gravel to cobble), overlying lag deposits of boulders or gently dipping shore platforms. The very low erosion rates in the nearby rocky cliffs (Marques, 1997) and the small catchment areas of streams that drain to the coast result in a generally negligible fluvial or coastal sediment supply. The absence of dune systems backing the beaches, and acting as sand reservoirs, contributes also to the sediment deficiency of these embayments. Enclosed by 30 to 70 m-high limestone cliffs, Salema embayment is, however, relatively unconstrained by headlands, which allows the beach to range from 600 to 1100 m-long (Fig. 1.6). With a general WSW-ENE orientation, the embayment is directly exposed to south-easterly waves, yet the relatively unconstrained setting enables the dominant south-westerly waves to also reach the beach. These generally

impinge on the shoreline with significant angles. Salema beach is composed of fine to medium sand (D_{50} ≈ 0.31 mm), overlying coarse gravel layers and boulders at the western and eastern ends. Typical gradients for the intertidal and nearshore zones are 0.07 and 0.02, respectively.

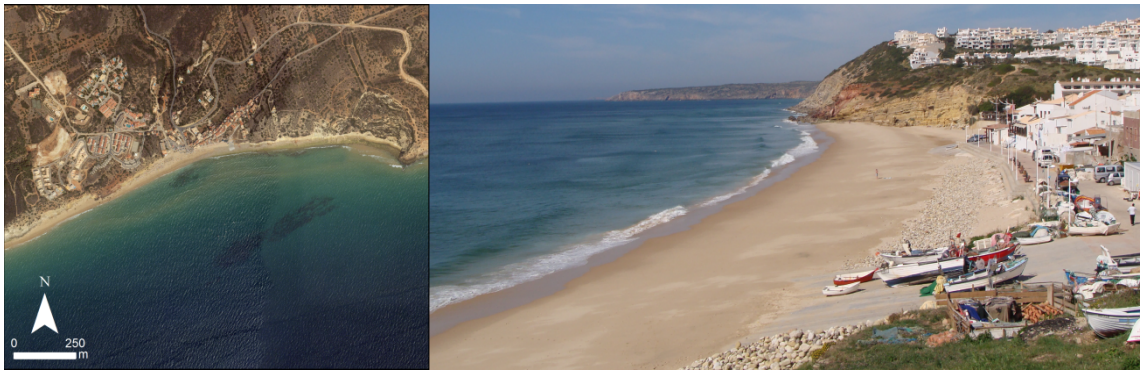

Figure 1.6 Salema embayment: aerial view (left) and oblique photograph taken in April 2009 from the eastern headland (right)

Boca do Rio is a short and narrow beach, approximately 180 m-long, in a small bay, laterally enclosed by 30 to 60 m-high limestone cliffs (Fig. 1.7). With a WSW-ENE general orientation, this beach is directly exposed to south-easterly waves, but the reduced seaward protrusion of the bordering headlands enables waves from south-westerly to also impact the beach. Boca do Rio beach corresponds to the terminal part of a small estuary, which has been completely infilled and where a small stream, with episodic discharge, drains through the eastward end of the beach during periods of significant rainfall. The beach is composed of medium sand (D_{50} ≈ 0.43 mm), overlying lag deposits of boulders along with small layers of coarse gravel. The beach is separated from land by a storm ridge and rock spur in the centre that constitute a barrier to storm wave overtopping (Hindson *et al.*, 1996), and by an erosional bluff in the west (Carrasco *et al.*, 2007). Typical intertidal and nearshore gradients are 0.07 and 0.02, respectively.



Figure 1.7 Boca do Rio embayment: aerial view (left) and oblique photograph taken in April 2009 from the eastern cliff (right)

Cabanas Velhas is an approximately 500 m-long narrow beach located to the west of Ponta de Almádena, a Jurassic limestone headland that constrains the beach to the east (Fig. 1.7). Cabanas Velhas is directly exposed to the dominant south-westerly waves, which are also associated with more intense storms, while south-easterly waves arrive significantly diffracted to the central and eastern sectors beach. The beach is typically composed of fine to medium sand ($D_{50} \approx 0.29$ mm), which overlies boulders and shore platforms on the western sector and cobbles on the central and eastern sectors. The latter are reworked under high-energy wave conditions, forming beach cusps and erosion scarps. Identical to Salema and Boca do Rio, typical intertidal and nearshore gradients in Cabanas Velhas are 0.07 and 0.02, respectively.



Figure 1.8 Cabanas Velhas embayment: aerial view (left) and oblique photograph taken in May 2009 from the western cliff (right)

1.3 THESIS OBJECTIVES AND OUTLINE

The broad aim of this study is to *define the medium-term (months to years) morphodynamic variability of embayed beaches in contrasting geomorphological settings*. A greater understanding of the mechanisms driving, yet also constraining, the interactions between hydrodynamic processes and beach morphology at embayed beaches will be obtained. To achieve this main goal, a two-year survey program was established in six embayments located in southwestern Portugal, exposed to contrasting geodynamic conditions, aiming to obtain datasets of morphological change with enough resolution to capture not only seasonal/cyclic beach variability, but also beach response to high-energy events.

From the general aim, the study is organized into four primary objectives structured from a broader, morphodynamic and morphological embayment-wide scale, towards a focused, morphodynamic processes-oriented scale, to better understand the morphodynamic behavior and mechanisms acting on embayed beaches:

(i) Assess the applicability of beach morphodynamic state classification for geologically controlled embayed beaches.

There are indications that geological control significantly impacts beach morphodynamic state. Consequently, existing beach state models may not be adequate for characterizing morphodynamic state at embayed beaches. This is explored using averaged environmental parameters and is further extended considering joint probability analysis.

(ii) Evaluate the dominant modes of embayment morphological variability and how they are determined by the presence of geological boundaries.

Topographic monitoring performed on the embayments allows dominant modes of embayment variability to be analysed and related to forcing

mechanisms using statistical techniques. The spatial and temporal response observed in the embayments and the nature of the forcing mechanisms are used to explore and quantify the effect of geological boundaries in embayed beach morphological variability

(iii) *Characterize morphodynamic mechanisms driving morphological change in high-energy embayed beaches.*

Temporal and spatial morphological changes observed in embayed beaches exposed to high-energy conditions presents both seasonal and episodic components. These are explored in order to identify morphodynamic mechanisms driving alongshore non-uniform embayment response in high-energy west coast embayments.

(iv) *Evaluate the development of megarips in high-energy embayed beaches and characterize their enhanced action during storm groups.*

Megarips occur in embayed beaches exposed to high-energy wave conditions, promoting beach erosion and driving alongshore non-uniform beach response. The conditions for their development are further explored and their persistence and enhanced action during storm groups is examined.

These four objectives are individually addressed in chapters 2, 3, 4 and 5, respectively. Each chapter corresponds to individual scientific papers that have been either submitted or already published in international peer-reviewed scientific publications. Presenting the thesis by individual papers allows each chapter to be considered independently, however, this format has the disadvantage of repeating certain details, particularly in terms of study area description and data collection

procedures, while in some sections details of data analysis are not explicitly provided, but instead referenced to the other papers. While it is acknowledged that such repetition and referencing may hinder the thesis readability, the present format was chosen in order to maintain the integrity of the original scientific papers. The thesis comprises six chapters:

CHAPTER 1 – provides a brief introduction detailing the motivation of the present work within the framework of beach morphodynamic research, further presenting the study area and detailing the thesis objectives and structure.

CHAPTER 2 – is a scientific paper entitled *Applicability of parametric beach morphodynamic state classification in embayed beaches* by C. Loureiro, Ó. Ferreira and J.A.G. Cooper, submitted to *Marine Geology*.

CHAPTER 3 – is a scientific paper entitled *Geologically constrained morphological variability and boundary effects on embayed beaches* by C. Loureiro, Ó. Ferreira and J.A.G. Cooper, in revision in *Marine Geology*.

CHAPTER 4 – is a scientific paper entitled *Morphologic change and morphodynamics at high-energy embayed beaches in southwestern Portugal* by C. Loureiro, Ó. Ferreira and J.A.G. Cooper, published in 2011 as a book chapter in the *Proceedings of the Seventh International Symposium on Coastal Engineering and Science of Coastal Sediment Processes – Coastal Sediments'11*.

CHAPTER 5 – is a scientific paper entitled *Extreme erosion in high-energy embayed beaches: influence of megarips and storm grouping* by C. Loureiro, Ó. Ferreira and J.A.G. Cooper, published in 2012 in *Geomorphology*.

CHAPTER 6 – provides a final synthesis and general conclusions of the thesis.

1.4 REFERENCES

Carrasco, A.R., Ferreira, Ó., Matias, A., Dias, J.M.A., 2007. Historic monuments threatened by coastal hazards at Boca do Rio, Algarve, Portugal. *Coastal Management* 35, 163-179.

Carter, R.W.G., 1988. *Coastal Environments: an introduction to the physical, ecological and cultural systems of coastlines*. Academic Press, London, 617 p.

Costa, M., Esteves, R., 2010. Clima de agitação marítima na costa oeste de Portugal Continental. Proceedings of XI Jornadas Técnicas de Engenharia Naval — O Sector Marítimo Português. Edições Salamandra, Lisboa, Portugal, pp. 413-426.

Costa, M., Silva, R., Vitorino, J., 2001. Contribuição para o estudo do clima de agitação marítima na costa Portuguesa. Proceedings of 2as Jornadas de Engenharia Costeira e Portuária. AIPCN, Aveiro, Portugal (20 pp. CD-ROM).

Dias, J.M.A., Boski, T., Rodrigues, A., Magalhães, F., 2002. Coast line evolution in Portugal since the Last Galcial Maximum until present – a synthesis. *Marine Geology* 170, 177-186.

Emery, K.O. and Kuhn, G.G., 1982. Sea cliffs: their processes, profiles and classification. *Geological Society of America Bulletin* 93, 644-654.

Feio, M., 1951. A evolução do relevo do Baixo Alentejo e Algarve. *Comunicações dos Serviços Geológicos de Portugal* 32, 303-481.

Finkelstein, K., 1982. Morphological variations and sediment transport in crenulated-bay beaches, Kodiak Island, Alaska. *Marine Geology* 47, 261-281.

Freire, P., Taborda, R., Bertin, X., Guerreiro, M., Fortunato, A.B., Silva, A.M., Andrade, C., Oliveira, A., Antunes, C., Freitas, M.C., Nahon, A., Rodrigues, M., Bruneau, N., 2011. Medium-term morphodynamic evolution of a small coastal inlet. *Journal of Coastal Research* SI 64, 666-670.

Gama, C., 2005. Dinâmica de Sistemas Sedimentares do Litoral Ocidental Português a Sul do Cabo Espichel. Ph.D Thesis, Universidade de Évora, Portugal.

Gama, C., Coelho, C., Baptista, P., Albardeiro, L., 2011a. Equilibrium configuration of sandy embayed beaches from the Southwest Portuguese rocky coast. *Journal of Coastal Research* SI 64, 2037-2041.

Gama, C., Dias, J.M.A., Ferreira, Ó., Taborda, R., 1994. Analysis of storm surge in Portugal, between June 1986 and May 1988. Proceedings of Littoral'94, EUROCOAST, Lisboa, Portugal. pp. 381-387.

Gama, C., Fortes, C.J.E.M., Baptista, P., Albardeiro, L., Pinheiro, L., Salgado, R., 2011b. Medium-term evolution of an intermediate beach with an intertidal bar (Amoreira beach, Southwest Portuguese rocky coast). *Journal of Coastal Research* SI 64, 80-84.

Hindson, R.A., Andrade, C., Dawson, A.G., 1996. Sedimentary processes associated with the tsunami generated by the 1755 Lisbon earthquake on the Algarve coast, Portugal. *Physics and Chemistry of the Earth* 21, 57-63.

Hsu, J.R.C., Yu, M.J., Lee, F.C., Benedet, L., 2010. Static bay beach concept for scientists and engineers: a review. *Coastal Engineering* 57, 76-91.

Inman, D.L. and Norstrom, C.E., 1971. On the tectonic and morphologic classification of coasts. *Journal of Geology* 79, 1-21.

Instituto Hidrográfico, 2008. Tabela de Marés, Volume I. Instituto Hidrográfico, Portugal.

Jackson, D.W.T. and Cooper, J.A.G., 2009. Geological control on beach form: accommodation space and contemporary dynamics. *Journal of Coastal Research* SI 56, 69-72.

Jackson, D.W.T., Cooper, J.A.G., del Rio, L., 2005. Geological control of beach morphodynamic state. *Marine Geology* 216, 297-314.

Klein, A.H.F., Benedet, L., Schumacher, D.H., 2002. Short-term beach rotation processes in distinct headland bay beach systems. *Journal of Coastal Research* 18, 442-458.

Klein, A.H.F, Ferreira, Ó., Dias, J.M.A., Tessler, M.G., Silveira, L.F., Benedet, L., Menezes, J.T., Abreu, J.G.N., 2010. Morphodynamics of structurally controlled headland-bay beaches in southeastern Brazil: a review. *Coastal Engineering* 57, 98-111.

Klein, A.H.F. and Menezes, J.T., 2001. Beach morphodynamics and profile sequence for a headland bay coast. *Journal of Coastal Research* 17, 812-835.

Laranjeiro, S.., Oliveira, F., Freire, P., 2003. Longshore sediment transport along a sandy coast with hard rock outcrops. *Shore and Beach* 71, 20-24.

LeBlond, P.H., 1979. An explanation of the logarithmic spiral plan shape of headland-bay beaches. *Journal of Sedimentary Petrology* 49, 1093-1100.

Marques, F.M.S.F, 1997. As Arribas do Litoral do Algarve. Dinâmica, processos e mecanismos. Ph.D. Thesis, Universidade de Lisboa, Portugal.

Oliveira, A., Fortunato, A.B., Guerreiro, M., Bertin, X., Bruneau, N., Rodrigues, M., Taborda, R., Andrade, C., Silva, A.M., Antunes, C., Freire, P., Pedro, S.L., Dodet, G., Loureiro, C., Mendes, A., 2010. Effect of inlet morphology and wave action on transport and sediment dynamics in a coastal stream. Proceedings of the Eleventh International Conference on Estuarine and Coastal Modeling. ASCE Conference Proceedings 388, 601-620.

Oliveira, F.S.B.F and Barreiro, O.M., 2010. Application of empirical models to bay-shaped beaches in Portugal. *Coastal Engineering* 57, 124-131.

Pereira, A.R., 1987. Acumulações arenosas eólicas consolidadas do litoral do Alentejo e Algarve ocidental. Linha de Acção de Geografia Física, Centro de Estudos Geográficos, n.º 27, 113 p.

Pereira, A.R., 1990. A Plataforma Litoral do Alentejo e Algrave Ocidental. Estudo de Geomorfologia. Ph.D Thesis, Universidade de Lisboa, Portugal.

Pereira, A.R., 1992. A Geomorfologia da Margem Continetal Portuguesa e a Interdependência das Plataformas Continental e Litoral. Linha de Acção de Geografia Física, Centro de Estudos Geográficos, n.º 30, 85 p.

Pereira, A.R., 2006. The southwest of Portugal's mainland: a heritage littoral. In Pereira, A.R., Trindade, J., Neves, M. (Eds.), Portugal: coastal dynamics. Publicações da Associação Portuguesa de Geomorfólogos, Vol. IV, pp. 81-87.

Pessanha, L.E. and Pires, H.O., 1981. Elementos sobre o clima de agitação marítima na costa sul do Algarve. Relatório do Instituto Nacional de Meteorologia e Geofísica, 66 p.

Pethick, J., 1984. *An Introduction to Coastal Geomorphology*. Edward Arnold, London, 260 p.

Phillips, J.D., 1985. Headland-bay beaches revisited: an example from Sandy Hook, New Jersey. *Marine Geology* 65, 21-31.

Pilkey, O.H., Neal, W.J., Kelley, J.T., Cooper, J.A.G., 2011. *The World's Beaches - a global guide to the science of the shoreline*. University of California Press, Berkeley, 283 p.

Pinto, C.A., Taborda, R., Andrade, C., Teixeira, S.B., 2009. Seasonal and mesoscale variations at an embayed beach (Armação de Pêra, Portugal). *Journal of Coastal Research* SI 56, 118-122.

Pita, C. and Santos, J.A., 1989. Análise dos temporais da costa oeste de Portugal Continental, Report NATO PO-WAVES 1/89-A. IH/LNEC, Lisboa, Portugal.

Psuty, N.P., Steinberg, P.E., Wright, D.J., 2004. Coastal and marine geography. In Gaile, G.L. and Willmott, C.J. (Eds.), Geography in America at the Dawn of the 21st Century. Oxford University Press. New York. 314-325.

Short, A.D., 1985. Rip current type, spacing and persistence, Narrabeen beach, Australia. *Marine Geology* 65, 47-71.

Short, A.D., 2002. Large scale behaviour of topographically-bound beaches. Proceedings of the 28th International Conference on Coastal Engineering. ASCE, Cardiff, Wales, pp. 3778-3890.

Short, A.D. and Jackson, D.W.T., in press. Beach morphodynamics. In Sherman, D.J. (Ed.), *Treatise on Geomorphology: Coastal and Submarine Geomorphology*. Elsevier, Amsterdam.

Short, A.D. and Masselink, G., 1999. Embayed and structurally controlled beaches. In: Short, A.D. (Ed.), *Handbook of Beach and Shoreface Morphodynamics*. John Wiley & Sons, Chichester, pp. 230–249.

Silvester, R. and Hsu, J.R.C., 1997. *Coastal Stabilization*. World Scientific, Singapore. 578 p.

Stephenson, W.J. and Brander, R.W., 2003. Coastal geomorphology into the twenty-first century. *Progress in Physical Geography* 27, 607-623.

Trenhaile, A.S., 1987. *The Geomorphology of Rock Coasts*. Oxford University Press, Clarendon. 384 p.

Trindade, J., 2010. Dinâmica Morfossedimentar de Praias Dominadas por Sistemas de Arriba (Peniche – Cascais). Ph.D Thesis, Universidade Aberta, Lisboa.

Trindade, J. and Pereira, A.R., 2009. Sediment textural distribution on beach profiles in a rocky coast (Estremadura – Portugal). *Journal of Coastal Research* SI 56, 138-142.

Wright, L.D. and Thom, B.G., 1977. Coastal depositional landforms: a morphodynamic approach. *Progress in Physical Geography* 1, 412-459.

CHAPTER 2

Applicability of parametric beach morphodynamic state classification in embayed beaches

Loureiro, C., Ferreira, Ó., Cooper, J.A.G.. Applicability of parametric beach morphodynamic state classification in embayed beaches. *Marine Geology* (submitted).

ABSTRACT

Use of parametric classification of beach morphodynamic state has been steadily increasing in coastal research, despite identification of several shortcomings of their representativeness as elementary beach descriptors. In this paper, we analyse the parametric classification of beach morphodynamic state in a set of six embayed beaches in southwestern Portugal, exposed to diverse conditions, from high-energy (dissipative to intermediate) to low-energy (intermediate to reflective) conditions. Applicability of parametric approaches considered within the dimensionless space defined by Ω (dimensionless fall velocity) and RTR (relative tidal range) according to averaged wave, tide and sediment characteristics of beaches, was assessed in association with a probabilistic analysis, implemented through a Bayesian network model, that considered the full range of wave, tide and sediment conditions at each site. Both parametric approaches were compared to field-based beach state classification implemented using a novel hierarchical framework for beach state analysis. The classification obtained within a probabilistic framework provided an innovative approach for analysis of beach state and mobility, extending the insights on beach morphodynamic behaviour obtained from averaged environmental parameters. Reflective to lower-intermediate beach conditions showed better agreement with parametric approaches, while poor beach state differentiation was achieved for intermediate beach types. Limitations in the application of beach classification models result from (*i*) an inadequacy of existing beach state types in differentiating beaches, particularly within the intermediate domain and for geologically controlled embayed beaches, and (*ii*) shortcomings involved in the parametric approaches. The beach state models disregard the major role of geological control in embayed beach morphodynamic behaviour (in modulating beach shape and segmentation, influencing sediment size and availability, causing alongshore variations

in the wave field and creating topographically induced nearshore circulations). Existing beach state models are unable to adequately represent the widely variable conditions observed in embayed beaches.

KEYWORDS: beach state models, probabilistic statistics, morphodynamic parameters, geological control, mesotidal, wave-dominated beaches

2.1 INTRODUCTION

Morphodynamic classification of beach states based on the parameterization defined by the dimensionless fall velocity Ω, given by

$$\Omega = H_b / (W_s T_p) \quad (2.1)$$

where H_b is breaking wave height, W_s is the sediment fall velocity and T is the wave period, according to the beach state model Wright and Short (1984), afterwards integrated with the relative tidal range RTR, given by

$$\mathrm{RTR} = TR/H_b \quad (2.2)$$

where TR is the tidal range, proposed in the beach state model of Masselink and Short (1993), has achieved widespread usage (Jackson *et al.*, 2005, Scott *et al.*, 2011). These parameterizations have, generally, been favoured over other parameters frequently employed to differentiate beach states, particularly the surf scaling parameter (Guza and Inman, 1975), given by

$$\varepsilon = (a\sigma^2)/(gT^2 tan^2\beta) \quad (2.3)$$

where a is the incident wave amplitude ($H_b/2$), σ is the incident wave radian frequency ($2\pi/T$), g is the acceleration due to gravity and β is the beach slope. The reason for such preference resides in the documented inability of the surf scaling to differentiate between intermediate beach states (Bauer and Greenwood, 1988). Shortcomings of both the Wright and Short (1984) and Masselink and Short (1993) models have also received increased attention (c.f. Anthony, 1998; Masselink and Pattiaratchi, 2001; Jackson *et al.*, 2005), and some have suggested (Scott *et al.*, 2011) that a universal morphodynamic beach classification model may not exist. Nonetheless there has been a steady increase in their application in coastal research (Fig. 2.1), as there is a clear demand to categorize beach states within a common framework for beach behaviour comparisons.

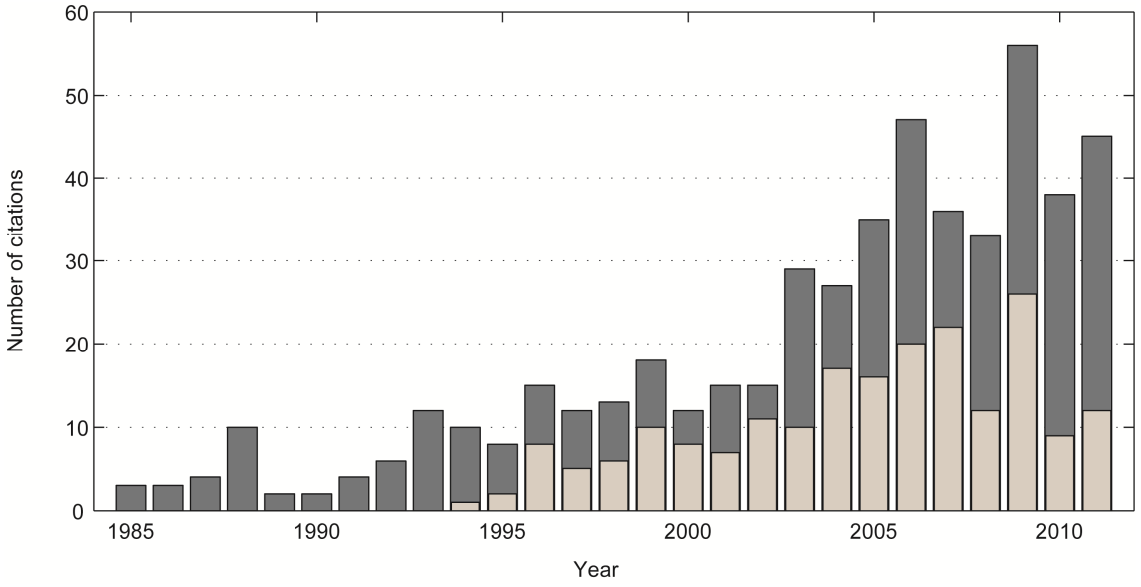

Figure 2.1 Yearly citations for Wright and Short (1984) (dark grey) and Masselink and Short (1993) (light grey) morphodynamic beach classification models based on Thomson Reuters ISI Web of Knowledge (V5.5) checked on 23/02/2012.

Rigid uses of the averaged Ω and RTR values have, however, been progressively discussed, as several factors have been shown to constrain the ability of the parametric approach to characterise beach states, including reduced discriminatory ability (*e.g.* Wright *et al.*, 1985), geological control (*e.g.* Jackson *et al.*, 2005), beach variability (*e.g.* Costas *et al.*, 2005), or local wave climate variability (*e.g.* Gómez-Pujol *et al.*, 2007).

For any given beach, the modal or mean value of the dimensionless parameter Ω, only indicates the prevailing combination of hydrodynamic and sedimentary conditions and the parametric beach state towards which a beach would eventually change, but it does not necessarily indicate the prevailing beach state (Short, 1987). A similar reasoning can be applied for RTR. Furthermore, the range of temporal variability in state and morphology for any given beach is equally important, and, possibly more informative than the average properties (Wright *et al.*, 1985). Overfocusing on parametric modal beach state implies that other, possibly more important aspects of beach morphology, including parameters that represent beach form, can be overlooked.

Despite wide recognition that geological inheritance and control have a major impact in beach morphodynamics (Short and Masselink, 1999; Klein and Menezes, 2001; Benedet *et al.*, 2004; Jackson *et al.*, 2005; Short, 2006; Jackson and Cooper, 2009; Short, 2010; Scott *et al.*, 2011), affecting beach morphodynamic classification (*c.f.* Jackson *et al.*, 2005), parametric approaches to beach morphodynamic state are large insensitive to geological control yet often applied in geologically constrained settings without further discussion. For an embayed coast, variables such as headland spacing, bay shape, wave obliquity, indentation ratio, nearshore morphology and substrate control are of primary importance in determining beach morphodynamic type

and behaviour (Roy and Stephens, 1981; Klein and Menezes, 2001), yet these remain absent from most beach morphodynamic classification studies and their influence is often disregarded.

Naturally, parameterization is important if one wishes to depart from a purely descriptive framework to analyse beach state. Empirical models have been shown to have some predictive skill (*e.g.* Plant *et al.*, 2006), offering a pragmatic alternative to limitations of process-based morphodynamic models (*c.f.* Cooper and Pilkey, 2004, 2007, 2008; Pilkey and Cooper, 2007). So far no other empirical approach to beach morphodynamic state classification has achieved wider applicability than the use of Ω. Acknowledging that there is uncertainty in the calculation of any parameter, and that a single value for any parameter is not a universal descriptor of beach characteristics (Bauer and Greenwood, 1988; Anthony, 1998), we explore and analyse the parametric classification of beach morphodynamic state defined by Ω and RTR in embayed beaches. Here, we take a probabilistic approach to beach morphodynamics that, although suggested initially by Wright and Short (1984) with the use of beach state histograms, has rarely been incorporated in the morphodynamic classification of beaches. A notable exception is the work of Gómez-Pujol *et al.* (2007) and further exploration by Jiménez *et al.* (2008).

Considering the full range of wave, tide and sediment conditions observed and modelled from a set of embayed beaches exposed to diverse conditions, from high-energy dissipative to intermediate conditions and low-energy intermediate to reflective conditions, we implement a probabilistic model to perform an assessment of beach morphodynamic state and mobility within the dimensionless space determined by Ω and RTR. The probabilistic distribution is then compared to the observed beach states and the single averaged parametric modal state. The overall aim is to explore the influence

of joint probability of beach states as opposed to the classical use of modal beach state, and to assess the applicability of parametric classification of morphodynamic state in geologically controlled embayed beaches exposed to contrasting environmental conditions. The paper is organized as follows. Section 2.2 provides a brief overview of the study sites setting, with an emphasis on hydrodynamic conditions and variability in the southwestern Portuguese coast. The Bayesian probabilistic model description and implementation are detailed in Section 2.3, followed in Section 2.4 by the exposition of the framework for observed beach state classification. Section 2.5 presents the results of the parametric probabilistic and single averaged value approaches and compares both with observed states at the study sites. The use of parametric beach state classification in embayed beaches is discussed in Section 2.6 and the conclusions are presented in Section 2.7.

2.2 STUDY SITES

The present assessment is performed with data from six embayments located along the rocky coastline of the southwestern coast of Portugal (Fig. 2.2), where topographic and sedimentary beach monitoring was performed over a period of two years from September 2007. The beaches are located in two clusters; the western one includes intermediate to dissipative beaches, while the southern cluster includes intermediate to reflective beaches. Western facing beaches (Amoreira, Mt. Clérigo and Arrifana) are fully exposed to the North Atlantic swell and storms and therefore experience a high-energy wave climate, with a marked oceanographic seasonality. Mean significant wave height ranges between 1.5 and 2 m and average peak period between 9 and 13 s for summer and winter periods, respectively. Waves reach this section of the

coastline mostly from the north-westerly quadrant (Costa and Esteves, 2010) (Fig. 2.2); yet nearly complete refraction of ocean swell renders most of these embayed beaches swash aligned.

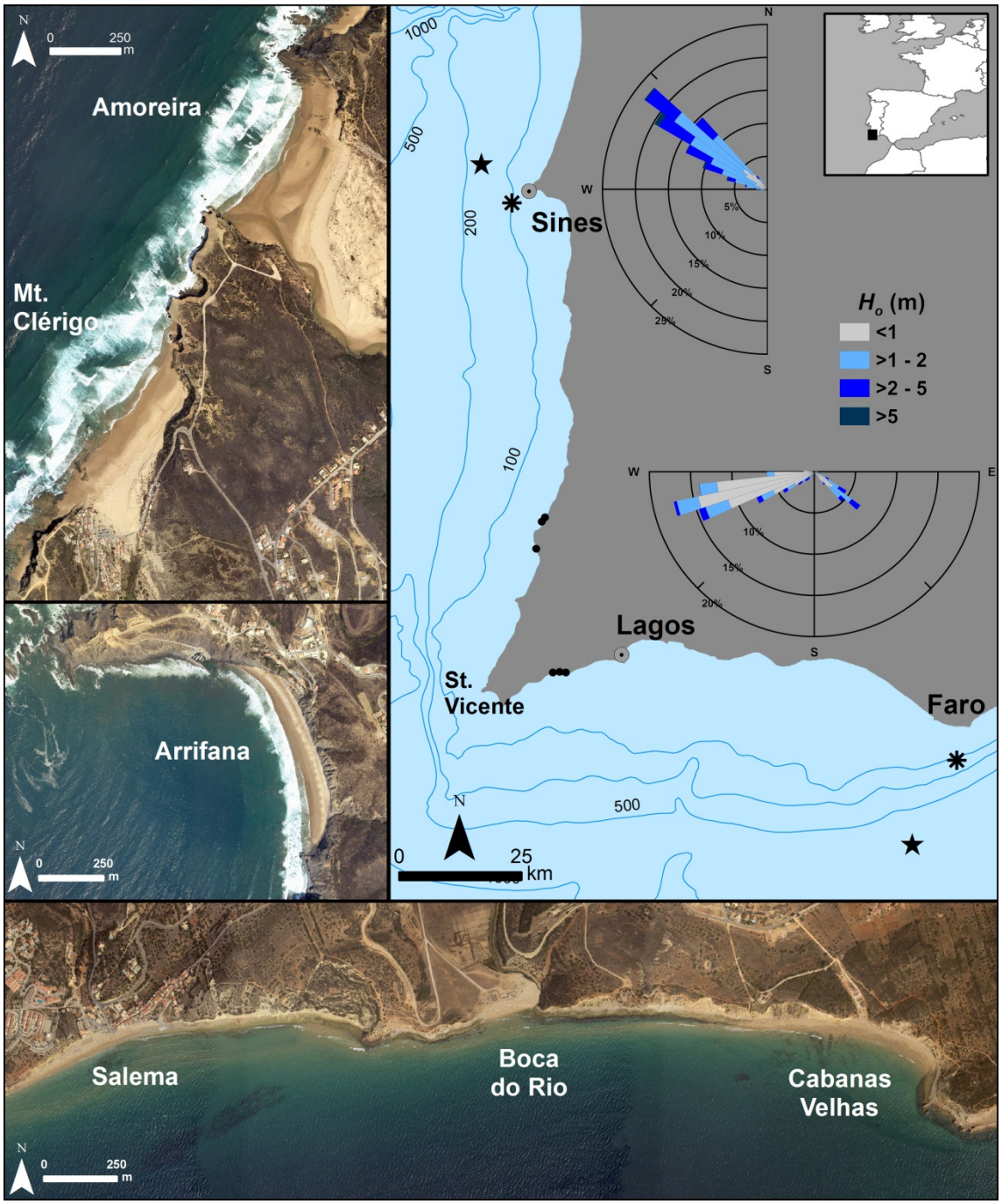

Figure 2.2 Geographic location and aerial view of the study sites (indicated by black circles in the map). Location of directional wave buoys, modelled WANA wave grid points and tide gauges indicated by asterisks, stars and doted circles, respectively. Wave roses for Sines and Faro computed from wave buoy data (asterisks in location image), from 2007 to 2009.

Southern facing beaches (Salema, Boca do Rio and Cabanas Velhas) are relatively sheltered from the full impact of the North Atlantic, experiencing attenuated swell waves combined with waves generated from SE winds across the Gulf of Cadiz. Offshore wave conditions are moderate, with mean wave heights around 0.9 m and peak periods of 8 s, experiencing only slight variations between summer and winter conditions. Dominant waves reach this southern coast from the south-westerly quadrant, yet shorter period south-easterly waves account for roughly a quarter of occurrences (Costa *et al.*, 2001) (Fig. 2.2). This oceanographic setting imposes a more complex bimodal wave climate on the southern coast embayments. Tide conditions along both sections of the coastline are identical and synchronous and characterized by a mesotidal, semi-diurnal regime with maximum spring tidal range around 3.5 m.

2.3 BAYESIAN PROBABILISTIC MODEL

Use of Bayesian probabilistic analysis has increased dramatically (Berger, 2000), and within coastal science several recent studies have highlighted its potential to address diverse issues in coastal morphodynamics. These include extreme wave analysis (*e.g.* Scotto and Guedes Soares, 2007; Sánchez-Arcilla *et al.*, 2008), modelling of surf-zone processes (*e.g.* Plant and Holland, 2011a, 2011b), coastal vulnerability to sea level rise (*e.g.* Gutierrez *et al.*, 2011), coastal evolution (*e.g.* Yates and Le Cozannet, 2012) and also cliff erosion (*e.g.* Hapke and Plant, 2010). Most of these studies use a condensed number of variables, reducing the dimensionality of the problem to be analysed. The variables are treated as conditional probability functions that are then combined by means of causal relationships within the Bayesian network in order to derive joint probability distributions of specific outcomes (Hapke and Plant, 2010;

Gutierrez *et al.*, 2011). Frequently, the conditional probabilities for the variables are obtained from assimilation of hundreds to thousands of observed or modelled cases, but they can also be derived from climatology, user-defined and parametric distributions. Bayesian networks are multi-dimensional implementations of Bayes theorem (Bayes, 1763), relating the probability of one event R given the occurrence of another event O according to:

$$p(R_i|O_j) = p(O_j|R_i)\ .p(R_i) / p(O_j) \tag{2.4}$$

Concisely, the left-hand term of Eq (2.4) is the updated conditional probability of a particular response (R_i) given a set of observations (O_j). The first right-hand term, $p(O_j|R_i)$, is the likelihood of the observation if the response is known, while the second term, $p(R_i)$, is the prior probability of the response and the last term, $p(O_j)$, is a normalization factor to account for the total likelihood of the observations (a concise review of Bayes theorem is provided by Plant and Holland (2011a)).

2.3.1 Model implementation

In this study, we implement a Bayesian network to calculate the joint probability distributions of Ω and RTR for each individual beach, determined by the specific distributions of the input variables. The Bayesian network was constructed using the Netica software package (Norsys, 1992-2011) and consists of a set of variables, or nodes, that are causally related. Our network uses six variables, divided into beach state drivers and response variables. Breaker height (H_b), peak period (T_p), sediment fall velocity (W_s) and tidal range (TR) are the variables included in the formulations of Ω and RTR and, therefore, considered as the beach state drivers, while the two parameters,

Ω and RTR, are the response variables. A schematic diagram of the Bayesian network demonstrating the parametric morphodynamic classification of beaches based on Ω and RTR is shown in Fig. 2.3. The design of the Bayesian network reflects the parametric approximation to beach morphodynamic classification and, therefore, this approach is not aimed at identifying all the possible relations between the variables nor does it attempt to include all the possible variables that may influence beach morphodynamics. Only the relations and variables that represent the parametric empirical approximations to beach morphodynamic state are considered.

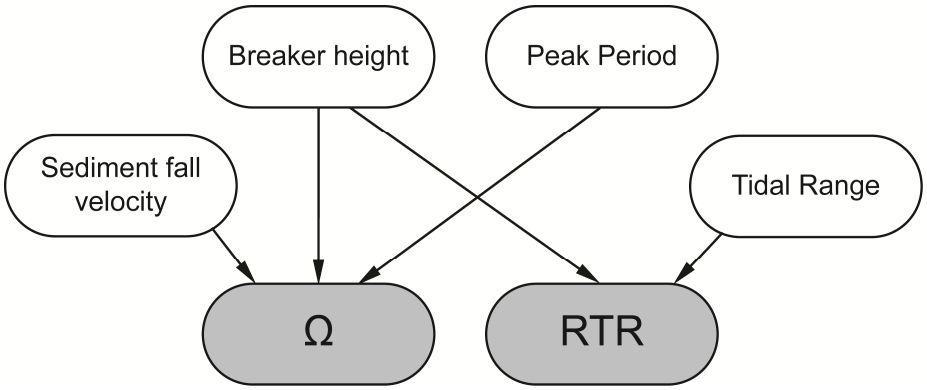

Figure 2.3 Schematic diagram of a Bayesian network for parametric beach morphodynamic classification

To implement the Bayesian network the variables, although they are continuous, had to be discretized according to user-defined bins (described in detail in the data section). The bin widths for the beach state drivers are variable and were selected in order to represent the commonly used environmental ranges of wave, tide and sediment classifications, while also attempting to contain uncertainty in the data itself. The response variable Ω was discretized according to the classification of Wright and Short (1984) considering the mean equilibrium values of Ω for each beach state (Wright *et al.*, 1985; Short, 1987), while the boundaries defined in the classification of Masselink and

Short (1993) were used for defining bin boundaries for RTR. The vectors connecting the beach state drivers and the response variables indicate the unidirectional causal relationships that are required to calculate the joint probability distribution of Ω and RTR according to the direct application of their respective formulations. In addition to the joint conditional probability, the mean or expected value (μ) of each variable (x) weighted by their respective probability distribution $p(x)$ was also determined, which for continuous variables is given by:

$$\mu = \int_{-\infty}^{\infty} x\, p(x)\, dx \tag{2.5}$$

When implementing equations for determining joint probabilities for continuous variables in the Bayesian network, it is necessary to identify the location within each bin to evaluate the equation. Such evaluation is done at random positions for each bin, with higher accuracy for increasing sampling numbers (Norsys, 1992-2011). Preliminary evaluation of the joint probabilities with sampling ranging from 10^2 to 10^6 random positions within each bin indicated that evaluation with 10^4 random sampling positions minimized differences in probability to values lower than 0.001, and this value was used throughout.

2.3.2 Data set

2.3.2.1 Wave forcing

Wave data used to obtain the distributions of H_b and T_p was derived from nearshore propagation of offshore wave conditions registered between September 2007 and September 2009 at Sines and Faro Buoy for the west and south coasts, respectively (see Fig. 2.2 for location). Both buoys are located roughly 7 km from shore in

approximately 100 m water depths, and provide records of offshore significant wave height, peak spectral period and peak wave direction. Missing records in the measured wave record during the two year monitoring period (≈15/5% in Sines/Faro) were filled using modelled wave data from neighbouring grid points of the WANA deepwater network (Lahoz and Albiach, 2005) (Fig. 2.2). Transference of offshore wave data to breaking conditions at each embayment was undertaken with the numerical wave model SWAN (Booij *et al.*, 1999), using a nested modelling scheme initialized at offshore boundaries with the parametric input from the wave buoy time series. Details of the SWAN implementation and bathymetric grids can be found in Loureiro *et al.* (2012) and the main specifications are provided in Table 2.1.

Table 2.1 Specifications of SWAN inplementation

Nesting Scheme	3 regular grids (offshore/intermediate/nearshore)
Grid resolutions	100 m / 20 m / 10 m
Wave spectral shape	JONSWAP
Physical processes	refraction diffraction non-linear triad wave-wave interaction bottom friction (JONSWAP variable) depth induced breaking (γ = 0.78)
Breaking location	first bin exceeding 1% of depth induced breaking

In order to balance computational effort and required accuracy, two levels of simplification where considered for the wave modelling:

(i) The wave propagation was performed using daily averages instead of the complete series with records every three hours or half-hourly during storms (significant wave height ≥ 5/3 m in the west/south coast).

(ii) For each simulation a single value of H_b and T_p was obtained by averaging alongshore the values of the 10 m cells fronting the beach that matched the breaking location definition.

Given the wide variation in breaking conditions for the study areas, bin widths of 0.5 m and 2 s were assigned for H_b and T_p distributions, respectively. The discretization of the variables has to be optimized in order to provide meaningful distributions while containing the uncertainties in observational and model data (Plant and Holland, 2011a), and the proposed bin widths are wide enough to absorb inaccuracy in modelling yet still able to represent differentiation of wave conditions.

2.3.2.2 Tidal range

Maximum daily tidal ranges for the duration of the monitoring period were computed from the observed tide records at Sines and predicted tide records at Lagos, for west and south coast beaches, respectively (see Fig. 2.3 for gauge location). Given the similarity of tide conditions for southern Portugal and proximity between embayments, no alongshore interpolation was deemed necessary. Bin widths of 0.5 m were implemented for discretizing this variable, providing a more comprehensive distribution than the commonly used classification of Davies (1964) separating tide ranges in micro-tidal (< 2 m), meso-tidal (2-4 m) and macro-tidal (> 4 m), as this strict division has been found inadequate in beach morphodynamic classification (Short, 1991).

2.3.2.3 Sediment fall velocity

Seasonal sediment sampling was conducted in all beaches twice a year. Samples were collected in March, after the most intense storm activity period and then again at the end of the summer season, in September. Sampling was performed along three cross-shore beach profiles in each embayment, and samples collected along existent morphologies of the intertidal beach, including berm, beach face, and low-tide terrace. A total of 40 to 60 samples was obtained from each beach and sediment fall velocity of each sample was computed according to Soulsby (1997) using the median grain diameter (d_{50}).

From the complete distribution of sediment fall velocities for each beach, percentages of occurrence were determined for classes discretized according to the thresholds of the Udden-Wenthworth sediment classification (Blott and Pye, 2012), after conversion of the grain size thresholds to sediment fall velocity values. A further division separating medium sand ($0.03 \geq W_s < 0.07$) in two bins at 0.04 m/s was included to provide higher discrimination at this class, as medium fine sand ($0.03 \leq W_s < 0.04$) was found to dominate sediment distribution at most sites.

2.4 FIELD CLASSIFICATION OF BEACH STATE

To provide a basis for evaluating parametric beach state classification, either by the probabilistic or single averaged value approaches, beach states were independently and non-parametrically classified into the morphodynamic beach states devised by the Wright and Short (1984) and Masselink and Short (1993) models. Several studies compared parametric and observed states, mostly inferring beach state through the use of expert visual observation, interpretation of beach imagery and cross-shore beach

profile data (*e.g.*, Wright *et al.*, 1985; Ranasinghe *et al.*, 2004; Jackson *et al.*, 2005; Sénéchal *et al.*, 2009). While determining observed beach state comprises some degree of subjectivity, by combining the aforementioned information sources in a structured framework, it is possible to assign beach states with confidence. Grounded on the basic premises of the morphological classification procedures of Lippmann and Holman (1990) and Ranasinghe *et al.* (2004), beach types can be fundamentally distinguished at the field based on bar morphology, profile geometry, and alongshore variability. Accordingly, a classification framework for each beach state model was derived (Fig. 2.4) and used to define observed beach state using topographic data collected at each embayment along with digital imagery (procedures of data collection are provided in Loureiro *et al.*, 2012).

The hierarchical classification framework proposed here assumes the presence or absence of the inner bar to be the primary descriptor of observed beach state. Following Lippmann and Holman (1990) the presence of outer bar or multiple offshore bars is disregarded. When an inner bar can be identified, the classification further considers the presence/absence of a continuous trough separating the inner bar from the lower beach section, distinguishing between attached and detached conditions. The latter generally occur in higher intermediate beach types, while attached bars are common for the lower intermediate beach types. Profile geometry is then evaluated, with three basic configurations distinguishing steep, flat and composite profiles. The latter occur when there is a clear break in slope between the higher and lower intertidal sections of the beach profile. Alongshore variability is the final beach descriptor, and is used here to differentiate between intermediate beach types with common bar and rip characteristics. Within this classification, alongshore variability is expressed by the presence of rip current and/or feeder channels within the lower section of the beach

profile and beach cusps at approximately high-tide level. The hierarchical classification frameworks of Wright and Short (1984) and Masselink and Short (1993) were applied for each survey completed during the monitoring period (20 surveys on the west coast beaches and 32 on the south coast beaches), and used to calculate observed beach state frequency distributions for each embayment.

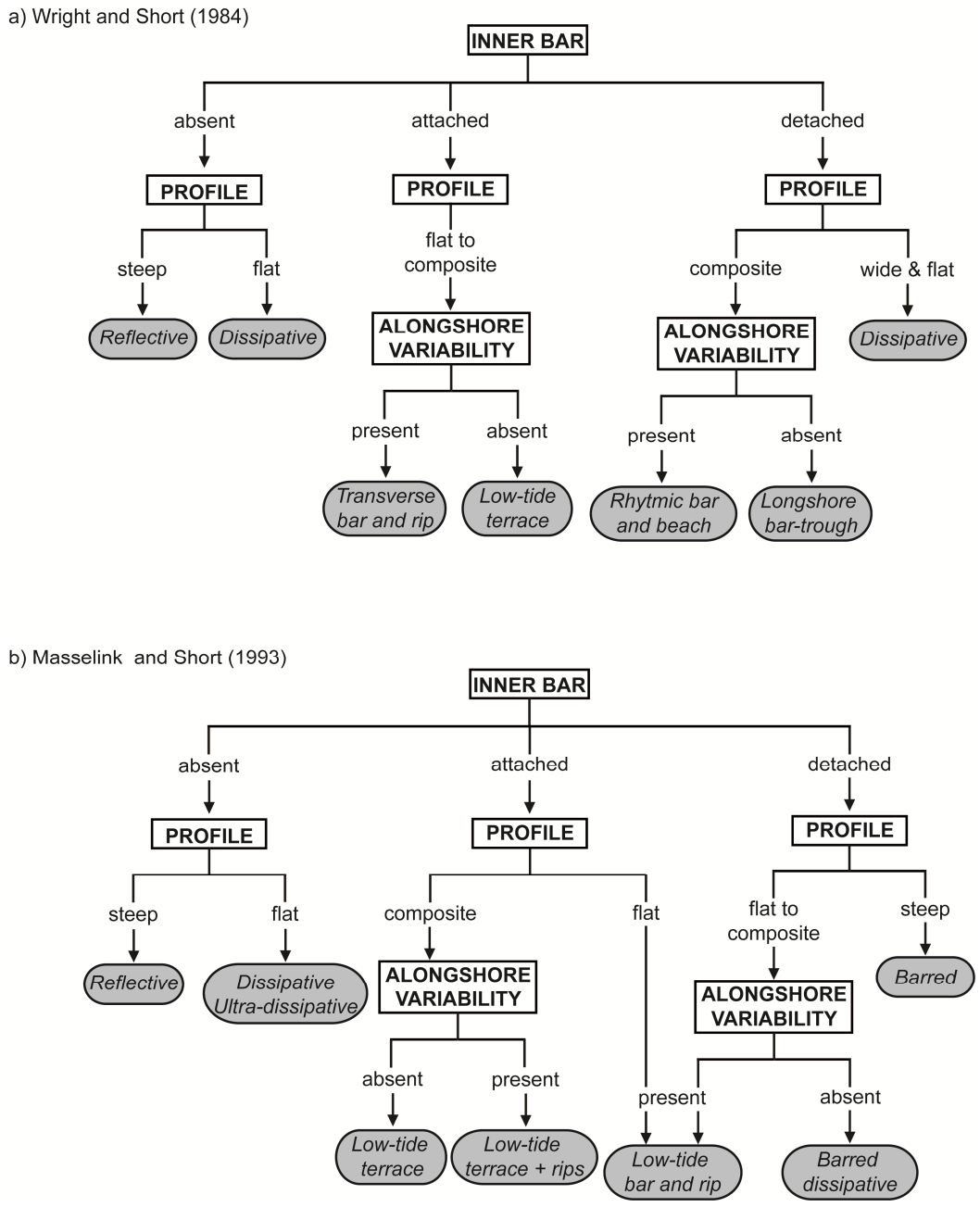

Figure 2.4 Hierarchical frameworks for field based classification of beach states according to a) Wright and Short (1984); and b) Masselink and Short (1993) models of beach morphodynamic state.

2.5 RESULTS

Once the Bayesian network was implemented and compiled with the input variables distribution for each embayment, a joint probability distribution for the response variables for each beach was obtained, termed the 'prior distribution' (Fig. 2.5 and 2.6). The prior distribution captures the broad range of conditions that occur in the input variables, implying that, for these sites, the beaches could range along all the possible states presented by the beach morphodynamic classifications, although with widely diverse likelihoods.

Conditions for west coast embayments are generally similar in terms of hydrodynamic forcing (Fig. 2.5a-i), with noticeable differences only in terms of breaker height distribution in Arrifana (Fig. 2.5c), which is skewed towards lower values. Breaking wave heights are below 1 m for roughly 60% of the distribution in Arrifana, while in Amoreira and Mt. Clérigo such low waves barely represent 20%. Sediment fall velocity distributions (Fig. 2.5j-l) show only noteworthy differences regarding the less representative classes, as medium fine sand ($0.03 \leq W_s < 0.04$) represents more than 70% of sediment distributions for the west coast embayments.

An immediate outcome of the prior distribution of Ω in these three embayments (Fig. 2.5m-o) is that reflective conditions ($\Omega \leq 1.5$) are very unlikely ($P < 8\%$) for Amoreira and Mt. Clérigo and, despite being higher ($P < 16\%$), are still relatively unlikely in Arrifana, as would be expected in an energetic environment with medium to fine sand beaches. The prior distribution further highlights that the outcome with the highest probability for Ω is identical in Amoreira and Mt. Clérigo ($\Omega > 5.5$ which represents dissipative conditions). It is worth mentioning that the entire range of intermediate conditions ($1.5 \leq \Omega \leq 5.5$) amounts to probabilities above 65%, suggesting that most of the time west coast beaches are likely to be wavering between intermediate

states, with a clear prevalence for lower intermediate conditions in Arrifana ($P(1.5 \leq \Omega \leq 2.8) = 35\%$). The prior distribution of RTR indicates a high likelihood of wave-dominated conditions (Fig. 2.5p-r), particularly noticeable at Amoreira and Mt. Clérigo ($P > 85\%$), but still substantial at Arrifana ($P = 68\%$).

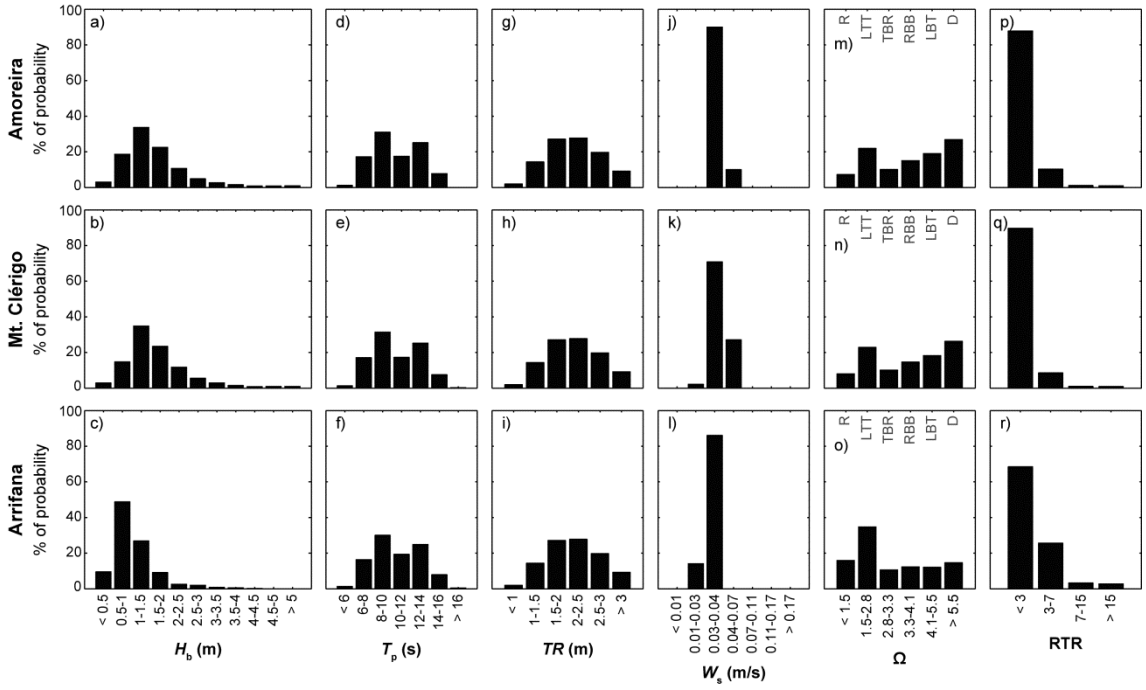

Figure 2.5 Prior probability distributions for the variables in the Bayesian networks for west coast embayments. Beach states as defined by Wright and Short (1984): R - reflective; LTT – low-tide terrace; TBR – transverse bar and rip; RBB – rhythmic bar and beach; LBT – longshore bar-trough; D - dissipative.

Similar to the west coast, hydrodynamic conditions are identical amongst the three beaches on the south coast (Fig. 2.6a-i). Breaker heights display the only perceptible difference, with a more uniform distribution between the two lower classes in Cabanas Velhas (Fig. 2.6c), each representing around 40% of the distribution. Nevertheless, for all south coast embayments, low energy breaking conditions ($H_b < 1$ m) represent more than 80% of the distribution. Slightly coarser sediments are found in Boca do Rio beach, with medium coarse sand ($0.04 \leq W_s < 0.07$) representing more than

60% of the distribution of sediment fall velocity, along with inexpressive percentages of coarse sand and gravel, which, nevertheless, only occur at Boca do Rio embayment (Fig. 2.6k).

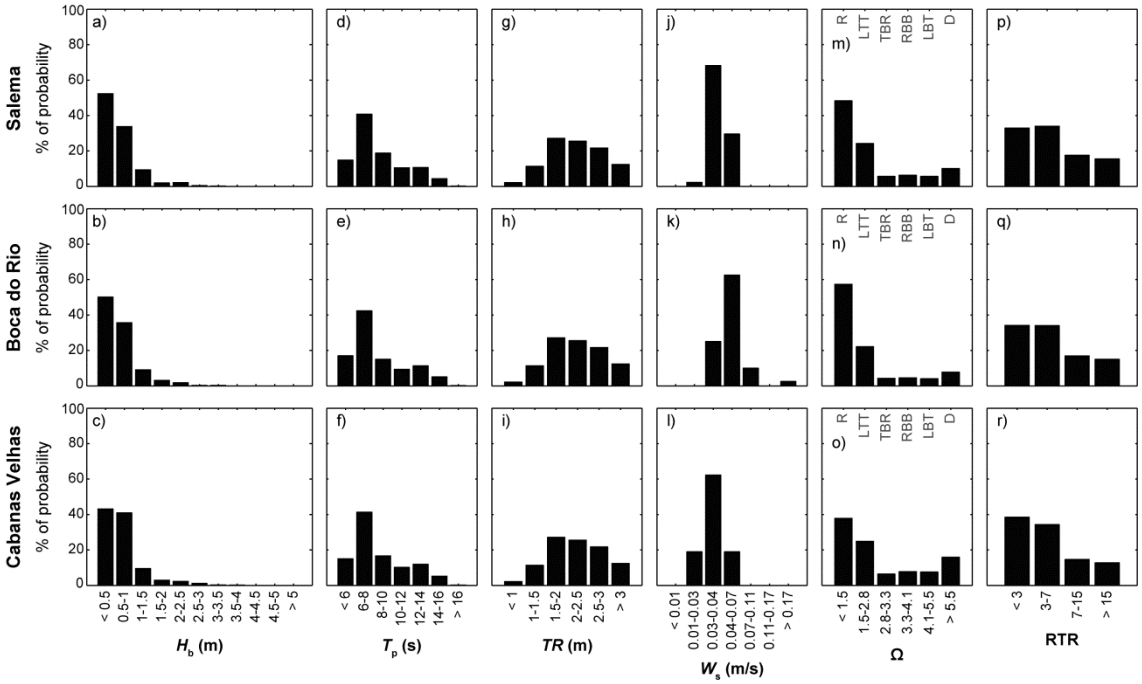

Figure 2.6 Prior probability distributions for the variables in the Bayesian networks for south coast embayments. Beach states as defined by Wright and Short (1984): R - reflective; LTT – low-tide terrace; TBR – transverse bar and rip; RBB – rhythmic bar and beach; LBT – longshore bar-trough; D - dissipative.

The prior probability distribution of Ω in south coast embayments (Fig. 2.6m-o) explicitly indicates reflective conditions as the most likely in all three sites. Nonetheless, likelihoods diverge between embayments, with P ($1.5 < \Omega$) increasing from 38% in Cabanas Velhas, to 48% in Salema and finally reaching 57% in Boca do Rio. Dissipative conditions are unlikely in all south coast embayments ($P(\Omega > 5.5) <$ 16%), while intermediate conditions are dominated in the three beaches by the lower intermediate class ($P(1.5 \leq \Omega \leq 2.8) > 22\%$). RTR prior distribution indicates similar likelihoods ($P \approx 35\%$) for wave-dominated (RTR < 3) and mixed wave-dominated (3 ≤

RTR ≤ 7) conditions in south coast beaches (Fig. 2.6p-r), further specifying that higher RTR values are unlikely ($P \approx 15\%$).

Alongside the prior distribution inspection, we examined the agreement between the prior probabilities of beach states predicted using the Bayesian network and the frequency of observed beach states for the duration of the monitoring period (Fig. 2.7 and 2.8). In addition, the parametric single averaged values of Ω and RTR were also determined using the mean hydrodynamic and sedimentary characteristics for each beach and assessed in conjunction with the mean probabilistic weighted value for both parameters (Fig. 2.7 and 2.8; Table 2.2)

Dispersion amongst four to five beach states based on Ω values was observed in west coast embayments (Fig. 2.7a-c), as generally suggested by the prior distribution. There is, however, significant divergence between the class with higher likelihood in the prior distribution and the most frequently observed state. Transverse bar and rip state occurrence rates are above 50% in Amoreira and Mt. Clérigo, ranking just below that value in Arrifana (48%), yet the prior distribution indicates a reduced likelihood for this state ($P(2.8 \leq \Omega \leq 3.3) < 11\%$). In general, intermediate conditions are under predicted by the Bayesian network for west coast beaches, with probabilities for these states around 65%, while observed frequencies range from 70% in Arrifana, 80% in Mt. Clérigo and 90% in Amoreira. Agreement between the prior distribution of Ω and observed states for south coast embayments is significantly more successful, and the most likely state predicted for the three embayments, indicative of reflective conditions, is matched in terms of observations (Fig. 2.7d-f). Furthermore, the ranking between the two most frequently observed and more likely states is also coincident, although the exact values of frequency of occurrence and probability may differ by up to 15%. A

peak at observed longshore bar-trough state in Boca do Rio is not matched in terms of prior probability (Fig. 2.7e).

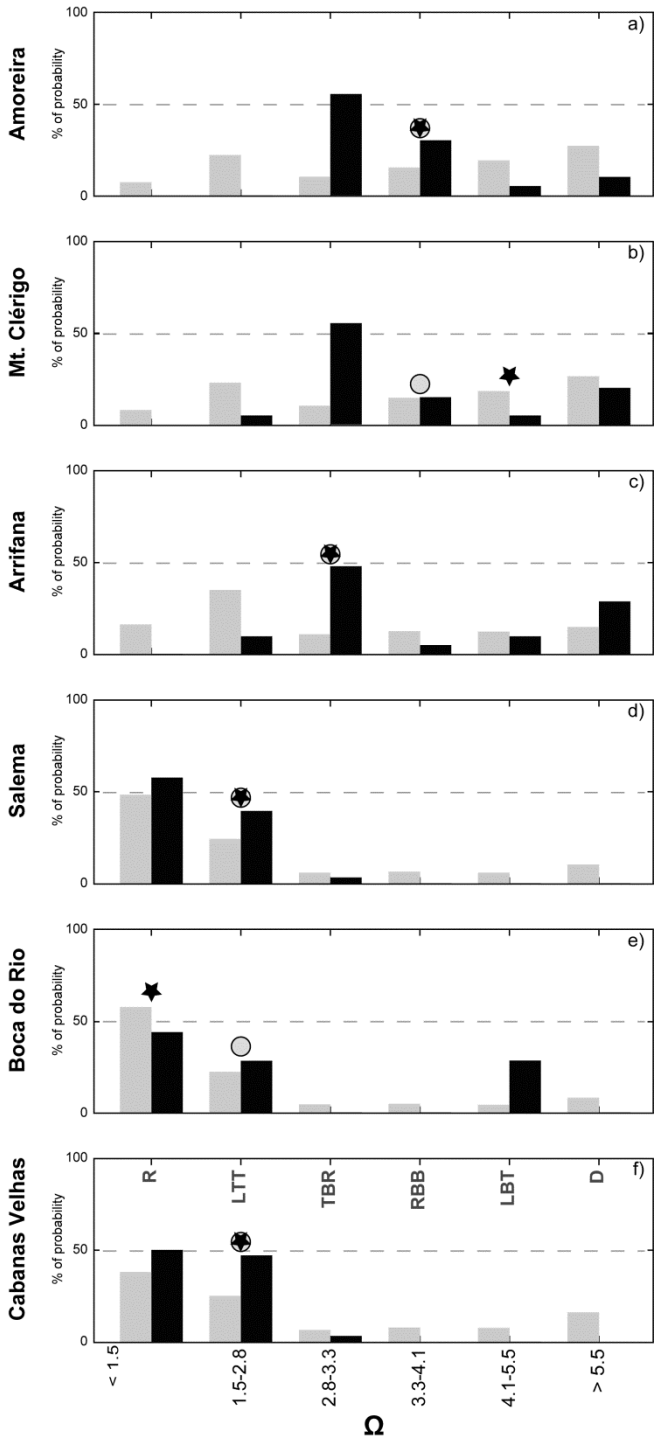

Figure 2.7 Prior probability distributions of Ω (light grey) and observed beach state histograms (black) according to Wright and Short (1984) beach states. Stars indicate the beach state determined by Ω single averaged value calculation and circles the beach state determined by the mean probabilistic weighted value.

Table 2.2 Mean beach hydrodynamic and sediment characteristics and parametric classifications (single averaged value – *sv* – and probabilistic weighted mean – μ)

Embayment	H_b (m)	T_p (s)	*MSR* (m)	D_{50} (mm)	W_s (m/s)	Ω (sv)	RTR (sv)	Ω (μ)	RTR (μ)
Amoreira	1.60	10.5	2.90	0.307	0.038	4.01	1.81	3.96	2.11
Mt. Clérigo	1.65	10.5	2.90	0.307	0.038	4.14	1.76	3.90	2.04
Arrifana	1.04	10.6	2.90	0.273	0.033	2.97	2.79	3.12	3.18
Salema	0.61	8.4	2.85	0.308	0.039	1.86	4.67	2.18	7.07
Boca do Rio	0.63	8.4	2.85	0.427	0.057	1.32	4.52	1.88	6.92
Cabanas Velhas	0.69	8.5	2.85	0.287	0.035	2.32	4.13	2.64	6.31

Consideration of beach state within the two-dimensional space determined by Ω and RTR following the classification of Masselink and Short (1993) reveals that west coast beaches, Amoreira, Mt. Clérigo and Arrifana, are parametrically positioned within the barred intermediate beach type (Fig. 2.8), given mean values of RTR below 3 and Ω values ranging between 2 and 5 (Table 2.2). Mean probabilistic weighted values closely follow the single averaged value classification, yet the most frequent observed beach states generally differs between the two approaches. Only for Arrifana is there agreement between observed beach state and the mean probabilistic weighted value, although considerable dispersion of observed beach states at this embayment precludes the clear definition of a modal beach state. Observed beach states for the west coast embayments positioned in the parametric wave-dominated domain (RTR < 3) represent only 15 to 25% of observations (corresponding to the barred dissipative state) despite the generally energetic conditions experienced along this stretch of coastline. Significant profile variability and frequent intertidal bar and rip morphology, induce low-tide terrace with rips and low-tide bar and rip states on more than 50% of observations for the three west coast beaches.

The second group of beaches, Salema, Boca do Rio and Cabanas Velhas, is positioned towards the lower intermediate beach conditions, yet the parametric approaches are unable to clearly identify the prevalence for reflective beach states observed for the south coast beaches (Fig. 2.8). Agreement between the single averaged values of RTR with the respective mean probabilistic weighted values is lower than exhibited for west coast beaches, as the probabilistic approach is clearly displaced to higher RTR values (Table 2.2). This positioning does, however, appear to reflect the dispersion between reflective to low-tide terrace states observed in the beaches.

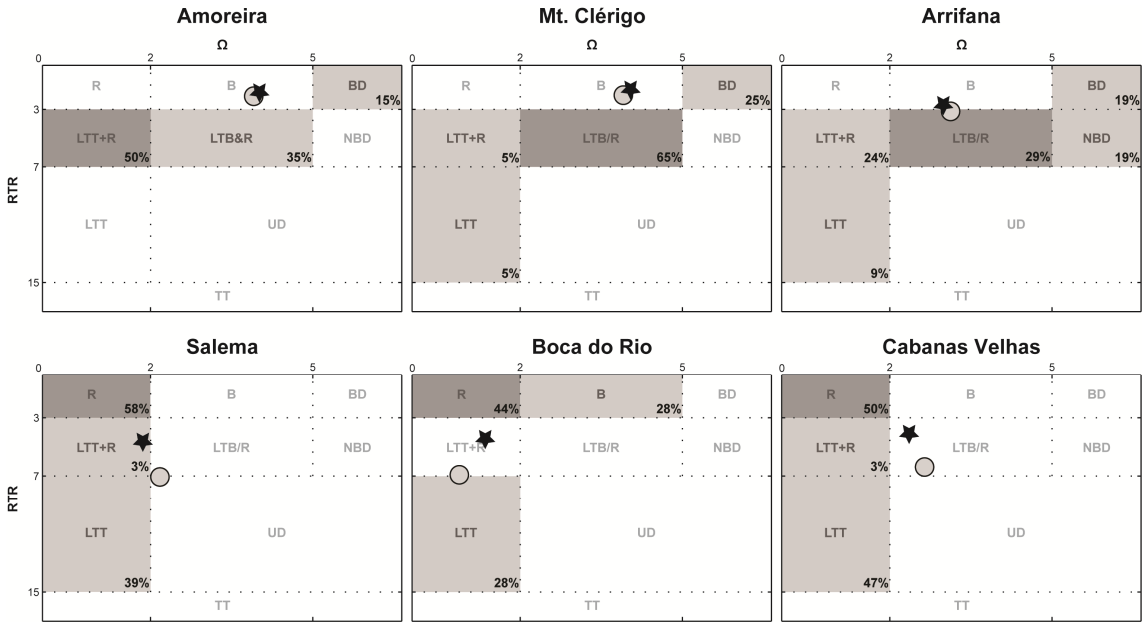

Figure 2.8 Beach state classification within the dimensionless Ω - RTR space according to Masselink and Short (1993). Observed beach states and frequency (grey rectangles) with modal state indicated by darker shading. Stars indicate the beach state determined by single averaged value calculation and circles the beach state determined by the mean probabilistic weighted value. Beach types as defined by Masselink and Short (1993): R - reflective; B - barred; BD - barred dissipative; LTT+R – low-tide terrace + rip; LTB/R – low-tide bar/rip; NBD – non-barred dissipative; LTT – low-tide terrace; UD – ultra-dissipative; TT – transition to tidal flats.

2.6 DISCUSSION

Parametric classification of beach morphodynamic state approached classically, according to the averaged and static representation of beach environmental parameters following the models of Wright and Short (1984) and Masselink and Short (1993), was here paralleled by a probabilistic approach designed to incorporate the full range of wave, tide and sediment conditions experienced on a set of embayed beaches. Both approaches showed agreement difficulties when compared with conditions observed on the beaches. A comparative assessment of the two approaches will constitute the initial part of this section, followed by a more general discussion of the limitations of parametric beach state classifications with an emphasis on embayed beaches.

2.6.1 Modal values and probabilistic distributions in parametric beach classification

Both the single averaged value and the probabilistic approaches to parametric beach state classification presented here share the same underlying assumption: that a simplified mathematical combination of wave, tide and sediment properties can be used to differentiate a sequential combination of beach morphodynamic states. Constraining a beach to averaged values disregards the wide variability of conditions actually experienced (Scott *et al.*, 2011), assuming also that a mean value would indicate a prevailing state, which may not necessarily occur (Short, 1987). Consideration of an extended range of wave, tide and sediment conditions, as demonstrated with the probabilistic model presented here, allows the extension of the parametric approach to beach classification, providing indications of the beach state mobility that is likely to be experienced. For example, when different sediment populations exist, the probabilistic

approach eliminates the necessity of (unrealistically) selecting only one or averaging. Similarly, when wave conditions vary abruptly between low energy conditions and high energy events (*e.g.* Costas *et al.*, 2005), a single average value is likely to be a poor representation of environmental conditions, as is the restriction of tidal range to a single value. However, expanding the approach to include the entire range of wave, tide and sediment conditions observed at a beach is also likely to produce a wide dispersion, as evidenced for west coast embayments. Such dispersion, despite the low agreement with the distinct beach states observed, is still a constructive outcome of a probabilistic approach, as it appropriately indicates that beaches would experience a wide range of states, given widely varying conditions. On the other hand, when conditions are variable, yet within restricted intervals, agreement between probabilistic approaches and observed conditions is improved, as recognized in the two most frequent states and their relative rankings for south coast embayments. This is an encouraging result of the probabilistic approach, and previous investigations of beach type based on Ω values within a probabilistic framework by Gómez-Pujol *et al.* (2007) indicated similar concentration and scatter of probabilistic distributions for reflective and intermediate conditions, respectively. Comparatively, an averaged value, either calculated directly from the mean parameters or obtained from a weighted integration of the probabilistic distribution, as also presented here, provides a very limited, and often meaningful, characterization of a beach (Anthony, 1998). This is evident at the studied embayments, particularly on the west coast sites, as the observed dominant beach states do not coincide with the parametric approaches. Geological constrains may also contribute to the disagreement between observed and parametric beach states, yet it appears to be mostly a result of the inability of an averaged parametric approach to correctly identify the most frequent morphodynamic state.

Consideration of the complete distribution of environmental forcing parameters embodied in the parametric probabilistic approach assumes that beaches respond instantaneously to forcing. Such assumption implies that any combination of environmental parameters would have an immediate morphological response. Several reasons have been presented for disproving this assumption, from the dependence on antecedent beach state (Wright *et al.*, 1985), to the importance of energy levels and event duration (Jiménez *et al.*, 2008) to state variable relaxation time effects (Scott *et al.*, 2011). Site variable response times, particularly within geologically constrained environments (Loureiro *et al.*, in revision), are a further reason for considering that, despite suggested by probabilistic distributions, the full realization of beach states suggested by the combinations of environmental parameters is unlikely to be accomplished in any given beach and, particularly, at embayed ones. Reflective conditions in west coast embayments indicated by probabilistic distributions, although with low likelihood values, cannot be attained as wave conditions never remain low enough for a significant amount of time. Oppositely, reduced duration of energetic conditions in south coast embayments, imply that dissipative conditions suggested by the probabilistic distributions are unattainable. Furthermore, realization of all beach states suggested by the probabilistic distributions is also hindered in embayed beaches due to the constrained morphodynamic variability imposed by the existence of geological constrains to profile mobility (Loureiro *et al.*, in revision) and nearshore hydrodynamic circulation (Loureiro *et al.*, 2012).

2.6.2 Parametric values and beach morphodynamic states

At the onset, comparing parametric and observed beach states considers that individual states can be readily and objectively separated into the types proposed by

beach state models. Previous research has demonstrated that this is not always possible, as beaches are dynamic systems in constant adjustment to environmental forcing. The few beach state discrimination tests available in the literature revealed agreement rates around 75% (Lippmann and Holman, 1990; Ranasinghe *et al.*, 2004), while other studies acknowledge that in some conditions a beach state cannot be classified from observations with certainty (*e.g.* Sénéchal *et al.*, 2009). Although sequential classification frameworks were here devised for classifying observed beach conditions into the states proposed by Wright and Short (1984) and Masselink and Short (1993) models, the differentiation between classes is always problematic and subject to disagreement. For relatively short beaches, as the ones presented here, how much longshore variability separates a LBT from RBB states was a difficulty identified for west coast embayments, and also reported by Sénéchal *et al.* (2009). Identically problematic was the definition of when does the morphologic expression of rips is sufficient to separate a TBR from LTT beach type, or a LTT from a LTT+R in the Masselink and Short (1993) classification. Apart from such difficulties of distinction between beach state types, the adequacy of existing classes is also debatable, as new beach types have frequently been presented (*e.g.* Hegge *et al.*, 1996; Short, 2006; Scott *et al.*, 2011). Classification of Boca do Rio as belonging to a LBT type on 28% of occurrences represents a case where the resolution of the Wright and Short (1984) model is inadequate to correctly typify the beach. The existence of a longshore uniform detached bar, which determines the classification as LBT, does not conform to the conditions described by the authors for this morphotype, which is associated to energetic wave regimes and closer to the dissipative part of the classification (Wright and Short, 1984). A subtidal longshore inner-bar detached from the beach was clearly identified during surveys, but its existence is dependent on geological constraints posed

by subtidal rock outcrops and the maintenance of low energy conditions, which are unable to remobilize the sediment towards the beach. In such conditions, Boca do Rio would more adequately be classified as *linear sub-tidal barred* beach type recently presented by Scott *et al.* (2011).

Differentiating beach types based on Ω alone or combined with RTR was shown to perform with relative success in south coast embayments, while for west coast beaches agreement is widely variable and inconclusive. Such variable agreement conforms to an established body of research explicitly demonstrating inadequacies in the applicability of the parametric approach to beach state classification (*e.g.* Wright *et al.*, 1985; Anthony, 1998; Benavente *et al.*, 2000; Levoy *et al.*, 2000; Klein and Menezes, 2001; Masselink and Pattiaratchi, 2001; Jackson *et al.*, 2005; Gómez-Pujol *et al.*, 2007; Jiménez *et al.*, 2008; Scott *et al.*, 2011). While the extremes of classification schemes are more likely to be correctly identified, it is unrealistic to define static boundaries to classify beach types (mainly intermediate) based on wave, tide and sediment parameters (Scott *et al.*, 2011). As an example, on the only continental scale beach type classification study reported so far, Short (2006) analyzed approximately 5000 wave dominated beaches, reporting average values of Ω for each beach type according to Wright and Short (1984) model. Intermediate beach types LTT, TBR, RBB and LBT, presented average Ω values of 2.5, 3.6, 3.1, and 2.4, respectively. Only for dissipative beaches (average Ω = 9) and reflective beaches (average Ω = 1.1) does the average Ω value appear to conform to the model. Not even the increasing Ω value expected between lower to higher intermediate beach states can be recognized from Short (2006) dataset, as higher values are found in TBR and RBB classes, while the lower average Ω value is in fact obtained for the higher energy intermediate LBT class. Given such widely recognized inabilities to differentiate beach states, parametric

classifications based on Ω appear to be no more successful than the surf scaling parameter – ε – in differentiating beach types, particularly within the intermediate domain. Remarkably, the same statement that the surf-scaling parameter is a poor descriptor of intermediate conditions, following the work of Bauer and Greenwood (1988), has not achieved a similar level of recognition for Ω, despite the growing body of research affirming the very same conclusion.

2.6.3 Embayed configuration and geological influence on beach state

The role of geological control on beach morphodynamic state has been highlighted by Jackson *et al.* (2005), who concluded that inherited geological factors, particularly accommodation space and sediment availability, are fundamental determinants of beach morphodynamic type. These are not embodied within the parametric approach to beach classification. Reduction in breaker height along with control of sediment size and availability are commonly considered the major impacts of geological inheritance, and assumed to be represented in parametric beach state classification by the incorporation of H_b and W_s in the calculation of Ω. However, the recognized role of headlands and/or rocky outcrops in modulating embayed beach shape and segmentation, alongshore variations in the incident wave field and topographic induced nearshore circulation, produce beach types and behaviours unlikely to be captured by existing parametric approaches, especially considering average tide and sediment characteristics and monochromatic wave fields (Jackson *et al.*, 2005). For example, geological constraints in embayed beaches frequently imply modifications in the nearshore wave and current field inducing topographic rips (Short, 2010). Given that these geological constraints are permanent, topographic rips are frequently a persistent feature observed on embayed beaches (Gallop *et al.*, 2011; Loureiro *et al.*, 2012), which

is not necessarily dependent on the level of forcing and will modify beach state. Likewise, since embayed beaches are not as free to evolve as unconstrained beach environments, the embayed setting is likely to restrain the potential for the realization of the full beach state spectrum determined by the dynamic forcing parameters for the probabilistic approach.

Recognition of particularities imposed by geological control on beach state has resulted in the development of new geologically-controlled beach types by Short (2006) to classify Australian beach systems. Such new states, *beaches plus rock flats* and *beaches plus fringing coral reefs*, are not supported by a clear parameterization, as their site specificity hinders the identification of suitable environmental control parameters. Following a similar reasoning, Jackson and Cooper (2009) suggested that geologically constrained beaches represent a new type of beach that likely operates outside the bounds of existing parametric beach state models. While acknowledging the usefulness of Wright and Short (1984) and Masselink and Short (1993) models to provide a qualitative framework for characterizing observed beach morphologies, they do not account for all beach morphological types and their dependence on wave, tide and sediment variables is frequently inadequate and even meaningful at geologically controlled beaches. As new beach classifications studies continue to be presented, it is most likely that new/adapted beach types will be proposed (*e.g.* Klein and Menezes, 2001; Jackson and Cooper, 2009; Scott *et al.*, 2011), particularly in geologically controlled settings where embayed beaches prevail.

While a universal beach state model may not exist (Scott *et al.*, 2011), particularly within intermediate states, the fundamental distinction between reflective, intermediate and dissipative beach types appears to remain meaningful and adequate for most wave-dominated beach environments. Even considering site-specific

morphodynamic behaviour at embayed beaches, distinction between these three morphodynamic states can still be embodied within simplified embayed beach classification models (Short and Masselink, 1999; Klein and Menezes, 2001). Finally, the use of the empirical parameterization provided by the dimensionless fall velocity - Ω - as an elementary descriptor of beach state may still offer some exploratory ability to differentiate between the reflective-intermediate-dissipative beach morphodynamic states. However, intermediate embayed beach types cannot be meaningfully distinguished based on wave, tide and sediment parameters.

2.7 CONCLUSION

1) A new hierarchical framework for classification of beach morphodynamic state based on field observations was proposed and applied to a set of six embayed beaches in southwestern Portugal monitored regularly for a period of two years. Parametric beach state obtained by single averaged values and joint probability distributions of wave, tide and sediment variables was then compared to the field based observed beach states in order to analyse beach morphodynamic state classification in embayed settings.
2) Parametric classification of beach morphodynamic state within a probabilistic framework provides a wider avenue for beach state and mobility analysis, extending the insights on beach morphodynamic behaviour obtained with averaged environmental parameters.
3) Full realization of a parametric probabilistic distribution of beach states is unlikely, as beaches do not respond immediately to forcing and, in embayed settings, geological control constrains the variability in beach response.

4) Differentiating intermediate beach state according to boundaries within the dimensionless Ω and RTR space has reduced applicability, similarly to what is generally acknowledged for the surf scaling parameter.
5) Ω parameter provides limited information and is generally insufficient to provide a meaningful characterization of beach state, particularly in embayed settings where geological control modulate beach shape and segmentation, sediment size and availability, alongshore variations in the incident wave field and topographic induced nearshore circulation.
6) The beach state types of Wright and Short (1984) are generally better suited for characterizing wave-dominated environments, even within mesotidal conditions, as the Masselink and Short (1993) model presents reduced discriminatory ability for intermediate wave-dominated conditions. However, parametric approaches based on Ω should only be used as elementary descriptor of beach state assisting in the generic differentiation between the three major beach types (reflective-intermediate-dissipative).
7) Geological inheritance is a major determinant of embayed beach morphodynamics, and existent state models are unable to fully represent the observed variability. New geologically-controlled beach types have been presented and it is likely that new classes will be required for a more widely representation of the effects of geological control on beach morphodynamics. Consideration of a simplified classification consisting of reflective, intermediate and dissipative beach states is preferable, particularly in geologically constrained settings, further detailed on a regional scale according to observations of embayed beach behaviour.

2.8 ACKNOWLEDGEMENTS

This work is a contribution to Project BAYBEACH – Evolution and Management of Embayed Beaches in Contrasting Environments, funded by FCT under contract PTDC/CTE-GEX/66893/2006. Carlos Loureiro was supported by FCT, grant reference SFRH/DB/27878/2006. Hydrodynamic data was provided by Instituto Hidrográfico. Modelled WANA wave data were supplied by Puertos del Estado. We gratefully acknowledge the help of everyone involved in fieldwork data collection. We are especially thankful to Mara Nunes (CIMA-UALG) for valuable assistance during surveying and Eduardo Ferreira (CESAM-UA/UNICV) for insights regarding Bayesian statistics. Comments and examples from Nathaniel Plant and Cheryl Hapke (USGS) about the application of Bayesian networks in coastal research are gratefully acknowledged.

2.9 REFERENCES

Anthony, E., 1998. Sediment-wave parametric characterization of beaches. *Journal of Coastal Research* 14, 347-352.

Bauer, B.O. and Greenwood, B., 1988. Surf-zone similarity. *Geographical Review* 78, 137-147.

Bayes, T., 1783. An essay towards solving a problem in the doctrine of chances. *Philosophical Transactions of the Royal Society of London* 53, 370-418.

Benavente, J., Gracia, F.J., López-Aguayo, F., 2000. Empirical model of morphodynamic beachface behaviour for low-energy mesotidal environments. *Marine Geology* 167, 375-390.

Benedet, L., Finkl, C., Klein, A.H.F., 2004. Morphodynamic classification of beaches on the Atlantic coast of Florida: geographical variability of beach types, beach safety and coastal hazards. *Journal of Coastal Research* SI39, 360-36.

Berger, J.O., 2000. Bayesian analysis: a look at today and thoughts of tomorrow. *Journal of the American Statistical Association* 95, 1269-1276.

Blott, S.J. and Pye, K., 2012. Particle size scales and classification of sediment types based on particle size distributions: review and recommended procedures. *Sedimentology* (accepted article: doi 10.1111/j.1365-3091.2012.01335.x).

Booij, N., Ris, R.C., Holthuijsen, L.H., 1999. A third-generation wave model for coastal regions - 1. Model description and validation. *Journal of Geophysical Research* 104 (C4), 7649–7666.

Cooper, J.A.G. and Pilkey, O.H., 2004. Longshore drift: trapped in an Expected Universe. *Journal of Sedimentary Research* 74, 599-606.

Cooper, J.A.G. and Pilkey, O.H., 2007. Quantification and measurement of longshore sediment transport: an unattainable goal? In: Balson, P. and Collins, M. (Eds.) Coastal and Shelf Sediment Transport. *Geological Society of London Special Publication* 274, 37-43.

Cooper, J.A.G. and Pilkey, O.H., 2008. Discussion of "Brøker *et al.*, 2008. Morphological modelling: a tool for optimisation of coastal structures. Journal of Coastal Research 23, 1148-1158". *Journal of Coastal Research* 24, 814-816.

Costa, M. and Esteves, R., 2010. Clima de agitação marítima na costa oeste de Portugal continental. Proceedings of XI Jornadas Técnicas de Engenharia Naval — O Sector Marítimo Português. Edições Salamandra, Lisboa, Portugal, pp. 413–426.

Costa, M., Silva, R., Vitorino, J., 2001. Contribuição para o estudo do clima de agitação marítima na costa Portuguesa. Proceedings of 2as Jornadas de Engenharia Costeira e Portuária. AIPCN, Aveiro, Portugal (20 pp. CD-ROM).

Costas, S., Alejo, I., Vila-Concejo, A., Nombela, M.A., 2005. Persistence of storm-induced morphology on a modal low-energy beach: a case study from NW-Iberian Peninsula. *Marine Geology* 224, 43-56.

Davies, J.L., 1964. A morphogenetic approach to world shorelines. *Zeitschrift für Geomorphologie* 8, 27-42.

Gallop, S.L., Bryan, K.R., Coco, G., Stephens, S.A., 2011. Storm-driven changes in rip channel patterns on an embayed beach. *Geomorphology* 127, 179–188.

Gómez-Pujol, L., Orfila, A., Cañellas, B., Alvarez-Ellacuria, A., Méndez, F.J., Medina, R., Tintoré, J., 2007. Morphodynamic classification of sandy beaches in low energetic marine environment. *Marine Geology* 242, 235-246.

Gutierrez, B.T., Plant, N.G., Thieler, E.R., 2011. A Bayesian network to predict coastal vulnerability to sea level rise. *Journal of Geophysical Research* 116, F02009.

Guza, R.T. and Inman, D.L., 1975. Edge waves and beach cusps. *Journal of Geophysical Research* 80, 2997-3012.

Hapke, C. and Plant, N.G., 2010. Predicting coastal cliff erosion using a Bayesian probabilistic model. *Marine Geology* 278, 140-149.

Hegge, B., Eliot, I., Hsu, J., 1996. Sheltered sandy beaches of Southwestern Australia. *Journal of Coastal Research* 12, 748-460.

Jackson, D.W.T. and Cooper, J.A.G., 2009. Geological control on beach form,: accommodation space and contemporary dynamics. *Journal of Coastal Research* SI 56, 69-72.

Jackson, D.W.T., Cooper, J.A.G., del Rio, L., 2005. Geological control of beach morphodynamic state. *Marine Geology* 216, 297-314.

Jiménez, J.A., Guillén, J., Falqués, A., 2008. Comment on the article ”Morphodynamic classification of sandy beaches in low energetic marine environment.” By Gómez-Pujol, L., Orfila, A., Cañellas, B., Alvarez-Ellacuria, A., Méndez, F.J., Medina, R., Tintoré, J. Marine Geology, 242, pp. 235-246, 2007. *Marine Geology* 255, 96-101.

Klein, A.H.F. and Menezes, J.T., 2001. Beach morphodynamics and profile sequence for a headland bay coast. *Journal of Coastal Research* 17, 812-835.

Lippmann, T.C. and Holman, R.A., 1990. The spatial and temporal variability of sand bar morphology. *Journal of Geophysical Research* 95, 11575-11590.

Lahoz, M.G. and Albiach, J.C.C., 2005. Wave forecasting at the Spanish coasts. *Journal of Atmospheric & Ocean Science* 10, 389-405.

Levoy, F., Anthony, E.J., Monfort, O., Larsonneur, C., 2000. The morphodynamics of megatidal beaches in Normandy, France. *Marine Geology* 171, 39-59.

Loureiro, C., Ferreira, Ó., Cooper, J.A.G., 2012. Extreme erosion on high-energy embayed beaches: influence of megarips and storm grouping. *Geomorphology* 139-140, 155-171.

Loureiro, C., Ferreira, Ó., Cooper, J.A.G., in revision. Geologically constrained morphological variability and boundary effects in embayed beaches. *Marine Geology*.

Masselink, G. and Pattiaratchi, C.B., 2001. Seasonal changes in beach morphology along the coastline of Perth, Western Australia. *Marine Geology* 172, 243-263.

Masselink, G. and Short, A.D., 1993. The effect of tide range on beach morphodynamics and morphology: a conceptual beach model. *Journal of Coastal Research* 9, 785-800.

Norsys, 1992-2011. Netica. www.norsys.com, Version: 5.02.

Pilkey, O.H. and Cooper, J.A.G., 2007. Lifting the flap or why coastal models don't work. *Journal of Coastal Research* SI50, 585-587.

Plant, N.G. and Holland, K.T., 2011a. Prediction and assimilation of surf-zone processes using a Bayesian network. Part I: forward models. *Coastal Engineering* 58, 119-130.

Plant, N.G. and Holland, K.T., 2011b. Prediction and assimilation of surf-zone processes using a Bayesian network. Part II: inverse models. *Coastal Engineering* 58, 256-266.

Plant, N.G., Holland, K.T., Holman, R.A., 2006. A dynamical attractor governs beach response to storms. *Geophysical Research Letters* 33, L17607.

Ranasinghe, R., Symonds, G., Black, K., Holman, R., 2004. Morphodynamics of intermediate beaches: a video imaging and numerical modelling study. *Coastal Engineering* 51, 629-655.

Roy, P.S. and Stephens, A.W., 1981. Geological controls on process-response, S.E. Australia. Proceedings of the 17th International Conference on Coastal Engineering. ASCE, Sydney, Australia, pp. 913–933.

Sánchez-Arcilla, A., Aguar, J.G., Egozcue, J.J., Ortego, M.I., Galiatsatou, P., Prinos, P., 2008. Extremes from scarce data: the role of bayesian and scaling techniques in reducing uncertainty. *Journal of Hydraulic Research* 46, 224-234.

Scott, T., Masselink, G., Russel, P., 2011. Morphodynamic characteristics and classification of beaches in England and Wales. *Marine Geology* 286, 1-20.

Scotto, M.G. and Guedes Soares, C., 2007. Bayesian inference for long-term prediction of significant wave height. *Coastal Engineering* 54, 393-400.

Sénéchal, N., Gouriou, T., Castelle, B., Parisot, J.-P., Capo, S., Bujan, S., Howa, H., 2009. Morphodynamic response of a meso- to macro-tidal intermediate beach based on a long-term data set. *Geomorphology* 107, 263-274.

Short, A.D., 1987. A note on the controls of beach type and change, with S.E. Australian examples. *Journal of Coastal Research* 3, 387-395.

Short, A.D., 1991. Macro-meso tidal beach morphodynamics – an overview. *Journal of Coastal Research* 7, 417-436.

Short, A.D., 2006. Australian beach systems – nature and distribution. *Journal of Coastal Research* 22, 11-27.

Short, A.D., 2010. Role of geological inheritance in Australian beach morphodynamics. *Coastal Engineering* 57, 91-97.

Short, A.D. and Masselink, G., 1999. Embayed and structurally controlled beaches. In: Short, A.D. (Ed.), *Handbook of Beach and Shoreface Morphodynamics*. John Wiley & Sons, Chichester, pp. 230–249.

Soulsby, R.L., 1997. *Dynamics of Marine Sands: a manual for practical applications*. Thomas Telford, London. 249 p.

Wright, L.D. and Short, A.D., 1984. Morphodynamic variability of surf zones and beaches: a synthesis. *Marine Geology* 56, 93-118.

Wright, L.D., Short, A.D., Green, M.O., 1985. Short-term changes in the morphodynamic states of beaches and surf zones: an empirical predictive model. *Marine Geology* 62, 339-364.

Yates, M., Cozannet, G., 2012. Evaluating European coastal evolution using Bayesian networks. *Natural Hazards and Earth Systems Sciences* 12, 1173-1177.

CHAPTER 3

Geologically constrained morphological variability and boundary effects on embayed beaches

Loureiro, C., Ferreira, Ó., Cooper, J.A.G.. Geologically constrained morphological variability and boundary effects in embayed beaches. *Marine Geology* (in revision).

ABSTRACT

Headlands, rock outcrops and engineering structures impact beach and nearshore dynamics of coastal embayments, inducing boundary effects that constrain the lateral and vertical beach variability. This study analyses morphological change in six embayed beaches with diverse levels of exposure to wave action and various degrees of geological control in the mesotidal coast of southwestern Portugal. The aim is to identify whether geological boundaries constrain the morphological behaviour of embayed beaches and assess whether their effects can be decoupled from datasets of morphological change. Topographic data, obtained over a two-year period on each of the six embayments, were analysed using empirical orthogonal functions (EOF) to decompose temporal and spatial variability in the datasets. First and second mode eigenfunctions were explored using time-variable linear correlation analysis with several nearshore parameters that include hydrodynamic variables, sedimentary and geometric characteristics of each embayment in order to derive forcing-response relationships.

Our results demonstrate that natural geological boundaries constrain the morphological behaviour of embayed beaches, producing conspicuous alongshore variability in all embayments. Localized responses induced by lateral and vertical boundary interference with nearshore dynamics include beach rotation, topographically-controlled rip circulation and reduced profile fluctuation. Spatial decoupling in cross- and longshore responses is accompanied by a temporal decoupling in response times, both of which increase in more constrained embayments (from 1 day in exposed embayments to 1 week or more in the most sheltered ones). Normalized wave power was correlated at the 99% confidence level with the primary mode of morphological variability at most embayments, which represented 67% to 94% of the variance in the

datasets. This correlation stresses the importance of combined parameterization of wave and tide forcing in process-response relations between hydrodynamics and morphological change for mesotidal coastal environments. Lateral and vertical geological boundaries exert their effects fundamentally by restraining longshore sediment transport, inducing cellular surf zone circulation and by impacting cross-shore sediment transport. It is postulated that decreasing sediment abundance and substrate depth intensify vertical boundary effects, while higher indentation and wave obliquity enhance the effects of lateral boundaries.

KEYWORDS: beach morphodynamics; geological control; empirical orthogonal functions; hydrodynamic forcing; Southwestern Portugal.

3.1 INTRODUCTION

The presence of physical boundaries, in the form of headlands, rocky outcrops or even engineering structures, significantly impacts planform, sediment transport and morphodynamics of embayed beaches (Short, 1999). Suggestions that these geological constraints can be as important as dynamic forcing by waves and currents in determining contemporary beach morphology (Jackson *et al.*, 2005) have, however, not been fully realised into the present thinking of beach morphodynamic behaviour (Jackson and Cooper, 2009). Influences of headlands, outcrops, and engineering structures in beach and surfzone dynamics are, nevertheless, frequently acknowledged regarding patterns of wave refraction and attenuation, development of cellular circulation, occurrence of sediment by-passing, and notably in the constraining of cross and longshore processes (*e.g.* Sanderson and Eliot, 1999; Short, 1999; Larson and Kraus, 2000; Gallop *et al.*, 2011b; Scott *et al.*, 2011).

While the presence of a geological framework is suggested to constrain the ability of a beach to fluctuate both laterally and vertically (Jackson and Cooper, 2009), effects of lateral boundaries, mainly due to headland control on equilibrium shoreline configuration (Silvester, 1985), have traditionally received most of the attention in the embayed beach literature (Ojeda and Guillén, 2008). Under oblique wave conditions,

headland protection offers a decreasing lateral sheltering from wave action in the downdrift coastline, promoting the development of a segmented beach based on curvature, energy levels and even textural characteristics (Finkelstein, 1982; Phillips, 1985; Silvester and Hsu, 1997). This lateral boundary effect downdrift of headlands, widely explored in coastal engineering, decreases as wave obliquity and curvature are reduced, with the entire beach experiencing similar morphological changes (Klein *et al.*, 2010). Irrespective of wave approach angle, as headland spacing decreases and seaward protrusion increases, other lateral boundary effects progressively modify embayed beach response (Short, 1999). In the last decade several studies have investigated the effects of lateral boundaries in natural and artificial embayed beach morphodynamics, focusing on headland restriction and modification of longshore sediment transport that imposes medium- to short-term beach rotation (*e.g.* Short *et al.*, 2000; Masselink and Pattiaratchi, 2001; Klein *et al.*, 2002, 2010; Ranasinghe *et al.*, 2004; Harley *et al.*, 2008, 2011; Ojeda and Guillén, 2008; Martins *et al.*, 2010; Ruiz de Alegria-Arzaburu and Masselink, 2010; Thomas *et al.*, 2010, 2011; Archetti and Romagnoli, 2011). However, while knowledge of lateral constraints has been advancing, effects of vertical boundaries posed by underlying rocky substrata in the morphological evolution and morphodynamic responses of embayed beaches have received only limited attention. Few studies have, so far, explored the effects of geological control in beach systems underlain by rocks, often classified as perched beaches (Gallop *et al.*, 2011b). Recently, Jackson and Cooper (2009) presented a conceptual model detailing the general mobility of beaches with varying degrees of underlying geological control. The authors propose three types of beaches based on the relative depth of the vertical boundary (unconstrained, semi-constrained and highly constrained). However, quantitative information about the thickness of sediment veneers below which vertical geological

control becomes unimportant remains undetermined (Jackson and Cooper, 2009), and field data describing vertical boundary effects is still scarce (Gallop *et al.*, 2011a).

Various statistical methods have proved to be useful for extracting characteristic behaviour patterns from coastal morphological data (Kroon *et al.*, 2008) and the application of empirical orthogonal functions (EOF) is considered particularly suitable for detecting and quantifying signals from different types of forcing and disturbances (Larson *et al.*, 2003). EOF analysis has been used in beach studies for three decades, following the classical work by Winant *et al.* (1975), and was recently reviewed by Miller and Dean (2007a; 2007b). Those authors demonstrated the ability of EOF analysis to characterize lateral boundary effects in 20 to 45 km-wide coastal cells, while previous studies using EOF analysis had also highlighted the role of lateral boundaries in embayed beaches (*e.g.* Clarke and Eliot, 1982; Short *et al.*, 2000). It is therefore naturally appealing to consider EOF analysis as a method for quantitatively characterising the effects of both lateral and vertical boundaries.

Building on the body of work on the analysis of boundary effects in beach dynamics, this paper explores the range of lateral and vertical geologic constraints on the medium-term (months to years) morphologic behaviour of embayed beaches. Due to similarities between natural headlands and outcrops with engineering structures, an increased knowledge of the mechanisms of geological beach control and boundary effects is important for understanding beach behaviour in the presence of engineering structures that intend to mimic natural geological control in embayed beaches (Hsu *et al.*, 2008). In this paper we hypothesized that lateral and vertical geological boundaries constrain the morphological behaviour of embayed beaches and that their effects can be decoupled from datasets of embayed beach morphological change. To test this, four specific objectives are outlined:

(i) Decompose the spatial and temporal variability of embayed beach morphology at diverse sites;

(ii) Evaluate the forcing mechanisms driving the observed morphological change;

(iii) Analyse the role of vertical and lateral geological constraints on the morphological response;

(iv) Characterize boundary effects on the morphological behaviour of embayed beaches.

To address the questions and objectives raised, this paper explores EOF analysis, which, although widely used to determine shoreline and beach profile evolution, has been scarcely applied to analyse the evolution of coastal areas controlled by headlands, rocky outcrops or underlying bedrock. Datasets of morphological change from six embayed beaches from southwestern Portugal are used. The beaches are clustered into two groups of three closely located embayments, with the beaches within each group exposed to identical offshore forcing. However, due to geological constraints, each beach experiences different morphological changes. The quantitative analysis based on EOF decomposition is complemented by time-variable correlation analysis with several forcing parameters combining hydrodynamic variables, sedimentary and geometric characteristics of each embayment.

3.2 FIELD SITE DESCRIPTION

The southwestern coast of Portugal is an indented rocky coastline with marked geodynamic contrasts between the western and southern sections. Despite both being bedrock-framed, with a prevalence of embayed beaches in coastal re-entrants fronting

the cliffs or associated with small streams, both geological and environmental characteristics differ significantly between these two sections. Carved in Carboniferous shale and greywacke, the high-energy western coastline is directly exposed to the North Atlantic swell, with several intermediate to dissipative embayed beaches experiencing energetic conditions throughout the year. Mean offshore significant wave heights (H_o) between 1.5 and 2 m, and peak wave periods (T_p) between 9 and 13 s for summer and winter periods, respectively, induce a marked oceanographic seasonality (Costa and Esteves, 2010). Waves reach this coastline predominantly from north-westerly to westerly directions (Fig 3.1); yet nearly complete refraction of swell waves renders most of these embayed beaches swash aligned. Jurassic to Miocene calcareous cliffs constitute the majority of the rocky section of the southern coastline, which is relatively sheltered from direct exposure to the North Atlantic swell. Offshore wave conditions are moderate, with mean H_o around 0.9 m and mean T_p of 8 s (Costa *et al.*, 2001). Slight variations occur between summer and winter conditions, but not as markedly as on the west coast. Dominant waves reach this coastline from a W-SW direction (Fig. 3.1), yet shorter period SE waves generated within the Gulf of Cadiz account for roughly a quarter of occurrences (Costa *et al.*, 2001). This oceanographic setting imposes a markedly bimodal wave climate on the sediment-deprived, intermediate to reflective south coast embayed beaches. Tidal conditions are identical and nearly synchronous for both sections of the coastline. Tidal regime is classified as semidiurnal and mesotidal, with maximum spring tidal range around 3.5 m.

Six embayed beaches were selected as study sites, three in each section of the coastline (Fig. 3.1). West coast beaches, Amoreira, Mt. Clérigo and Arrifana, are all composed of well-sorted, medium sand, and being exposed to a high-energy wave climate these beaches are modally dissipative or intermediate skewed to dissipative.

Amoreira beach is roughly 500 m-long, but is wide and backed by an extensive dune field. This embayment contains a bay-barrier estuary, with a small tidal stream that runs through a shallow channel adjacent to the southern headland. The beach has a persistent low tide terrace, occasionally crossed by the tidal stream, which creates a ridge and runnel-like morphology. Similarly to Amoreira, the Mt. Clérigo embayment faces directly the dominant NW waves. This beach is wide and backed by partly vegetated dunes in the south and central sections, while the northern part is narrow and backed by 50 m-high cliffs. The intertidal area is wide, with rocks outcropping in the southern section of the embayment. Arrifana is a swash-aligned beach, completely enclosed by up to 100 m-high cliffs, and partially protected from dominant NW waves by a prominent northern headland. A lag deposit, composed of coarse gravel and boulders, separates the narrow subaerial beach from the cliffs.

The south coast embayments, Salema, Boca do Rio and Cabanas Velhas, are composed of relatively thin layers of medium to coarse sand, which generally overlie lag deposits of cobbles, boulders and/or shore platforms. These sediment-deprived beaches are modally intermediate skewed to reflective. Salema beach is relatively unconstrained by protruding headlands, which allows it to range from 600 to 1100 m in length. Being openly exposed to SSE, this beach receives waves from the dominant SW swell as well as SE sea, which generally impinge on the beach with significant angles. Boca do Rio is a short, narrow beach that corresponds to the terminal part of a small infilled estuary, with a temporary stream that crosses the eastern section of the beach following rainfall events. It is also roughly exposed to SSE, and the reduced seaward protrusion of the bordering headlands also enables waves from both dominant directions to reach the shoreline. Cabanas Velhas is also narrow, and backed by 10 to 50 m-high

cliffs. It is exposed directly to the dominant SW waves, being partially protected from SE waves by a protruding eastern headland.

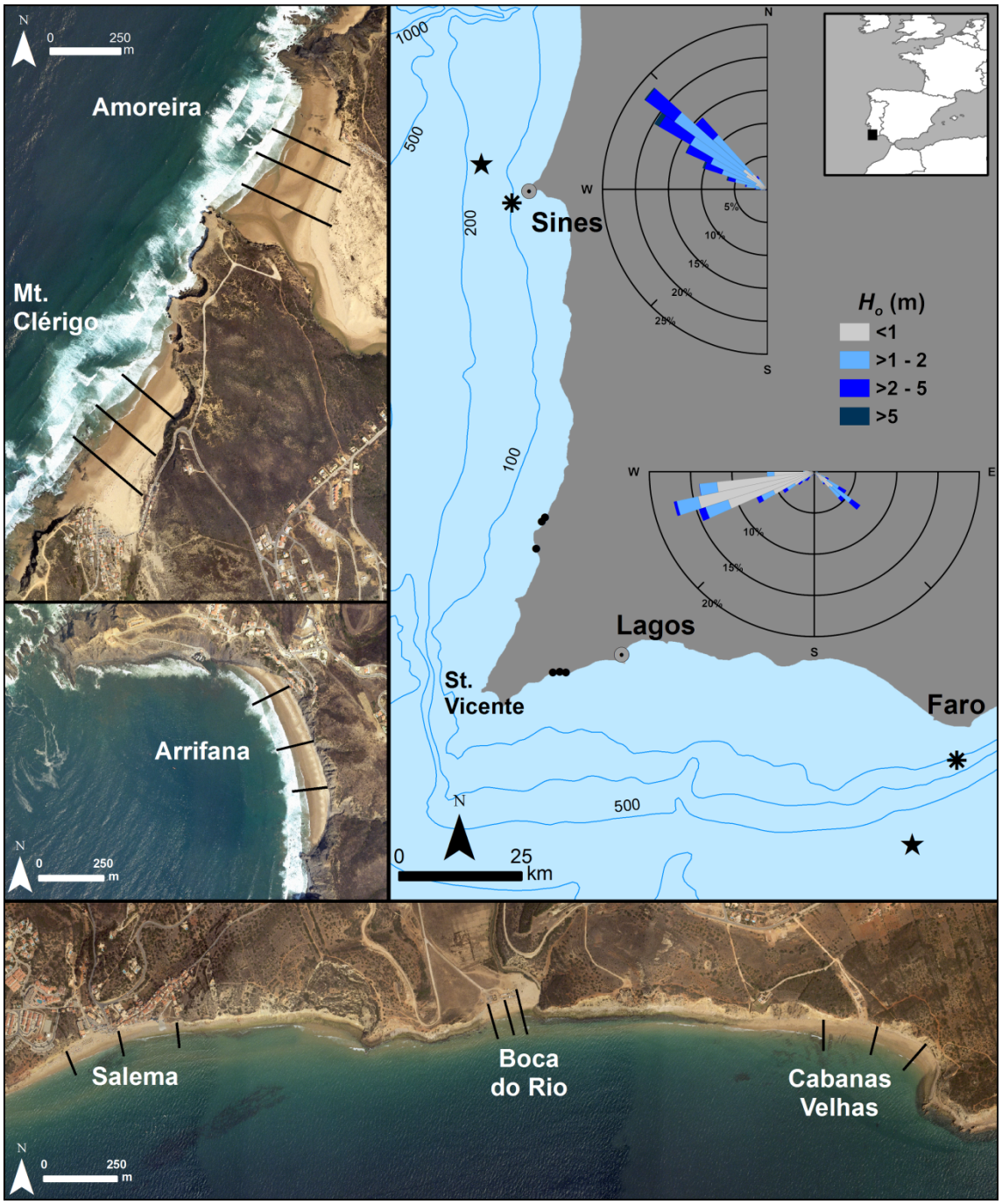

Figure 3.1 Geographic location and aerial view of the study sites (indicated by black circles in the map). Location of beach profiles, directional wave buoys, modelled wave points and tide gauges indicated by black lines, asterisks, stars and doted circles, respectively. Wave roses for Sines and Faro were computed from wave buoy data (asterisks in location image), from 2007 to 2009.

3.3 DATA AND METHODS

3.3.1 Topographic data

Topographic surveys along cross-shore beach profiles were performed bimonthly on the study sites between September 2007 and September 2009, and complemented by event-driven surveys immediately after storm events and two to three weeks later to monitor beach recovery. Three profiles, with variable alongshore spacing (Fig. 3.1; Table 3.1), were measured in each embayment using RTK-GNSS (Real Time Kinematic Global Navigation Satellite System). Surveys were undertaken at low tide and extended from the frontal dune or cliff base to the mean low water spring level (MLWS), 1.4 m below mean sea level (MSL), or further seaward.

The selection of proxies to represent the overall beach response is non-trivial. Recent EOF analyses of alongshore beach variability have used datum-based shoreline positions, mainly extracted from time-exposure video images or profile surveys (*e.g.* Miller and Dean, 2007a; Fairley *et al.*, 2009; Ruiz de Alegría-Arzaburu *et al.*, 2010). These are, however, generally restricted to the upper portion of the cross-shore beach profile. Alternatively, EOF analyses of beach variability have also been performed using a sediment budget approach, using either digital elevation models (*e.g.* Larson *et al.*, 1999; Haxel and Holman, 2004; Gómez-Pujol *et al.*, 2011), or linear volume along cross-shore beach profiles (*e.g.* Clarke and Eliot, 1982, 1988). The latter proxy was selected in the present study. Profile volume was computed by trapezoidal integration with the upper limit defined by the profile surface and the MLWS level as lower limit. The MLWS level was chosen because it indicates a vertical morphodynamic separation of the beach profile for exposed beaches in southern Portugal, based on results

presented by Almeida *et al.* (2011), due to the existence of a nodal point at this level that separates the cross-shore sectors dominated by berm and subtidal terrace changes.

Table 3.1 Summary of the relevant characteristics of the monitoring sites and correlation criteria

Dataset	Dimensions			Sediment		Beach profiles		Correlation criteria		
	S_l (m)	C_l (m)	B_l (m)	d_{50} (mm)	W_s (m/s)	Spacing (m)	Surveys	*DOF*	$R_{crit\ 95\%}$	$R_{crit\ 99\%}$
Amoreira	815	575	600	0.298	0.037	115	20	18	0.44	0.56
Mt. Clérigo	955	785	580	0.309	0.039	140	20	18	0.44	0.56
Arrifana	2055	1340	830	0.268	0.032	205	21	19	0.43	0.55
Salema	1300	1235	560	0.304	0.038	195	33	31	0.34	0.44
Boca do Rio	255	195	180	0.406	0.054	55	32	30	0.35	0.45
Cabanas Velhas	835	715	650	0.281	0.034	170	32	30	0.35	0.45

S_l - embayment shoreline length; C_l - chord length (distance between headlands); B_l - beach length; d_{50} - median grain diameter; W_s – sediment fall velocity; *DOF* - degrees of freedom; R_{crit} - confidence levels

3.3.2 Empirical orthogonal function analysis

EOF analysis is here applied to decompose the spatial and temporal variability within each dataset. Application of this multivariate statistical technique, often referred as Principal Component Analysis, to coastal geomorphology datasets has been widely described (*e.g.* Winant *et al.*, 1975; Vincent *et al.*, 1976; Aubrey, 1979; Wijnberg and Terwindt, 1995; Muñoz-Pérez *et al.*, 2001; Dean and Dalrymple, 2002; Larson *et al.*, 2003; Miller and Dean, 2007a). In brief, a data matrix $y(s,t)$ can be represented by a series of linear combinations of spatial and temporal functions, denoted by:

$$y(s,t) = \sum_{k=1}^{n} n_k\, e_k\,(s)\, c_k\,(t) \qquad (3.1)$$

where e_k (s) are the kth spatial eigenfunctions, c_k (t) are the kth temporal eigenfunctions, or temporal coefficients, and n_k the normalizing factor. The new sets of variables, e_k (s) and c_k (t), are orthogonal and therefore, uncorrelated, and ordered in terms of their ability to explain the variance in the original dataset. EOF application allows the dimensionality of a dataset to be reduced (Larson *et al.*, 2003), as generally it is necessary to retain only the first few eigenfunctions, which will account for most of the variance, providing a compact representation of the original data (Miller and Dean, 2007a).

The way the data matrix is specified for EOF analysis is central to the outcome of the calculations (Clarke and Eliot, 1988). The most important distinction involves the scaling of the variables, which were here de-meaned prior to the calculations. Such choice of scale determines that the matrix used to perform the EOF analysis is a covariance matrix. This is the most common option for EOF applications to coastal morphologic data (Larson, *et al.*, 2003), as detailed in recent studies (*e.g.*, Kroon *et al.*, 2008; Fairley *et al.*, 2009; Hansen and Barnard, 2010; Gómez-Pujol *et al.*, 2011). The EOF modes, or eigenfunctions, obtained are thus considered in terms of deviation from the mean, which otherwise would tend to dominate the signal (Larson *et al.*, 2003). The first EOF modes are often given physical interpretations based on resemblance of the spatial eigenfunctions with morphological features (*e.g.* Winant *et al.*, 1975, Aubrey, 1979), or correlation of temporal eigenfunctions with forcing parameters (*e.g.* Miller and Dean, 2007b; Fairley *et al.*, 2009).

3.3.3 Comparison with forcing parameters

Establishing relationships between different variables can provide insights into the behaviour of a beach and how it responds to forcing (Larson *et al.*, 2003).

Accordingly, a set of commonly used hydrodynamic and morphodynamic parameters were selected to characterize the forcing and relate it to the temporal eigenfunctions. The variables considered here combine wave, tide, sediment characteristics and embayment geometry, and details of their collection, transformation and application are described below.

3.3.3.1 Offshore waves and tides

Wave data have been collected by Instituto Hidrográfico (IH) for Portuguese western and southern offshore coastal waters using Datawell directional wave buoys near Sines and Faro (Fig. 3.1), located both roughly 7 km from shore in approximately 100 m water depths. The buoys provide measurements of offshore significant wave height (H_o), peak spectral period (T_p) and peak wave direction (θ_o). Gaps in the measured wave record, accounting for roughly 15% at Sines and 5% at Faro buoy for the duration of the study, where filled using modelled wave data from WANA deepwater network (Lahoz and Albiach, 2005), provided by Puertos del Estado for grid points near the wave buoys (Fig. 3.1). Linear correlation analysis indicated a statistically significant correlation between observed and modelled wave heights ($R \geq 0.82$ for $p < 0.01$; RMSE $\leq$ 0.4m).

Tide level observations and predictions for the west coast beaches were obtained from the IH tide gauge in Sines (Fig. 3.1). The amount of missing records in the dataset was reduced, around 2%, and these were filled using the predicted tide levels at Sines. Equipment malfunction in Lagos tide gauge (Fig. 3.1) truncated the observed tide levels, rendering it useless, and predicted tide levels at Lagos were used for the south coast beaches.

3.3.3.2 Forcing parameters

Numerous dimensional and non-dimensional hydrodynamic and morphodynamic parameters are often used for characterizing the forcing driving beach changes. Ten parameters are considered here, namely breaker height (H_b), breaker angle (θ_b), peak wave period (T_p), wave steepness (H_o/L_o), wave energy (E_o), wave power (P_o), normalized wave power (Pn_o), alongshore wave energy flux (Pl_b), dimensionless fall velocity (Ω) and the dimensionless embayment scaling parameter (δ').

Deepwater conditions (H_o, T_p and θ_o) are provided directly from the buoy measurements, while breaking conditions (H_b and θ_b) were computed using the formula presented by Larson *et al.* (2010), developed to derive wave properties at incipient breaking based on a simplified solution of the wave energy flux conservation equation combined with Snell's law. Depth limited breaking is imposed with the commonly used depth breaker ratio of 0.78. Wave angles were converted in positive/negative angles for waves approaching northwards/southwards to beach normal for the west coast beaches, and waves approaching westwards/eastwards to beach normal for the south coast beaches.

Wave steepness, H_o/L_o, was calculated using linear wave theory with L_o, the deepwater wave length, given by:

$$L_o = (gT_p^2) / (2\pi) \tag{3.2}$$

where g is the acceleration due to gravity. Offshore wave energy density (E_o), or simply wave energy, was also computed considering linear wave theory:

$$E_o = (1/8)\, pgH_o^2 \tag{3.3}$$

where ρ is the density of water. Combining wave energy with the deepwater group velocity (C_g) it is possible to compute the rate at which wave energy is transferred by moving waves, the wave power (P_o):

$$P_o = EC_g \tag{3.4}$$

where C_g is given by

$$C_g = (1/(4\pi))\, gT_p \tag{3.5}$$

Recognizing the importance of tidal levels for coastal morphological evolution in Southern Portugal, Morris *et al.* (2001) proposed the normalized wave power (Pn_o) in order to include the tidal range according to:

$$Pn_o = P_o(\eta_{dtr} / \eta_{str}) \tag{3.6}$$

where η_{dtr} is the maximum daily tidal range and η_{str} is the maximum spring tidal range. This parameter conveniently reflects the enhanced wave erosion potential during spring tides, restricting it for lower tidal ranges (Morris *et al.*, 2001).

In order to obtain an indicator of the alongshore sediment transport, the alongshore component of the wave energy flux (Pl_b) was computed using:

$$Pl_b = (E_b C_g) \sin\theta_b \cos\theta_b \tag{3.7}$$

where E_b was obtained for breaking conditions according to Eq. (3.3) replacing H_o by H_b, and C_g as given by the shallow water approximation to wave group velocity:

$$C_g = \sqrt{(gh_b)} \tag{3.8}$$

where h_b is the water depth at breaking. According to the conversion of wave directions to wave angles positive/negative alongshore energy fluxes correspond to southward/northward transport for west coast beaches, and eastward/westward transport for the south coast beaches.

Besides the purely hydrodynamic parameters presented above, the nearshore forcing can also be represented by parameterizations that incorporate sedimentary characteristics of the embayments. A natural parameter to consider, for its generalized application to beach studies, is the dimensionless fall velocity (Ω) (Gourlay, 1968; Dean, 1973):

$$\Omega = H_b / (W_s T_p) \tag{3.9}$$

where W_s is the sediment fall velocity, computed according to Soulsby (1997) using the median grain diameter (d_{50}) averaged for each embayment from beach face samples collected seasonally during the two year study period (Table 3.1).

All the aforementioned parameters are well established in the literature and have proven skilfulness in characterizing morphological changes in the coastal environment. However, no parameter considers explicitly the impact of embayment dimensions and geometry in characterizing the nearshore environment. Short (1996; 1999) based on unpublished work by Marteens and collaborators presented the dimensionless embayment scaling parameter (δ'), which relates the embayment configuration to the incident breaking wave conditions according to:

$$\delta' = S_l^{\,2} / 100 C_l H_b \tag{3.10}$$

where S_l is the embayment shoreline length and C_l is the chord length (distance between headlands). This empirical approximation was derived from morphometric analysis of embayed beaches in order to describe parametrically the degree of headland impact on surf zone circulation considering a typical surfzone gradient of 0.01 (Short and Masselink, 1999).

3.3.3.3 Correlation analysis

Linear correlation analysis was used to test the hypothesis that EOF modes have a physical meaning, and are not simply by-products of the mathematical decomposition. Accordingly, if the temporal eigenfunctions of the EOF modes are related to the time series of at least one of the forcing parameters considered, their physical meaning should be elucidated by the characteristics of such forcing parameters (Miller and Dean, 2007b). Correlation between variables was considered statistically significant at the 95% confidence level when the Pearson's product moment correlation coefficient (R) exceeded the critical level ($R_{\text{crit }95\%}$) based on two-tailed normal distribution for n-2 degrees of freedom (DOF) (Table 3.1). More stringent correlation ($R_{\text{crit }99\%}$), at the 99% confidence level, is further used in order to distinguish the strongest correlations between the temporal eigenfunctions and the forcing parameters.

As beach changes occur at different frequencies and response times may be site specific, a variable averaging interval for correlation with the temporal eigenfunctions was implemented. The forcing parameters were averaged over 1 to 30 days prior to each survey date, regardless of survey intervals, following Hansen and Barnard (2010) and Alvarez-Ellacuria *et al.* (2011). As there is no consensus about the optimal averaging interval for correlation of forcing parameters with temporal eigenfunctions (or the beach changes they are supposed to represent), the varying averaging window implemented

provides a more flexible approach, enabling further exploration of the response times of each beach. Moreover, by extending from 1 to 30 days (D), the varying averaging window allows the incorporation of daily, weekly and monthly averaging intervals as in other studies (*e.g.* Miller and Dean, 2007b; Quartel *et al.*, 2008). The averaging interval that produced the first peak in correlation above the critical level was assumed to be the optimal time scale of beach response, regardless of the fact that higher correlation may be obtained for larger averaging windows (refer to Fig. 3.2 for an example of how peak correlation was obtained). The reasoning behind this option is that larger averaging intervals reflect responses to the seasonal variation in wave climate, as suggested by Miller and Dean (2007b), while the first peak in correlation more likely refers to the effects of boundaries in embayed beach response.

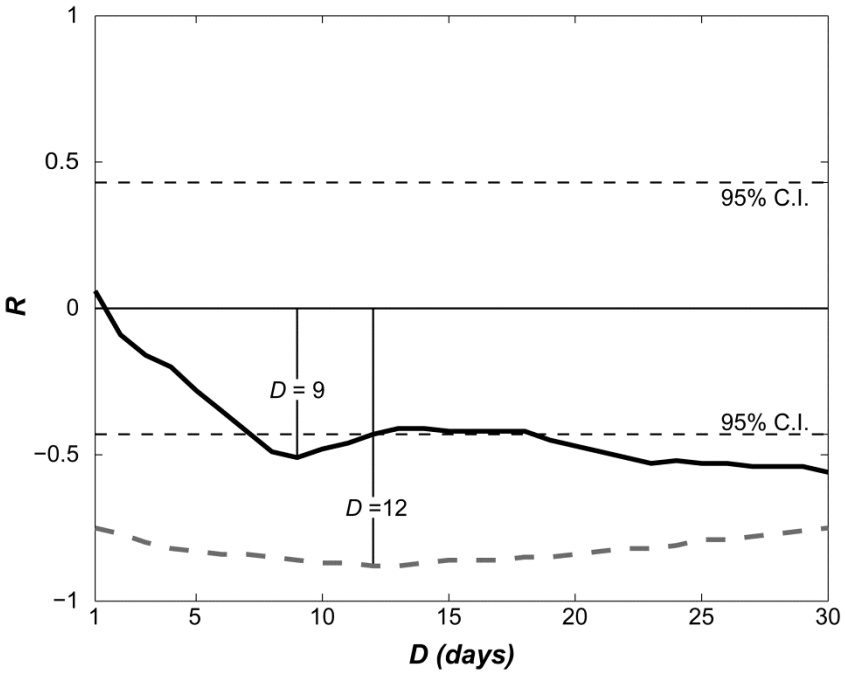

Figure 3.2 Linear correlation (R) between forcing parameters Ω (black line) and Pn_o (grey dotted line) and the first temporal eigenfunction ($c_1(t)$) for Arrifana beach. Results are presented for the averaging windows of 1 to 30 days prior to each survey. Averaging days (D) for the first peak in correlation above the $R_{crit\ 95\%}$ level are indicated for each forcing parameter.

3.4 RESULTS

The results of the EOF decomposition indicate that the first two eigenfunctions explain the majority of morphologic change, accounting for over 95% of the total variability in each embayment (Table 3.2). The first eigenfunction is undoubtedly the most important, contributing 67% to 94% of the total variance of each dataset, while the second eigenfunction only explains 4% to 29%. The first two eigenfunctions, $e_1(s,t)$ and $e_2(s,t)$, will be analysed in detail bellow, based on the interpretation of spatial patterns and temporal amplitudes for each embayment (Figs. 3.3 to 3.8), and evaluation of their relation with forcing parameters (Table 3.3).

Table 3.2 Percentage of the variance explained by the first two eigenfunctions at each site

Dataset	Percentage of variance explained		
	$e_1(s,t)$	$e_2(s,t)$	Remaining
Amoreira	86,43%	10,93%	2,64%
Mt. Clérigo	91,41%	6,94%	1,65%
Arrifana	93,96%	4,44%	1,60%
Salema	66,66%	29,40%	3,94%
Boca do Rio	87,45%	8,48%	4,07%
Cabanas Velhas	92,10%	4,33%	3,57%

3.4.1 Amoreira

The primary mode of variability in Amoreira beach, representing 86% of the variance, consists of a nearly uniform alongshore pattern of beach response. The spatial eigenfunction $e_1(s)$ represents a coherent pattern of morphological change along the entire embayment, although with increased variability in the northern and central sections (Fig. 3.3). Despite this slight alongshore variation, it is evident that the beach

responds as a whole, with changes characterized by alongshore uniform accretion and erosion. From January 2009, the temporal eigenfunction $c_1(t)$ exhibits a marked decrease (Fig. 3.3), most likely related to extreme storm events along the southwestern Portuguese coast reported in Loureiro *et al.* (2011). Coefficients for $c_1(t)$ remained negative with reduced variation throughout the rest of the monitoring period. The temporal variability of the first eigenfunction is only significantly correlated with the normalized wave power (Pn_o) (Table 3.3). The negative correlation between $c_1(t)$ and Pn_o, with a peak correlation value of R = -0.51 at D = 1 day, highlights an immediate inverse association between the normalized wave power and beach volume.

Table 3.3 Pearson's product moment correlation coefficient's between the temporal eigenfunctions ($c_n(t)$) for the peak D days averages of the hydrodynamic forcing parameters preceding each survey (only correlations at the 95% or higher confidence levels are presented).

Dataset	Correlation with forcing parameters									
	H_b	θ_b	T_p	H_o/L_o	E_o	P_o	Pn_o	Pl_b	Ω	δ'
Amoreira										
$c_1(t)$	--	--	--	--	--	--	-0.51 (1)	--	--	--
$c_2(t)$	0.65 (8)	--	0.68 (8)	--	0.62 (7)	0.65 (7)	--	0.48 (6)	0.52 (8)	-0.58 (8)
Mt. Clérigo										
$c_1(t)$	--	--	--	--	--	--	-0.65 (1)	--	--	--
$c_2(t)$	-0.49 (1)	--	--	--	--	--	--	--	-0.51 (1)	0.59 (1)
Arrifana										
$c_1(t)$	-0.52 (9)	--	-0.49 (24)	--	-0.54 (9)	-0.54 (9)	-0.88 (12)	0.49 (5)	-0.51 (9)	--
$c_2(t)$	--	--	--	--	--	--	--	--	--	--
Salema										
$c_1(t)$	--	--	-0.38 (15)	--	-0.40 (20)	-0.38 (11)	-0.53 (10)	--	--	--
$c_2(t)$	--	0.41 (6)	0.63 (15)	-0.41 (18)	--	0.36 (24)	0.37 (25)	0.35 (7)	--	-0.43 (15)
Boca do Rio										
$c_1(t)$	--	--	--	--	--	--	--	--	--	--
$c_2(t)$	--	0.55 (4)	0.44 (4)	-0.38 (2)	--	--	--	0.55 (3)	-0.35 (2)	--
Cab. Velhas										
$c_1(t)$	-0.35 (30)	--	--	-0.36 (14)	-0.37 (29)	-0.36 (30)	-0.49 (4)	--	-0.40 (19)	0.37 (17)
$c_2(t)$	0.37 (17)	--	--	--	0.36 (18)	0.37 (17)	--	--	0.37 (17)	--

Values between parentheses indicate the averaged D days preceding each survey when the first peak in the correlation was observed. Highlighted values identify correlations exceeding the 99% confidence level. All symbols and abbreviations indicated in the text.

The second mode of variability $e_2(s,t)$ accounts for 11% of the variance and exhibits opposing responses for the northern and southern beach ends. This alongshore non-uniform pattern of $e_2(s)$ presents a nodal point located near the centre of the embayment (Fig. 3.3), and higher variability for the southern section of the beach, adjacent to the stream inlet. Phase shifts between opposing ends of embayed beaches are associated with rotation phenomena (Short, 1999; Klein *et al.*, 2002), and at Amoreira positive/negative phases correspond to clockwise/anticlockwise rotation about the nodal point in the central section of the beach. Mode two temporal eigenfunction $c_2(t)$ is strongly correlated with several forcing parameters (Table 3.3). Highly significant correlations include the forcing parameters H_b, T_p, E_o, P_o and δ', while Pl_b and Ω are also significantly correlated but at 95% confidence level. The averaging windows for peak correlations with the aforementioned parameters are similar, ranging from 6 to 8 days preceding surveys. Correlation is positive for all these parameters (except δ'), implying that increases in H_b and T_p, with concomitant increases in E_o, P_o and Ω (and decrease in δ') are translated into a clockwise rotation of the embayment with sediment transferences from the northern section towards the southern section. Anti-clockwise rotation occurs for low waves, and is possibly mediated by the increasing influence of stream discharge and tidal prism under low waves, allowing the development of a secondary stream channel flowing northwards along the foreshore (Freire *et al.*, 2011). Although breaker angle alone lacks any significant correlation with $c_2(t)$, correlation with Pl_b provides additional support to the rotation interpretation, as a positive linear relationship implies clockwise (anticlockwise) rotation due to positive-southwards (negative-northwards) alongshore wave energy flux.

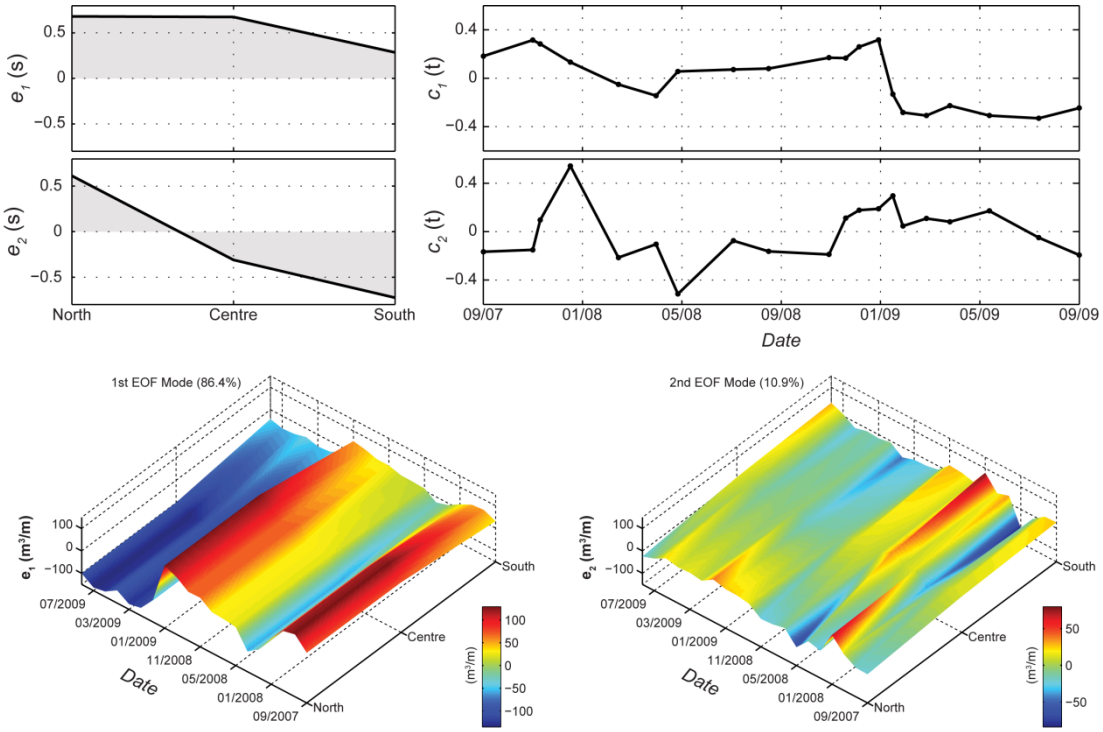

Figure 3.3 Normalized spatial ($e_n(s)$) and temporal ($c_n(t)$) eigenfunctions for Amoreira beach dataset (upper panels). Reconstruction of the first two EOF modes, based on the combined analysis of the spatial and temporal eigenfunctions (lower panels). North, Centre and South are relative to the profiles location at the beach.

3.4.2 Mt. Clérigo

The spatial eigenfunction $e_1(s)$ at Mt. Clérigo beach indicates a uniform pattern of morphological change, with a slightly higher variability in the central section (Fig. 3.4). Similarly to Amoreira beach, the combined eigenfunctions for $e_1(s,t)$ (Fig. 3.4), demonstrate an embayment-wide morphological response, with a seasonal signal. Accretion occurs during summer conditions and erosion in winter. Again, the negative peak after January 2009 marks the occurrence of extreme storm events. This temporal variability of $c_1(t)$ is significantly correlated with Pn_o (R = -0.65 at D = 1). The strong negative correlation peaking at the shorter averaging window suggests a prompt morphological response to changing wave conditions when normalised by the tide.

The second mode eigenfunction for Mt. Clérigo is alongshore non-uniform (Fig. 3.4). This alongshore non-uniform pattern is consistent with beach rotation behaviour, characterized by the out of phase response between both ends of the embayment (Fig. 3.4). Significant correlations were found between $c_2(t)$ and the parameters H_b, Ω and δ', with peak values obtained for D = 1 day (Table 3.3). While the spatial eigenfunction $e_2(s)$ is consistent with a rotation scenario, the absence of correlation between $c_2(t)$ and the two forcing parameters that include directional information, θ_b and Pl_b, indicates that rotation is not likely related with directional forcing. Highly significant correlation with δ' does, however, suggest that surf zone circulation may be the cause of this apparent rotation between opposite extremes of the beach.

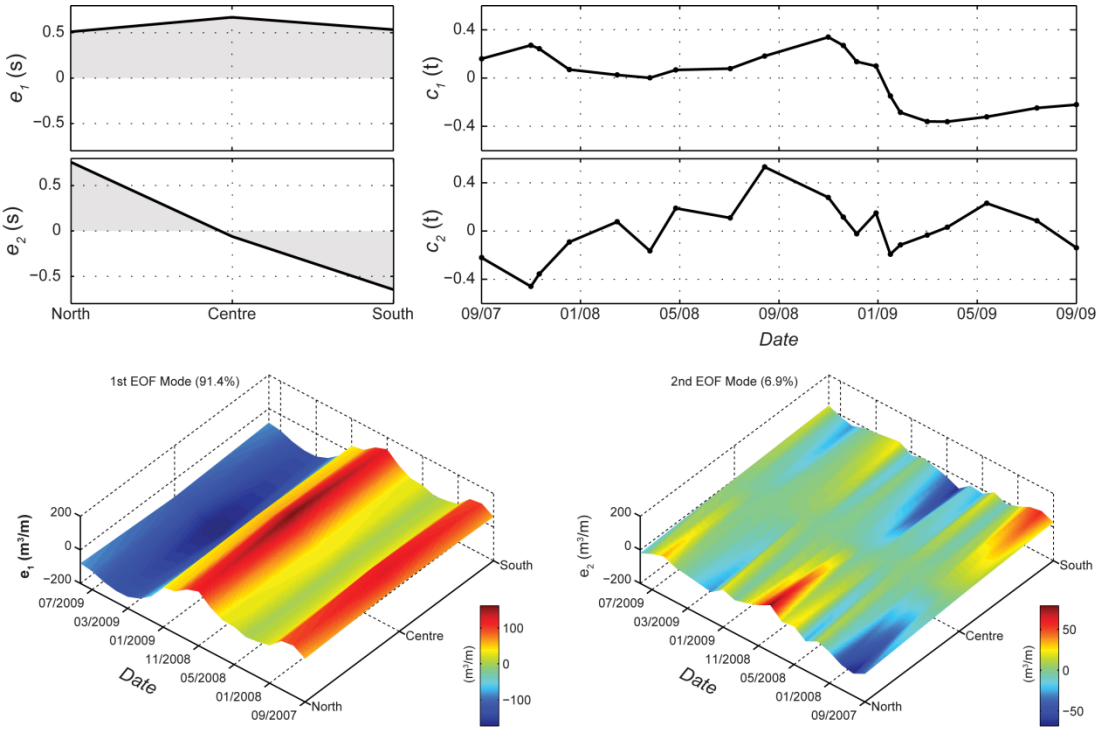

Figure 3.4 Normalized spatial ($e_n(s)$) and temporal ($c_n(t)$) eigenfunctions for Mt. Clérigo beach dataset (upper panels). Reconstruction of the first two EOF modes, based on the combined analysis of the spatial and temporal eigenfunctions (lower panels). North, Centre and South are relative to the profiles location at the beach.

3.4.3 Arrifana

Arrifana is the longest yet most indented embayment among the westerly exposed beaches. Mode one eigenfunction $e_1(s,t)$ for this beach follows the general pattern identified for the other embayments. The spatial variability$e_1(s)$ indicates that the beach responds uniformly with both ends experiencing similar, but more extreme, changes than the central section (Fig. 3.5). The timing of these changes displays identical seasonal signal to those described for Mt. Clérigo and Amoreira. Several forcing parameters are significantly correlated with $c_1(t)$, (H_b, T_p, E_o, P_o, Pn_o, Pl_b and Ω). Given the particularly strong negative correlation with Pn_o (Table 3.3), already noted for the other embayments, but with a wider peak averaging window (D = 12), it is likely that the higher confinement of Arrifana promotes a delayed morphological response comparing to the more exposed embayments, possibly due to enhanced attenuation of the local wave climate.

Mode two spatial eigenfunction $e_2(s)$ presents an alongshore non-uniform behaviour, characterized by higher variability in the central section (Fig. 3.5). Two nodal points occur near the extremities of the beach, lessening the magnitude of changes close to site boundaries for this eigenfunction. None of the forcing parameters is significantly correlated with $c_2(t)$, which restricts the physical interpretation of this mode. Development of circulation cells at the extremities of the beach with onshore re-attachment of sub- to inter-tidal crescentic bars in the central section has been observed in this embayment. These possibly embody a mechanism for beach recovery following rip-induced erosion reported during storms at Arrifana (Loureiro *et al.*, 2012). However, such hypothesis cannot be confirmed, as the forcing parameter δ', which characterizes embayment surfzone circulation, provided no statistically significant support.

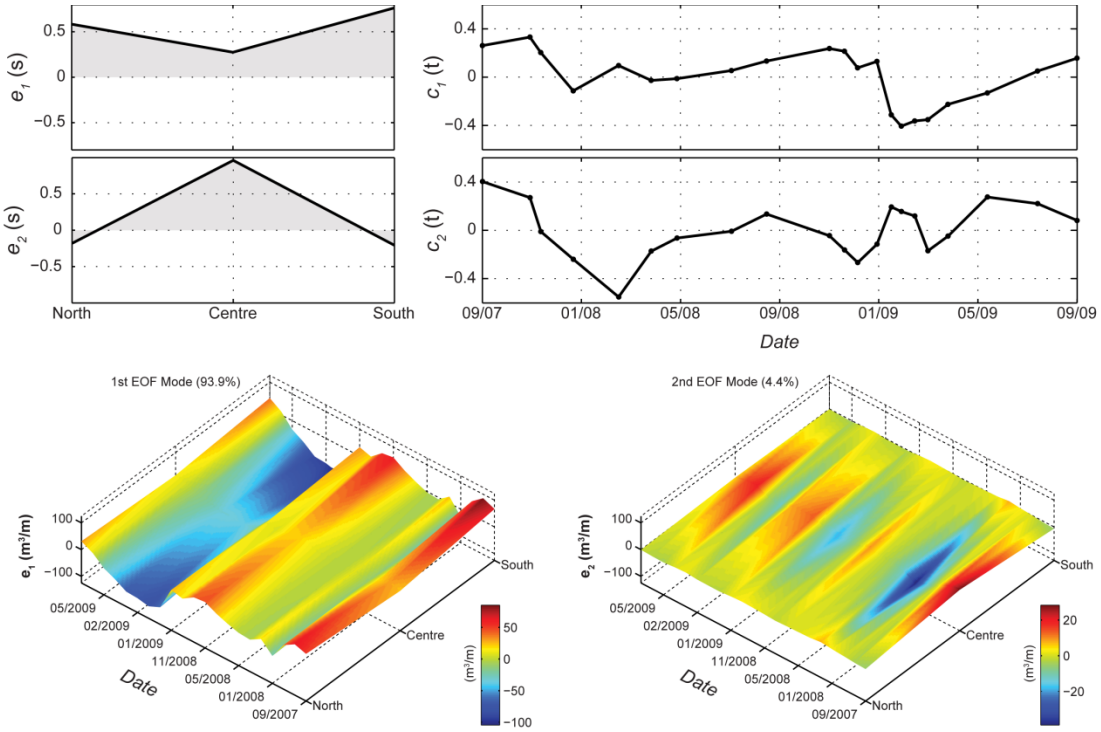

Figure 3.5 Normalized spatial ($e_n(s)$) and temporal ($c_n(t)$) eigenfunctions for Arrifana beach dataset (upper panels). Reconstruction of the first two EOF modes, based on the combined analysis of the spatial and temporal eigenfunctions (lower panels). North, Centre and South are relative to the profiles location at the beach.

3.4.4 Salema

Salema is the embayment where $e_1(s,t)$ ranks the lower relative importance, representing roughly 67% of the variance (Table 3.2). Absence of nodal points for $e_1(s)$ indicates that morphological changes are synchronous at the entire embayment, with the central and western sectors concentrating the bulk of the variability (Fig. 3.6). Correlation of $c_1(t)$ is statistically significant with several parameters, as indicated in Table 3.3, particularly those derived from an energetics-based approach to hydrodynamic forcing. The stronger correlations are again obtained with Pn_o, displaying a negative signal and peak correlations at D = 10 days.

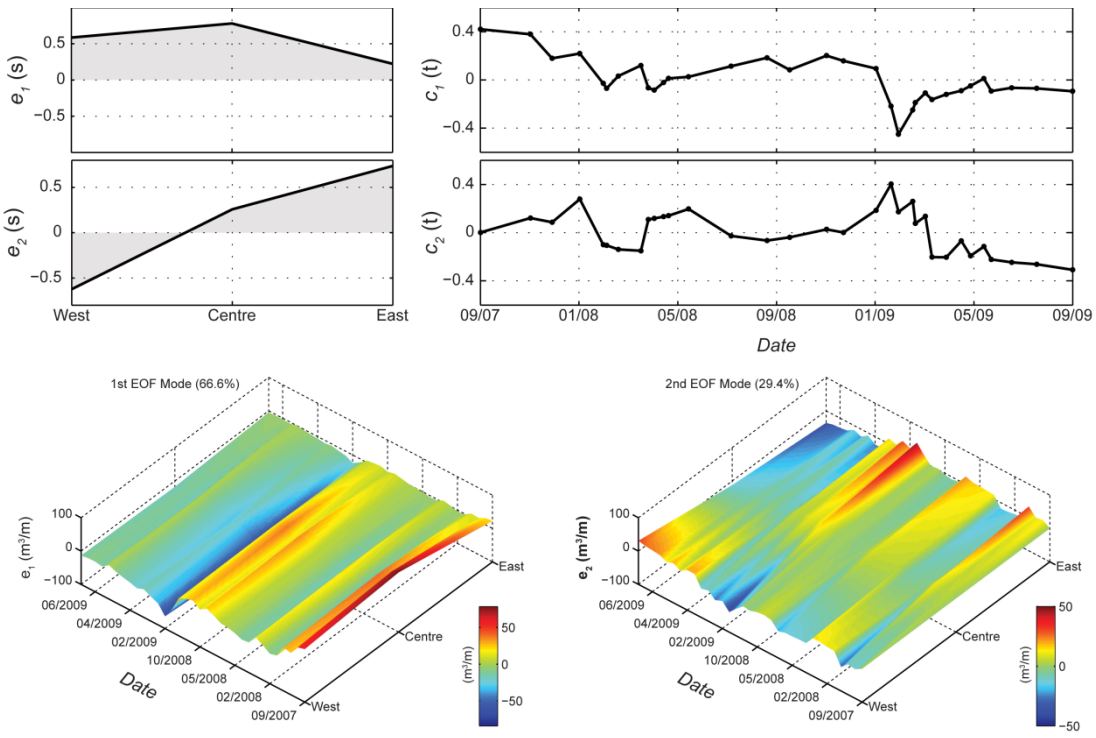

Figure 3.6 Normalized spatial ($e_n(s)$) and temporal ($c_n(t)$) eigenfunctions for Salema beach dataset (upper panels). Reconstruction of the first two EOF modes, based on the combined analysis of the spatial and temporal eigenfunctions (lower panels). West, Centre and East are relative to the profiles location at the beach.

Given the lower relative importance of $e_1(s,t)$, mode two eigenfunction $e_2(s,t)$ has a higher contribution for explaining the variability in Salema dataset (29%). This eigenfunction is consistent with the beach rotation scenario, with a nodal point close to the central section of the beach. The combined spatial and temporal eigenfunctions also support the hypothesis of beach rotation, and out-of-phase behaviour is evident in Fig. 3.6. Correlation analysis of $c_2(t)$ with forcing parameters reinforces this interpretation, with direction-dependent parameters (θ_b and Pl_b) presenting significant correlations, peaking at 6 to 7 days preceding surveys. Given the strong association between direction and wave period for the southern Portuguese coast (WSW swell with longer T_p or locally generated SE sea with shorter T_p), both T_p and H_o/L_o present very significant correlations with $c_2(t)$, further emphasising the wave-forced beach rotation scenario.

3.4.5 Boca do Rio

The primary mode of variability $e_1(s,t)$ in Boca do Rio presents an alongshore uniform pattern of beach change, with slight differences between beach sectors, generally describing a coherent response throughout the entire embayment (Fig. 3.7). The first mode eigenfunction is marked by a decrease in the temporal amplitude $c_1(t)$ in the first six months of study, followed by an invariant trend, occasionally disturbed by short lived peaks of beach accretion (Fig. 3.7). This unusual temporal variability is not correlated to any forcing parameter (Table 3.3) hampering the physical interpretation of mode one in Boca do Rio.

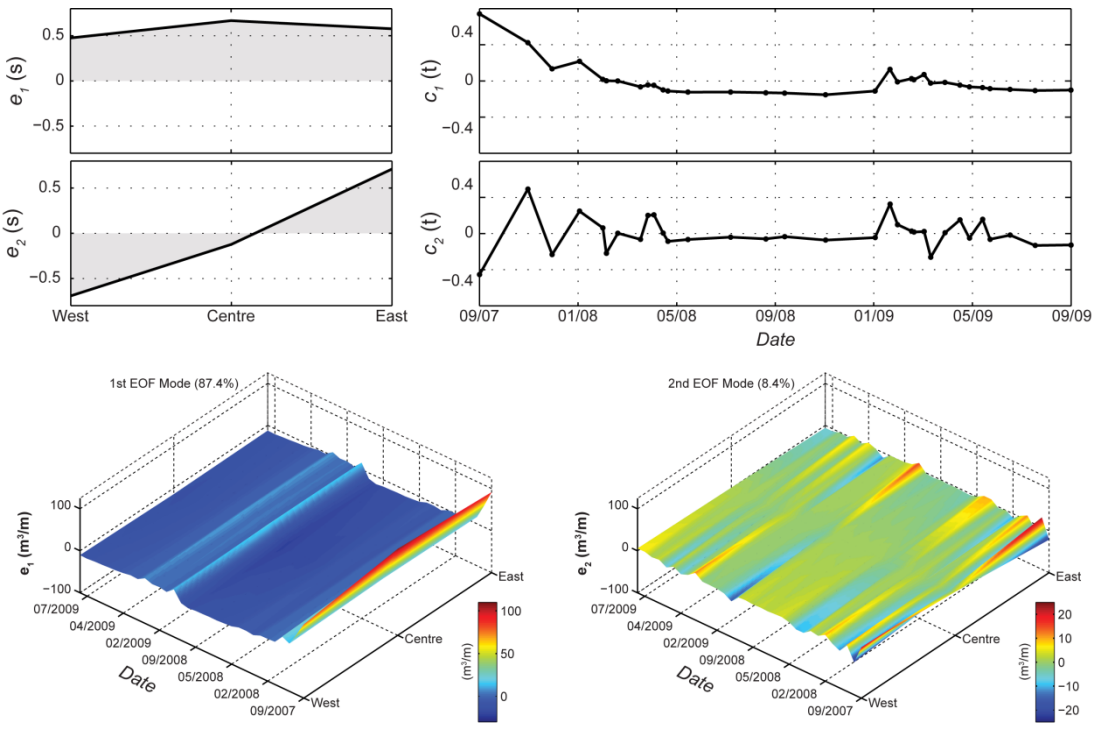

Figure 3.7 Normalized spatial ($e_n(s)$) and temporal ($c_n(t)$) eigenfunctions for Boca do Rio beach dataset (upper panels). Reconstruction of the first two EOF modes, based on the combined analysis of the spatial and temporal eigenfunctions (lower panels). West, Centre and East are relative to the profiles location at the beach.

Mode two spatial eigenfunction $e_2(s)$ for Boca do Rio follows the pattern of beach rotation previously described. The strong correlation of $c_2(t)$ with θ_b and Pl_b, for identical averaging windows (Table 3.3), confirms the hypothesis of a short-term beach rotation scenario at Boca do Rio.

3.4.6 Cabanas Velhas

Cabanas Velhas primary mode of variability $e_1(s,t)$ is also characterized by a coherent alongshore pattern with higher variability for $e_1(s)$ in the eastern sector (Fig. 3.8). The chronology of the changes described for Cabanas Velhas $c_1(t)$ is analogous to Boca do Rio $c_1(t)$, but with a sharper decrease in the first few months of study. Strong negative correlations were obtained between $c_1(t)$ and Pn_o, peaking at D = 4 days, reflecting the short-term inverse response to wave conditions along the entire embayment, enhanced by the effects of tidal range variation.

The second mode spatial variability $e_2(s)$ is alongshore non-uniform, with two nodal points closer to the extremes and an area of higher variability in the central section of the embayment (Fig. 3.8). Variability of $e_2(s,t)$ is consistent with the occurrence of erosion and accretion pulses in the central section of the beach, possibly with a partial contribution to and from the eastern section. Positive correlation values (R = 0.36 to 0.37) and long averaging windows (D = 17 to 18 days) between $c_2(t)$ and wave forcing parameters H_b, E_o, P_o, Ω, suggests that accretionary pulses might occur under moderate to high waves. Although necessarily below the storm threshold value ($H_o \geq 3$ m), higher than average wave forcing is likely to promote the transfer of sediment from the subtidal terrace to the intertidal beach in the bedrock fronted central section of Cabanas Velhas, similar to the effect of large swells in reef-fronted beaches (Miller and Fletcher, 2003).

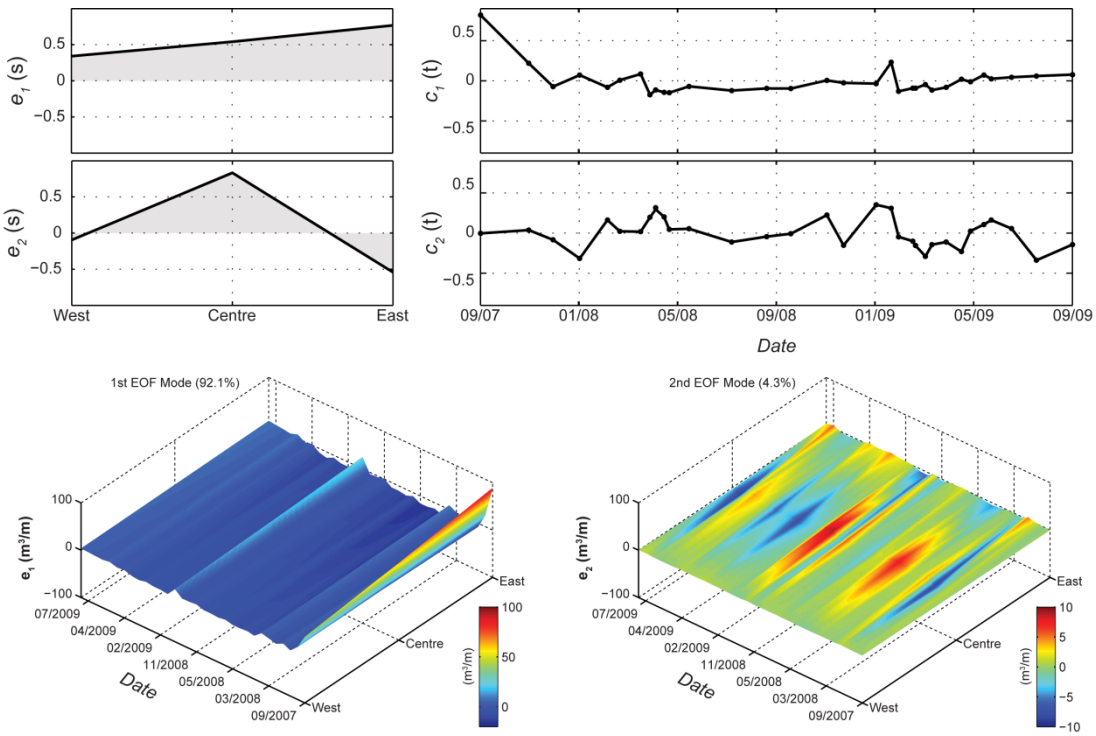

Figure 3.8 Normalized spatial ($e_n(s)$) and temporal ($c_n(t)$) eigenfunctions for Cabanas Velhas beach dataset (upper panels). Reconstruction of the first two EOF modes, based on the combined analysis of the spatial and temporal eigenfunctions (lower panels). West, Centre and East are relative to the profiles location at the beach.

3.5 DISCUSSION

3.5.1 Forcing parameters and response times

Selection of forcing parameters for exploring beach and nearshore morphological behaviour is not obvious or straightforward. Other parameters, reflecting similar nearshore forcing, where considered, for example, by Miller and Dean (2007b) and Fairley *et al.* (2009) in comparable EOF analysis of morphological change. However, observed significant correlations at the 99% confidence level with at least one of the selected parameters for most eigenfunctions substantiates the validity of our choices. In the results presented here, only two eigenfunctions, $c_2(t)$ in Arrifana and $c_1(t)$ in Boca do Rio, were uncorrelated with the forcing parameters selected. This highlights

the case for caution in the interpretation of EOF decompositions, as physical significance of EOF modes can be misleading (Dommenget and Latif, 2002). However, when statistically significant correlation can be identified with meaningful forcing parameters, as shown by the majority of the eigenfunctions analysed, physical interpretation of EOF modes should be considered with confidence (Miller and Dean, 2007b).

From all parameters considered, a marked consistency in strong negative correlation was identified between the first mode eigenfuntion and normalized wave power (Pn_o) for all but Boca do Rio embayment. Such correlation agrees with the findings of Fairley *et al.* (2009), where the first mode eigenfunction of shoreline variability behind detached breakwaters was also negatively correlated with a proxy combining wave and tidal forcing. Pn_o always provides the stronger correlation with $c_1(t)$, highlighting that the incorporation of tidal range variability for normalizing wave power enhances the explanatory ability of this parameter to describe morphological behaviour, as suggested by Morris *et al.* (2001). This has implications for energetics-based modelling of coastal changes, as this reasoning might be applied to template models of coastal change in meso to macrotidal beaches (*e.g.* Yates *et al.*, 2009).

Recent modelling and data-analysis work using EOFs on a Mediterranean embayed beach by Alvarez-Ellacuria *et al.* (2011) indicates a decoupling of response times in morphological behaviour. In their results, longshore response attributed to the second mode eigenfunction lags cross-shore response associated with the first mode eigenfunction by three days. This decoupling pattern is noticeable in several of the study sites presented here, although not holding consistently for all embayments. Most cases, however, appear to reflect a lag in response times, as evidenced for Amoreira with the first temporal eigenfunction peak correlation at D = 1 day, while the second

mode eigenfunction peaks at D = 7 to 8 days (Table 3.3). Less frequently, both modes peak at the same averaging interval (*e.g.* Mt. Clérigo with D = 1). Such site-specific response times are likely the result of diverse degrees of exposure and compartmentalization of the various embayments. The general lag for mode two confirms the suggestions of Alvarez-Ellacuria *et al.* (2011) that the cross-shore and longshore components elucidated do not respond simultaneously, and also of Miller and Dean (2007b) that each mode has a particular response time. Assumptions that on decadal timescales cross-shore processes have a shorter-term response time that longshore processes (Lazarus and Murray, 2007), seem to be applicable also on monthly to seasonal timescales even for highly localized responses. Compartmentalization appears, however, to significantly influence response times, with longer response times in more constrained embayments (*e.g.* Arrifana).

3.5.2 Mechanisms for alongshore variability

Although early spatial and temporal decompositions of morphological variability using EOF analysis in embayed beaches provide indications that morphological change is associated with nearshore circulation cells (Clarke and Elliot, 1982, 1988; Clarke *et al.*, 1984), most recent studies using this technique have identified beach rotation as the core mechanism of alongshore non-uniformity in embayed beaches (Short *et al.*, 2000; Munõz-Pérez *et al.*, 2001; Short and Trembanis, 2004; Harley *et al.*, 2008; Ruiz de Alegría-Arzaburu *et al.*, 2010). The results shown here, with four beaches presenting second mode eigenfunctions typical of rotation mechanisms, further emphasize the role of beach rotation as a prevailing mode of alongshore variability in embayed beaches. Our results also confirm the ability of EOF analysis to extract the rotation component from diverse datasets. Wave direction-forced beach rotation is,

however, not consistently supported for all cases. While at Salema and Boca do Rio statistically significant correlation of $c_2(t)$ with both θ_b and Pl_b translates a clear directionally-forced rotation behaviour, expectable under the bi-directional wave climate of southern Portugal, the out of phase pattern observed also in Amoreira and Mt. Clérigo is unlikely to be attributable to a similar mechanism.

The appearance of beach rotation (when the extremes of an embayment are out of phase and a nodal point or transition zone exists (Klein *et al.*, 2002)), can in fact be promoted by physical processes other than directionally forced alongshore sediment transport as recently demonstrated by Harley *et al.*, (2011). Given the strength and signal of the correlation between various forcing and $c_2(t)$ at Amoreira (Table 3.3), clockwise rotation occurs in this embayment under energetic waves, while anti-clockwise rotation develops during low wave conditions. Such behaviour is most likely the result of complex non-linear interactions involving wave conditions, tidal prisms and fluvial discharge of the shallow coastal stream within Amoreira embayment (Oliveira *et al.*, 2010; Freire *et al.*, 2011). In Mt. Clérigo, the surf zone circulation is suggested as the driver of the out-of-phase response within the embayment for the second mode eigenfunction. Three-dimensional cellular circulation, with extensive rip current systems, has been shown to determine morphological change in Mt. Clérigo (Loureiro *et al.*, 2012). The formation, evolution and clogging of rip and feeder channels, along with the displacement of nearshore bars drives alongshore non-uniform variability producing an inverse response between the extremes of the embayment, similar to findings of Ojeda and Guillén (2008). Strong correlation of $c_2(t)$ with δ' at Mt. Clérigo (Table 3.3) further validates this hypothesis.

3.5.3 Boundary effects

Presumed independence of two- and three-dimensional components in coastal morphological change renders EOF decomposition a particularly useful tool for coastal research (Ruessink *et al.*, 2000). Accordingly, nearly all studies of alongshore variability using EOFs in embayed beaches succeeded in isolating the cross-shore component present in the first eigenfunction, describing the bulk of the variability, from the alongshore components in lower-rank eigenfunctions (*e.g.* Clarke and Eliot, 1982; Short *et al.*, 2000; Harley *et al.*, 2008; Alvarez-Ellacuria *et al.*, 2011). General acceptance of this decoupled morphological response elucidated by the EOF analysis provides a further opportunity to examine the boundary effects in the morphological response of embayed beaches. Vertical boundary effects should be revealed by the variability of the first mode eigenfunction, assumed to represent two-dimensional cross-shore response, while the second mode eigenfunction, embodying three-dimensional alongshore response, ought to portray the effects of lateral boundaries

For all embayments presented here the first mode eigenfunction corresponds to a roughly uniform spatial trend without zero crossings (or nodal points), although not necessarily linear. In the present context, variability in the spatial amplitudes of this eigenfunction is presumed to represent variable two-dimensional geological constraints. Lower $e_1(s)$ amplitudes are indicative of the limitation to free profile fluctuation by underlying hard rock (Clarke and Eliot, 1982; Vousdoukas *et al.*, 2007), implying an effective vertical boundary control on beach profile evolution. The specific mechanisms that determine this constrained dynamics are not yet adequately understood (Gallop *et al.*, 2011b), as they are a result of complex morphodynamic interference of rocky hard-bottoms with beach morphologic change (Larson and Kraus, 2000; Vousdoukas *et al.*, 2007). However, it is generally considered that profile behaviour is dependent on the

depth and shape of the underlying geological control (Jackson *et al.*, 2005; Jackson and Cooper, 2009). As such, significant differences exist between the moderate-energy sediment-deprived south coast beaches and the high-energy sediment-richer west coast beaches. Considering both south and west coast embayments in the conceptual framework of Jackson and Cooper (2009), our results place west coast dissipative embayments within the vertical unconstrained beach type, while Salema more likely conforms to the semi-constrained and Boca do Rio and Cabanas Velhas are undoubtedly in the highly-constrained beach type.

South coast embayments, Salema, Boca do Rio and Cabanas Velhas, clearly show evidence of vertical boundary effects, and sectors where underlying geological control is shallower present reduced $e_1(s)$ amplitudes, increasing towards sections with deeper sediment veneers. This gradation can be observed in all three embayments, with the eastern sector in Salema and the western sector in Boca do Rio and Cabanas Velhas displaying minimums in the first mode spatial eigenfuntion (Fig. 3.6 to Fig. 3.8). Variable depths of the vertical boundary also imply diverse temporal response for hydrodynamic forced profile modification. Within the south coast beaches, Salema displays temporal variability of $c_1(t)$ broadly consistent with a seasonal forced response, while Boca do Rio and Cabanas Velhas present roughly invariant trends for $c_1(t)$ following severe erosion in the first months of monitoring. Muñoz-Perez *et al.* (2010) suggested that geologically controlled beach profiles are prone to erosive trends and less able to recover during accretionary periods, and this appears to be the case in the south coast beaches presented here. Thin veneers of sediment covering the underlying rocky substrate in Boca do Rio and Cabanas Velhas were easily eroded in the first months of monitoring. Recovery was limited and both embayments remained depleted by the end of the monitoring period. The limited sediment contained within Salema embayment is,

nonetheless, sufficient to enable the development of a sub-aerial beach profile that varies seasonally with significant recovery volumes, as demonstrated by the variability of $c_1(t)$. Such varied behaviour of south coast embayments confirms the suggestions of Muñoz-Perez *et al.* (2010), further emphasizing an enhancement in recovery ability as sediment depth increases.

Vertical boundary effects in west coast beaches are less readily apparent from the first mode eigenfunction. The underlying geological control is significantly deeper and was never exposed for most profiles, yet there are variations in the spatial amplitude of the first mode eigenfunctions, particularly noticeable in Arrifana embayment. Mechanisms other than direct influence of underlying rocky substrate must be considered for the west coast beaches. The highly three-dimensional nearshore behaviour of these high-energy beaches, where large scale rip systems develop during storms and persist for several months (Loureiro *et al.*, 2012), appears to be responsible for the variable spatial amplitudes of $e_1(s)$, as the topographically-controlled location of such rip systems is consistent with the areas of increased variability for $e_1(s)$.

Effects of lateral boundaries have received far more attention in studies of morphological variation in embayed beaches, and an established base of literature exists now demonstrating the utility of EOF analysis in extracting the rotation component from morphological change datasets (*e.g.* Short *et al.*, 2000; Munõz-Pérez *et al.*, 2001; Short and Trembanis, 2004; Miller and Dean, 2007a; Harley *et al.*, 2008; Ruiz de Alegría-Arzaburu *et al.*, 2010). A characteristic rotation pattern for the second mode spatial eigenfunction, with a nodal point separating sectors of inverse morphological response, facilitates interpretation. In most cases, such lateral boundary effects are manifested in embayed beaches through the interruption of longshore sediment transport by a downdrift headland, as a result of seasonal or periodic shifts in wave

climate (Short, 1999). When directional forcing can be associated with the spatial patterns of beach rotation, as in Salema and Boca do Rio, lateral boundaries unequivocally exert their effects by disrupting longshore sediment transport. However, lateral boundary effects can also be manifested through modification of nearshore circulation (Short, 1999). Interpretation of nearshore circulation mechanisms, particularly topographically-controlled rips, is not as straightforward as directionally forced beach rotation due to irregular EOF spatial amplitude patterns (Clarke and Eliot, 1982). Nevertheless, correlation with forcing parameters sensitive to beach type and morphodynamic behaviour, notably Ω and δ', does provide indications of the importance of laterally constrained nearshore circulation mechanisms in the three-dimensional behaviour of Cabanas Velhas, Mt. Clérigo and Amoreira embayments.

In coastal embayments it is generally assumed that boundary effects will influence only the sections close to the headlands, leaving a central section relatively unaffected by the site boundaries (Short, 1999; Miller and Dean, 2007a). While this is likely to be the case in wide embayments, the six study sites presented here are clearly small embayments and boundary effects are manifested along the entire beach. Our original hypothesis that vertical and lateral geological boundaries constrain the morphological behaviour of embayed beaches is abundantly supported by the results. Moreover, although it is not possible to state that the relative importance of two- and three dimensional changes directly relates to the variances explained respectively by the first and second mode eigenfunctions, a clear relation exists between these two variables, as postulated by Ruessink *et al.* (2000). Such distinction provides support to our secondary hypothesis that boundary effects can be decoupled from datasets of embayed beach morphological change.

Finally, a framework for boundary effects in geologically constrained embayed beaches is proposed (Fig. 3.9), which considers a basic control on boundary effects by the sedimentary budget. Sediment abundant embayed beaches, with large accommodation spaces, are generally unaffected by vertical boundary effects. They are, however, prone to exhibit lateral boundary effects through constraining of nearshore 3D circulation and/or longshore sediment transport. The relative importance of these processes varies inversely in response to changes in embayment indentation and obliquity of wave approach. Within sediment-deprived embayments the controls on boundary effects are determined mainly by substrate depth and wave obliquity. Increases in both parameters enhance lateral boundary effects, frequently promoting beach rotation, while reductions impose constrains on the cross-shore sediment transport leading to reduced profile fluctuation.

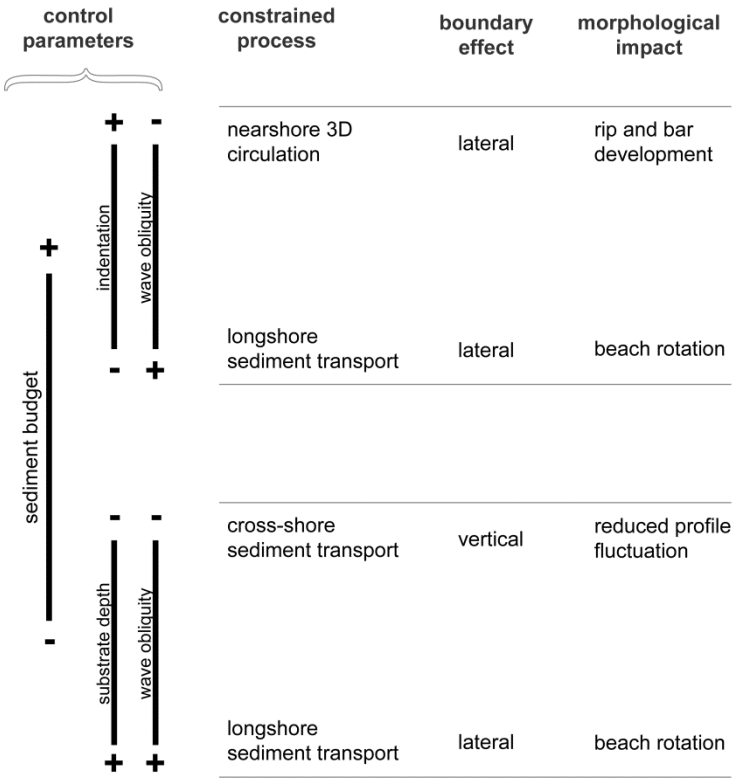

Figure 3.9 Conceptual framework describing boundary effects in embayed beaches

3.6 CONCLUSIONS

This study shows that natural geological boundaries constrain the morphological behaviour of embayed beaches, determining diverse spatial and temporal variability patterns within the six embayments analysed. Localized responses produced by lateral and vertical boundary interference with nearshore dynamics, including beach rotation, topographic-controlled rip circulation and subdued profile fluctuation, are suggested as the primary drivers of alongshore non-uniform morphological variability. Examination of second mode eigenfunction is consistent with recent work suggesting that directionally forced beach rotation is the most frequent mode of alongshore variability in embayed beaches. Rotation patterns can, however, also emerge due to cellular circulation mechanisms or even as a result of complex interactions involving wave conditions, tidal prisms and fluvial discharge of shallow coastal streams.

EOF decomposition confirms suggestions of a spatial decoupling in cross- and longshore responses. Variable peak correlation of temporal amplitudes and forcing parameters also indicates a decoupling in cross- and longshore response times, which appear to increase for more constrained embayments. Highly significant peak correlations of the normalized wave power with the first mode of morphological variability further suggests that, for exposed mesotidal coastal environments, a parameter combining wave and tide variability is likely to increase process-response relations between hydrodynamic forcing and morphological change.

Lateral and vertical geological boundaries exert their effects fundamentally by restraining longshore sediment transport, inducing cellular surf zone circulation and by impacting cross-shore sediment transport. While sediment abundance is suggested as the fundamental element determining boundary effects, embayment indentation, wave

obliquity and substrate depth are considered decisive to determine the morphological impact of vertical and lateral geological boundaries.

3.7 ACKNOWLEDGEMENTS

This work is a contribution to Project BAYBEACH – Evolution and Management of Embayed Beaches in Contrasting Environments, funded by FCT under contract PTDC/CTE-GEX/66893/2006. Carlos Loureiro was supported by FCT, grant reference SFRH/BD/27878/2006. Hydrodynamic data was provided by Instituto Hidrográfico. Modelled WANA wave data were supplied by Puertos del Estado. We gratefully acknowledge the help of everyone involved in the fieldwork data collection, frequently under severe weather conditions. We are especially grateful to Mara Nunes (CIMA - UALG) for valuable assistance during surveying and Lluís Gómez-Pujol (SOCIB - IMEDEA) for thoughtful insights and documentation regarding EOF analysis.

3.8 REFERENCES

Almeida, L.P., Ferreira, Ó., Pacheco, A., 2011. Thresholds for morphological changes on an exposed sandy beach as a function of wave height. *Earth Surface Processes and Landforms* 36, 523-532.

Archetti, R. and Romagnoli, C., 2011. Analysis of the effects of different storm events on shoreline dynamics of an artificially embayed beach. *Earth Surface Processes and Landforms* 36, 1449-1463.

Aubrey, D.G., 1979. Seasonal patterns of onshore/offshore sediment movement. *Journal of Geophysical Research* 84 (C10), 6347-6354.

Clarke, D.J. and Eliot, I.G., 1982. Description of littoral, alongshore sediment movement from empirical eigen-function analysis. J*ournal of the Geological Society of Australia* 29, 327-341.

Clarke, D.J. and Eliot, I.G., 1988. Low-frequency changes of sediment volume on the beachface at Warilla beach, New South Wales, 1975-1985. *Marine Geology* 79, 189-211.

Clarke, D.J., Eliot, I.G., Frew, J.R., 1984. Variation in subaerial beach sediment volume on a small sandy beach over a monthly lunar tidal cycle. *Marine Geology* 58, 319-344.

Costa, M. and Esteves, R., 2010. Clima de agitação marítima na costa oeste de Portugal Continental. Proceedings of XI Jornadas Técnicas de Engenharia Naval – O Sector Marítimo Português. Edições Salamadra, Lisboa, Portugal, pp. 413-426.

Costa, M., Silva, R., Vitorino, J., 2001. Contribuição para o estudo do clima de agitação marítima na costa Portuguesa. Proceedings of 2as Jornadas de Engenharia Costeira e Portuária. AIPCN, Aveiro, Portugal (20 p. CD-ROM).

Dean, R.G., 1973. Heuristic models of sand transport in the surf zone. Proceedings of the First Australian Conference on Coastal Engineering - Engineering Dynamics of the Coastal Zone. Institute of Engineers, Sydney, Australia, 208-214.

Dean, R.G. and Dalrymple, R.A., 2002. *Coastal Processes with Engineering Applications*. Cambridge University Press, Cambridge. 475 p.

Dommenget, D. and Latif, M., 2002. A cautionary note on the interpretation of EOFs. *Journal of Climate* 15, 216-225.

Fairley, I., Davidson, M., Kingston, K., Dolphin, T., Philips, R., 2009. Empirical orthogonal function analysis of shoreline changes behind two different designs of detached breakwaters. *Coastal Engineering* 56, 1097-1108.

Finkelstein, K., 1982. Morphological variations and sediment transport in crenulate-bay beaches, Kodiak Island, Alaska. *Marine Geology* 47, 261-281.

Freire, P., Taborda, R., Bertin, X., Guerreiro, M., Fortunato, A.B., Silva, A.M., Andrade, C., Oliveira, A., Antunes, C., Freitas, M.C., Nahon, A., Rodrigues, M., Bruneau, N., 2011. Medium-term morphodynamic evolution of a small coastal inlet. *Journal of Coastal Research* SI 64, 666-670.

Gallop, S.L., Bosserelle, C., Pattiaratchi, C.B., Eliot, I., 2011a. Hydrodynamic and morphological response of a perched beach during sea breeze activity. *Journal of Coastal Research* SI 64, 78-79.

Gallop, S.L., Bosserelle, C., Pattiaratchi, C.B., Eliot, I., 2011b. Rock topography causes spatial variation in the wave, current and beach response to sea breeze activity. *Marine Geology* 290, 29-40.

Gómez-Pujol, L., Orfila, A., Álvarez-Ellacuría, A., Tintoré, J., 2011. Controls on sediment dynamics and medium-term morphological change in a barred microtidal beach (Cala Millor, Mallorca, Western Mediterranean). *Geomorphology* 132, 87-98.

Gourlay, M.R., 1968. Beach and Dune Erosion Tests I. Report M935/M936, Delft Hydraulics Laboratory.

Hansen, J.E. and Barnard, P.L. 2010. Sub-weekly to interannual variability of a high-energy shoreline. *Coastal Engineering* 57, 959-972.

Harley, M.D., Turner, I.L., Short, A.D, Ranasinghe, R., 2008. Rotation and oscillation of an embayed beach. Proceedings of the 31st International Conference on Coastal Engineering. World Scientific Publishing, Singapore. 865-875.

Harley, M.D., Turner, I.L., Short, A.D, Ranasinghe, R., 2011. A reevaluation of coastal embayment rotation: the dominance of cross-shore versus alongshore transport

processes, Collaroy-Narrabeen Beach, southeast Australia. *Journal of Geophysical Research* 116, F040033.

Haxel, J.H. and Holman, R.A., 2004. The sediment response of a dissipative beach to variations in wave climate. *Marine Geology* 206, 73-99.

Hsu, J.R.C., Benedet, L., Klein, A.H.F., Raabe, A.L.A., Tsai, C.P., Hsu, T.W., 2008. Appreciation of static bay beach concept for coastal management and protection. *Journal of Coastal Research* 24, 198-215.

Jackson, D.W.T. and Cooper, J.A.G., 2009. Geological control on beach form: accommodation space and contemporary dynamics. *Journal of Coastal Research* SI 56, 69-72.

Jackson, D.W.T., Cooper, J.A.G., del Rio, L., 2005. Geological control of beach morphodynamic state. *Marine Geology* 216, 297-314.

Klein, A.H.F, Benedet, L., Schumacher, D.H., 2002. Short-term beach rotation processes in distinct headland bay beach systems. *Journal of Coastal Research* 18, 442-458.

Klein, A.H.F, Ferreira, Ó., Dias, J.M.A., Tessler, M.G., Silveira, L.F., Benedet, L., Menezes, J.T., Abreu, J.G.N., 2010. Morphodynamics of structurally controlled headland-bay beaches in southeastern Brazil: a review. *Coastal Engineering* 57, 98-111.

Kroon, A., Larson, M., Möller, I., Yokoki, H., Rozynsky, G., Cox, J., Larroude, P., 2008. Statistical analysis of coastal morphological data sets over seasonal to decadal time scales. *Coastal Engineering* 55, 581-600.

Lahoz, M.G. and Albiach, J.C.C., 2005. Wave forecasting at the Spanish coasts. *Journal of Atmospheric & Ocean Science* 10, 389-405.

Larson, M., Capobianco, M., Jansen, H., Rózynski, G., Southgate, H.N., Stive, M., Wijnberg, K.M., Hulscher, S., 2003. Analysis and modelling of field data on coastal morphological evolution over yearly and decadal time scales. Part 1: background and linear techniques. *Journal of Coastal Research* 19, 760-775.

Larson, M., Hanson, H., Kraus, N.C., Newe, J., 1999. Short- and long-term responses of beach fills determined by EOF analysis. *Journal of Waterway, Port, Coastal and Ocean Engineering* 125, 285-293.

Larson, M., Hoan, L.X., Hanson, H., 2010. Direct formula to compute wave height and angle at incipient breaking. *Journal of Waterway, Port, Coastal and Ocean Engineering* 136, 119-122.

Larson, M. and Kraus, N.C., 2000. Representation of non-erodible (hard) bottoms in beach profile change modelling. *Journal of Coastal Research* 16, 1-14.

Lazarus, E.D. and Murray, A.B., 2007. Process signatures in regional patterns of shoreline change on annual to decadal time-scales. *Geophysical Research Letters* 34, L19402.

Loureiro, C., Ferreira, Ó., Cooper, J.A.G., 2011. Morphologic change and morphodynamics at high-energy embayed beaches in southwestern Portugal. Proceedings of Coastal Sediments 2011. World Scientific Publishing, Singapore. Vol. 2, 1375-1389.

Loureiro, C., Ferreira, Ó., Cooper, J.A.G., 2012. Extreme erosion on high-energy embayed beaches: influence of megarips and storm groups. *Geomorphology* 139-140, 155-171.

Martins, C.C., Mahiques, M.M., Dias, J.M.A., 2010. Daily morphological changes determined by high-energy events on an embayed beach: a qualitative model. *Earth Surface Processes and Landforms* 35, 487-495.

Masselink, G. and Pattiaratchi, C.B., 2001. Seasonal changes in beach morphology along the sheltered coastline of Perth, Western Australia. *Marine Geology* 172, 243-263.

Miller, J.K. and Dean, R.G., 2007a. Shoreline variability via empirical orthogonal function analysis: Part I temporal and spatial characteristics. *Coastal Engineering* 54, 111-131.

Miller, J.K. and Dean, R.G., 2007b. Shoreline variability via empirical orthogonal function analysis: Part II relationship to nearshore conditions. *Coastal Engineering* 54, 133-150.

Miller, T.L. and Fletcher, C.H., 2003. Waikiki: historical analysis of an engineered shoreline. *Journal of Coastal Research* 19, 1026-1043.

Morris, B.D., Davidson, M., Huntley, D., 2001. Measurements of the response of a coastal inlet using video monitoring techniques. *Marine Geology* 175, 251-272.

Muñoz-Perez, J.J., Medina, R., 2010. Comparison of long-, medium- and short-term variations of beach profiles with and without submerged geological control. *Coastal Engineering* 57, 241-251.

Muñoz-Pérez, J.J., Medina, R., Tejedor, B., 2001. Evolution of longshore beach contour lines determined by the E.O.F. method. *Scientia Marina* 65, 393-402.

Ojeda, E. and Guillén, J., 2008. Shoreline dynamics and beach rotation of artificial embayed beaches. *Marine Geology* 253, 51-62.

Oliveira, A., Fortunato, A.B., Guerreiro, M., Bertin, X., Bruneau, N., Rodrigues, M., Taborda, R., Andrade, C., Silva, A.M., Antunes, C., Freire, P., Pedro, S.L., Dodet, G., Loureiro, C., Mendes, A., 2010. Effect of inlet morphology and wave action on transport and sediment dynamics in a coastal stream. Proceedings of

the Eleventh International Conference on Estuarine and Coastal Modeling. ASCE Conference Proceedings 388, 601-620.

Phillips, J.D., 1985. Headland-bay beaches revisited: an example from Sandy Hook, New Jersey. *Marine Geology* 65, 21-31.

Quartel, S., Kroon, A., Ruessink, B.G., 2008. Seasonal accretion and erosion patterns of a microtidal sandy beach. *Marine Geology* 250, 19-33.

Ranasinghe, R., McLoughlin, R., Short, A.D., Symonds, G., 2004. The Southern Oscillation Index, wave climate and beach rotation. *Marine Geology* 204, 273-287.

Ruessink, B.G., van Enckevort, I.M.J., Kingston, K.S., Davidson, M.A., 2000. Analysis of observed two- and three-dimensional nearshore bar behaviour. *Marine Geology* 169, 161-183.

Ruiz de Alegría-Arzaburu, A. and Masselink, G., 2010. Storm response and beach rotation on a gravel beach, Slapton Sands, UK. *Marine Geology* 278, 77-99.

Ruiz de Alegría-Arzaburu, A.R., Pedrozo-Acuña, A., Horrillo-Caraballo, J.M., Masselink, G., Reeve, D.E., 2010. Determination of wave-shoreline dynamics on a macrotidal gravel beach using Canonical Correlation Analysis. *Coastal Engineering* 57, 290-303.

Sanderson, P.G. and Eliot, I., 1999. Compartmentalisation of beachface sediments along the southwestern coast of Australia. *Marine Geology* 162, 145-164.

Scott, T., Masselink, G., Russel, P., 2011. Morphodynamic characteristics and classification of beaches in England and Wales. *Marine Geology* 286, 1-20.

Short, A.D., 1996. The role of wave height, period, slope, tide range and embaymentisation in beach classifications: a review. *Revista Chilena de Historia Natural* 69, 589-604.

Short, A.D., 1999. *Handbook of Beach and Shoreface Morphodynamics*. John Wiley & Sons, Chichester. 379 p.

Short, A.D., 2010. Role of geological inheritance in Australian beach morphodynamics. *Coastal Engineering* 57, 92-97.

Short, A.D., Trembanis, A.C., Turner, I.L., 2000. Beach oscillations, rotation and the southern oscillation , Narrabeen Beach, Australia. Proceedings of the 27th International Conference on Coastal Engineering. ASCE, Sydney. 2439-2452.

Short, A.D. and Trembanis, A.C., 2004. Decadal scale patterns in beach oscillation and rotation, Narrabeen Beach, Australia – time series, PCA and wavelet analysis. *Journal of Coastal Research* 20, 523-532.

Silvester, R., 1985. Natural headland control of beaches. *Continental Shelf Research*, 4, 581-596.

Silvester, R. and Hsu, J.R.C., 1997. *Coastal Stabilization*. World Scientific, Singapore. 578 p.

Soulsby, R.L., 1997. *Dynamics of Marine Sands: a manual for practical applications*. Thomas Telford, London. 249 p.

Thomas, T., Phillips, M.R., Williams, A.T., 2010. Mesoscale evolution of a headland bay: beach rotation processes. *Geomorphology* 123, 129-141.

Thomas, T., Phillips, M.R., Williams, A.T., Jenkins, R.E., 2011. Short-term beach rotation, wave climate and the North Atlantic Oscillation (NAO). *Progress in Physical Geography* 35, 333-352.

van Enckevort, I.M.J. and Ruessink, B.G., 2003. Video observations of nearshore bar behaviour. Part 2: alongshore non-uniform variability. *Continental Shelf Research* 23, 513-532.

Vincent, L., Dolan, R., Hayden, Resio, D., 1976. Systematic variations in barrier-island topography. *Journal of Geology* 84, 583-594.

Vousdoukas, M.I., Velegrakis, A.F., Plomaritis, T.A., 2007. Beachrock occurrence, characteristics, formation mechanisms and impacts. *Earth-Science Reviews* 85, 23-46.

Vousdoukas, M.I., Velegrakis, A.F., Karambas, T.V., 2009. Morphology and sedimentology of a microtidal beach with beachrocks: Vatera, Lesbos, NE Mediterranean. *Continental Shelf Research* 29, 1937-1947.

Wijnberg, K.M. and Terwindt, J.H.J., 1995. Extracting decadal morphological behaviour from high-resolution, long-term bathymetric surveys along the Holland coast using eigenfunctions analysis. *Marine Geology* 126, 301-330.

Winant, C.D., Inman, D.L., Nordstrom, C.E., 1975. Description of seasonal beach changes using empirical eigenfunctions. *Journal of Geophysical Research* 80, 1979-1986.

Yates, M.L., Guza, R.T., O'Reilly, W.C., 2009. Equilibrium shoreline response: observations and modelling. *Journal of Geophysical Research* 114, C09014.

CHAPTER 4

Morphologic change and morphodynamics at high-energy embayed beaches in southwestern Portugal

Loureiro, C., Ferreira, Ó., Cooper, J.A.G., 2011. Morphologic change and morphodynamics at high-energy embayed beaches in southwestern Portugal. In Wang, P., Rosati, J.D., Roberts, T.M. (Eds.), *Proceedings of the Seventh International Symposium on Coastal Engineering and Science of Coastal Sediment Processes – Coastal Sediments'11*. World Scientific Publishing, Singapore. Volume II, pp. 1375-1389.

ABSTRACT

Along the southwestern coast of Portugal, a high-energy, swell dominated environment with a markedly seasonal wave climate, morphologic change in three embayed beaches was regularly monitored over a two year period. While a general seasonal pattern was identified, the occurrence of a storm group induced dramatic beach response, producing marked interannual variability. Significant spatial variations in behaviour emerged during the monitoring period, inducing alongshore non-uniform beach change within each embayment. Megarips were the prevailing mechanism responsible for the extreme erosion experienced in all three beaches, and their specific location (controlled by topography) contributes to the variability observed within each beach. Despite severe beach erosion, dunes were unaffected, which suggests long-term stability of these high-energy, dissipative, embayed coastlines.

KEYWORDS: embayed beaches; seasonality; storm impacts; alongshore variability; beach erosion.

4.1 INTRODUCTION

Cycles of erosion and accretion in wave-dominated beaches have been extensively studied and documented around the world's coastlines. Initial models of winter "cut" and summer "fill" were progressively replaced by models of cyclic beach change in response to changing wave conditions (Hayes and Boothroyd, 1969; Nordstrom, 1980), and further extended to fully integrate the three-dimensional behaviour of beaches and surf zones (Wright and Short, 1984). Nevertheless, for coastal environments with a strong seasonal wave climate, as in swell-dominated beaches, morphologic change is commonly reflected in erosion and accretion patterns in phase with the seasons (Quartel *et al.*, 2008). Although periodic storm erosion is not unique to any particular season, there is a general tendency for higher intensity and frequency of storms during the winter season (Hayes and Boothroyd, 1969; Fox and Davis, 1978; Quartel *et al.*, 2008). More frequent storms means a shorter timeframe for the slow pace post-storm recovery to occur, and only partial recovery is accomplished before the following storm occurs, preventing complete recovery until the end of the storm season (Fox and Davis, 1978). This pattern of morphological change on swell-dominated beaches creates a seemingly seasonal cycle of beach change, with beach volume

variation characterized by a post-winter minimum and reaching a maximum volume at the beginning of the winter, following summer accretion (Quartel *et al.*, 2008).

On high-energy dissipative beaches observations of the seasonal pattern of morphological change increased in recent years, highlighting marked alongshore variations in shoreline change (*e.g.* Ruggiero *et al.*, 2005; Hansen and Barnard, 2010). Alongshore non-uniform morphological change on high-energy dissipative beaches arises because beach response, especially during storms, does not linearly depend on wave conditions (Russell, 1993), due to reduced contribution of the incident wave frequency band in the beach and inner surf zone (Wright *et al.*, 1982; Russell, 1993). Instead, it depends on a combination of waves and infragravity oscillations, tidal phase and surge level, antecedent morphology and geomorphologic control (Cooper *et al.*, 2004; Ruggiero *et al.*, 2005). For embayed beaches on high-energy coastal environments, conditions for alongshore non-uniform response are even more pronounced, as geomorphologic control in beach morphodynamics is highly significant (Jackson *et al.*, 2005), and sediment movement and hydrodynamics in embayed beaches are heavily impacted by headlands (Short, 1999). Earlier reports of alongshore variation in morphological change of embayed beaches exposed to energetic wave conditions identified complex interactions between large scale embayment circulation, particularly those associated with rip currents developed during storms (Eliot and Clarke, 1982). The beach response associated with such large scale rip currents, later termed megarips by Short (1985), was found to vary alongshore and deviate from the seasonal trend of morphological change (Eliot and Clarke, 1982). Recent work has highlighted megarips as an important mechanism of morphological change on embayed beaches (Short, 2010), but they still remain a little studied coastal process (MacMahan *et al.*, 2005).

The aim of this paper is to investigate the variability of beach change in embayed beaches exposed to high-energy wave conditions. The temporal variation, associated with seasonal and episodic changes, as well as the non-uniform alongshore patterns of beach change are analysed, and the morphodynamic mechanisms that drive the observed behaviour are discussed.

4.2 STUDY AREA

The southwestern coast of Portugal, a high-energy swell environment, is a bedrock-framed coastline where beaches occur generally in embayments associated with small streams or in coastal re-entrants within the rocky cliffs. Along this coastline three beaches, Amoreira, Mt. Clérigo and Arrifana, were selected as study sites (Fig. 4.1). The first two are directly exposed to the dominant north-westerly waves while Arrifana roughly faces west and is partially protected by a prominent northern headland. These three relatively short beaches (between 500 and 750 m long) are composed of well sorted medium sand and, being exposed to a high-energy wave climate, are modally dissipative or intermediate skewed to dissipative in state. Amoreira embayment contains a bay-barrier estuary, with a small tidal stream meandering along the intertidal zone. The beach is wide and backed by an extensive dune field, presenting a persistent low tide terrace occasionally crossed by the tidal stream, which creates a ridge and runnel-like morphology. Mt. Clérigo also presents a wide beach backed by dunes in the south and centre, while the northern sector is narrow and backed by 50-m high cliffs. During most of the year the beach is typified by a gently sloping beach face, extending shoreward to the toe of the cliffs on the northern sector. A similar gentle sloping beach face extending to a gravel deposit at the cliff base characterizes Arrifana, a swash

aligned beach enclosed by up to 100 m high cliffs. The subaerial beach is narrow and rarely contains a well-defined berm, while the intertidal beach is wide and planar.

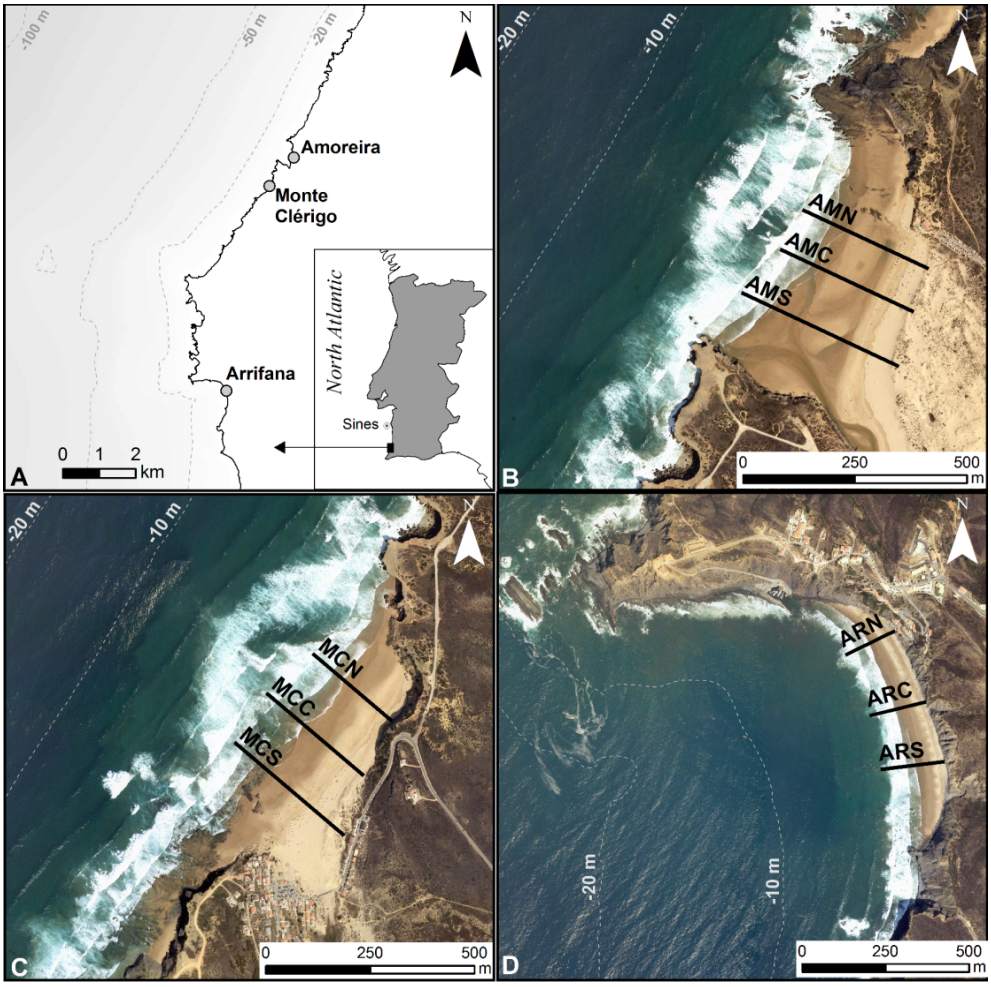

Figure 4.1 Location of the study area in the southwestern coast of Portugal (A). Amoreira (B), Mt. Clérigo (C) and Arrifana (D) embayments with profile identification (black lines).

Being exposed to the North Atlantic, the coastline of south-western Portugal experiences energetic conditions throughout the year, although with markedly seasonal variation. Mean monthly offshore significant wave heights (H_{so}) between 2 and 2.5 m occur from November to March, while during the remaining months H_{so} varies from 1 to 2 m (Costa and Esteves, 2010). Wave period follows a similar variation, with monthly peak periods (T_p) between 12 and 14 s from November to March and 9 to 12 s

during the rest of the year. Peak wave direction (θ) is constant throughout the year from NW-W direction (97.4% of the records) (Costa *et al.*, 2001; Costa and Esteves, 2010). Energetic wave conditions are relatively frequent, with H_{so} exceeding 3 m on 10% of the time. Storms along the western Portuguese coast are normally associated with $H_{so} \geq$ 5 m (Pita and Santos, 1989), and are generally caused by high to mid-latitude depressions crossing the North Atlantic towards Western Europe (Costa *et al.*, 2001). Storm groups occur frequently on the west coast of Portugal, on average once every year for groups of two storms and once every four years for a group of three storms (Ferreira, 2005). Tides along the south-western Portuguese coast are semidiurnal and mesotidal, with maximum spring tidal range of 3.6 m and maximum tidal elevation approximately 2 m above mean sea level (MSL). Barometric pressure effects can increase the water levels by up to an additional 0.5 m (Gama *et al.*, 1994).

4.3 METHODS

Topographic surveys were conducted along cross-shore beach profiles on the three beaches. Surveys were performed regularly every two months between September 2007 and September 2009. Episodic surveys were also undertaken after each storm and 15 to 30 days later to monitor beach recovery, as survey-storm timing is decisive to understand the variability in beach changes driven by storm events (Quartel *et al.*, 2008). In total, 20 surveys were completed on each beach over the two year period. Three profiles representative of different beach sectors and with alongshore spacing between 100 and 200 m (Fig. 4.1), were monitored on each beach using RTK-GPS. Surveys were performed always during low tide, preferentially during spring tides, at

least up to the mean low water spring level (MLWS), 1.4 m bellow MSL, or further seaward.

Wave and tide data were obtained continuously for the entire monitoring period from the Sines deepwater directional wave buoy, located in 97 m water depth, and from the Port of Sines tide gauge, both approximately 65 km north of the study area (Fig. 4.1). Gaps in the observed tidal record (~2% of the total record) where filled using the predicted tide levels, while gaps from the measured wave record (~20% of the total record) where filled using modelled data from a close WANA network deepwater grid point (Lahoz and Albiach, 2005), as significant correlation was obtained for H_{so} ($\rho \leq 0.001$, $n = 6137$, $R = 0.88$) and T_p ($\rho \leq 0.001$, $n = 6137$, $R = 0.61$). Correlation analysis was also performed between several WANA grid points along the southwest coast of Portugal to determine whether wave conditions close to Sines buoy were representative of the deepwater conditions further south, in locations closer to the study areas. Results indicate a highly significant correlation for both H_{so} and T_p at all points ($\rho \leq 0.001$, $n = 8276$, $R \geq 0.92$), suggesting a close similarity of deepwater wave conditions along this stretch of coastline.

Time series of beach width and volume variability were used to quantify beach changes. Beach width was calculated as the horizontal distance from the MSL shoreline position to the cliff base of frontal dune, which has not changed during the monitoring period. MSL was selected for beach width following several works using datum-based shorelines as proxies for beach width change (Farris and List, 2007), particularly using the intersection of the MSL with the foreshore on high-energy environments (*e.g.* Hansen and Barnard, 2010). Beach profile volume was obtained using trapezoidal integration with the upper limit defined by the profile surface and the MLWS level as lower limit. By taking MLWS level (-1.4 m MSL) as the lower limit for volume

calculation it was possible to incorporate the intertidal and subaerial beach change. A similar level, -1.3 m MSL, was recently identified for an exposed beach in southern Portugal by Almeida *et al.* (2011) as a nodal depth separating the cross-shore sectors dominated by berm and subtidal terrace changes, respectively above and below that depth. The existence of a nodal point at a depth close to MLWS level appears to indicate a vertical morphodynamic separation of the profile at this level, rendering it as an appropriate lower level for volume calculation. Net gain or loss of sediment over the MLWS level is then considered an indicator of cross-shore exchange of sediment between (*i*) the subaerial and intertidal beach and (*ii*) the subtidal beach. Profile volumetric mobility and envelopes where computed following Dolan *et al.* (1978). Mobility is defined as standard deviation of the mean profile volume (± σ), while the envelope corresponds to the maximum and minimum values of the detrended beach volume time series.

4.4 RESULTS

4.4.1 Wave forcing

Daily averages of offshore wave conditions, (Fig. 4.2) indicate that the largest values typically occur during winter (October to March), although most severe events are generally concentrated between December and February. During the remaining months wave conditions are moderate, even though energetic events occasionally occur, with H_{so} exceeding 3 m (*e.g.* April 2008 or September 2008). The seasonal character of the wave climate in southwestern Portugal is highlighted by the 3-month running average in Fig. 4.2. Both H_{so} and T_p display a similar seasonal variation, with average H_{so} around 2 m and T_p above 12 s in the peak of the winter season. Summer values

range between 1 and 1.5 m and 8 and 10 s for H_{so} and T_p, respectively. Average wave approach from WNW to NW shows little seasonal variation.

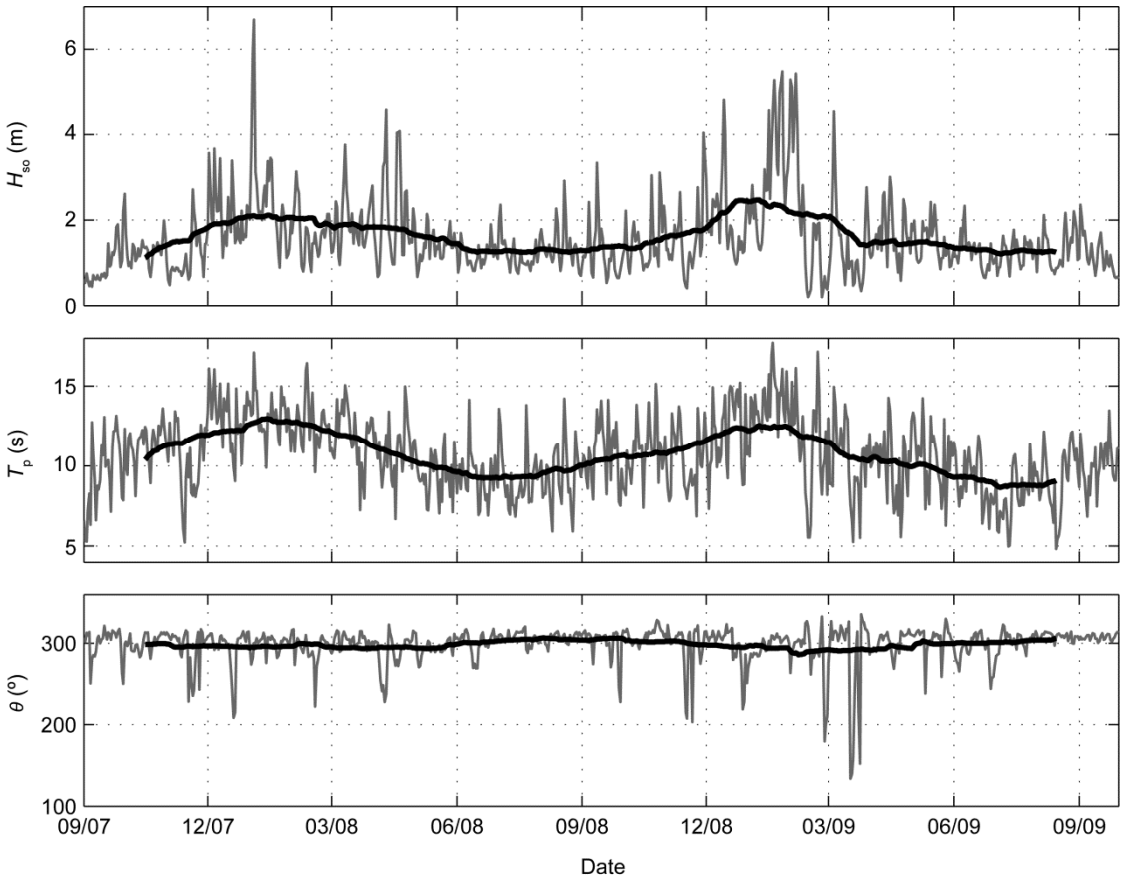

Figure 4.2 Daily averages of offshore wave conditions at Sines between September 2007 and September 2009. Thick black line depicts smoothed values using a 3-month running average.

The most significant events during the monitoring period occurred in January 2008 and January-February 2009 (Fig. 4.2). An extreme single storm, with daily H_{so} exceeding 6 m and maximum H_{so} up to 8 m, reached the coast during neap tide in early January 2008, with waves in excess of 5 m for 36 hours. By mid-January 2009 a series of storms in rapid succession was initiated, lasting for 22 days with continuously high waves. Considering a storm independence criterion of 30 hours between wave extremes, following Morton *et al.* (1997) according to the time-scale of mid-latitude depressions, 5 individual storms compose this storm group (Fig. 4.3). The storm group spanned

through neap and spring tides, although no storm peak was coincident with the highest tides between the 27th and 31st of January. Surge levels were significant, especially during the 4th and 5th storms, but maximum surge of 0.32 m did not reach the threshold of 0.35 m defined by Gama *et al.* (1994) as the yearly very significant surge level (above the 99th percentile) for the southwestern coast of Portugal.

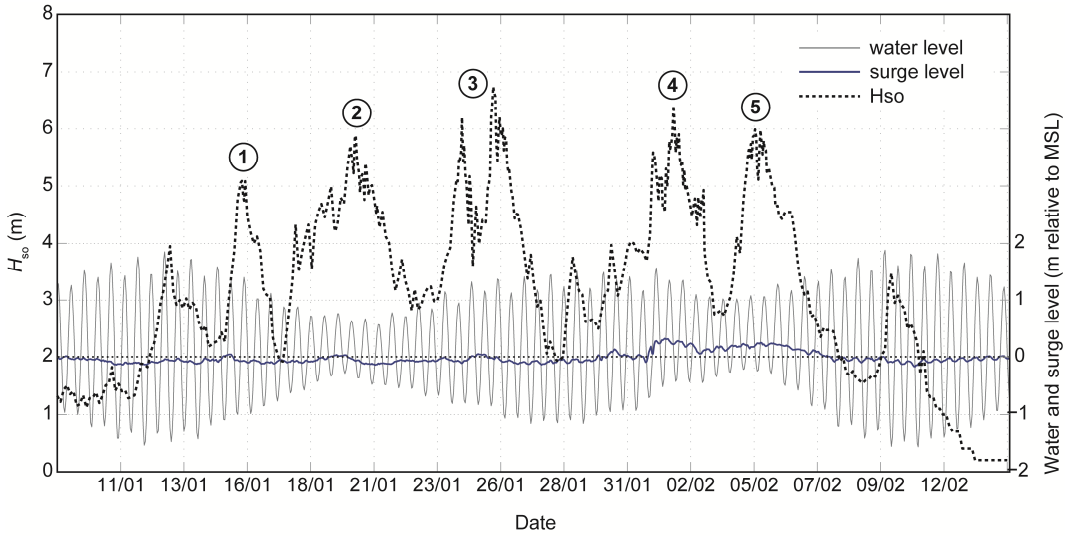

Figure 4.3 Offshore significant wave height, water level and surge level during the January-February 2009 storm group. Numbers indicate individual storm events considered.

4.4.2 Seasonal and storm induced beach change

Morphological change was evaluated using the variation of beach profile volume above MLWS level and beach width up to MSL (Fig. 4.4). Both proxies for beach change are significantly correlated at every profile ($R \geq 0.80$, $\rho \leq 0.001$), except Amoreira south profile ($R = 0.31$, $\rho > 0.05$). Peak profile volumes and widths are generally recorded in late October to early November, following a gradual accretion during the summer months. Abrupt changes took place during the winter, especially during the months of December to February, when high-energy events are more frequent. During the first year of monitoring the mean beach variation, in either volume

or width, fluctuated between ±100 m^3/m for profile volume and ±50 m for beach width. The variation in most individual profiles was also within these ranges, with exceptions of Amoreira north and south profiles and also Mt. Clérigo south profile. By early November 2008 most profiles presented volumes or widths similar to the ones recorded in November 2007, before the winter storms, suggesting a yearly cycle characterized by winter erosion and summer accretion, without significant sediment loss. Within this general seasonal variation in mean beach volume or width, however, individual profiles exhibit shorter term cyclic changes related to storm – post-storm cycles. Profiles Amoreira south and north, Monte Clérigo north and Arrifana south reveal more clearly these cycles that, despite the short-timescale, still involve sediment volumes and beach width changes similar to the values previously reported for the mean beach variation.

The January-February 2009 storm group promoted general erosion on all three beaches, being responsible for the most dramatic changes during the monitoring period. Erosion of 100 to 200 m^3/m occurred on most profiles during this cluster of 5 storms, and average shoreline retreat was 40 m. The response of the beaches to this storm group was not uniform, and there were variations especially in terms of magnitude of beach width change. These variations are evident in Amoreira beach, where changes are of higher magnitude (note the different y axis scale in Fig. 4.4). Following the storm group, beach recovery initiated immediately in Arrifana beach, while Amoreira and Mt. Clérigo beaches still experienced moderate erosion, reaching the lower sediment volumes by the beginning of the 2009 summer season, after which beach recovery was initiated. By the end of the monitoring period net sediment loss was significant in Amoreira and Mt. Clérigo beaches, amounting to approximately 150 m^3/m with a corresponding net shoreline retreat of roughly 50 m. Sediment losses were, however, restricted to the foreshore, resulting in significant berm retreat and intertidal beach

lowering. Despite the significant erosion observed, mostly under the action of the January-February 2009 storm group, there was no dune scarping or retreat on the profiles backed by dunes in Amoreira and Mt. Clérigo beaches.

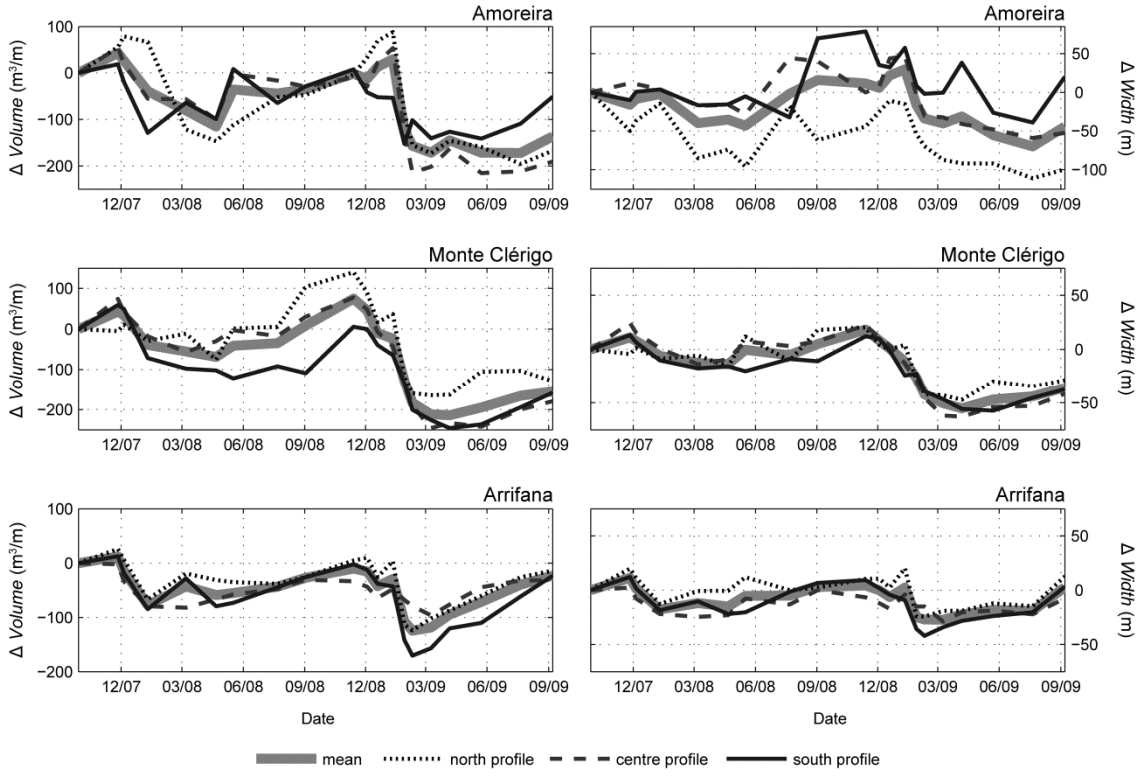

Figure 4.4 Cumulative beach change for each profile and averaged per beach. Left panels represent the beach volume (m^3/m) and beach width (m) is shown in the right panels.

4.4.3 Alongshore non-uniform beach change

Regardless of the reduced dimensions of the three beaches, with lengths of less than 1 km, differences in beach profile response within each beach were observed. Alongshore variations in profile response are generally in terms of magnitude of change, since erosion and deposition were mostly synchronous in all profiles. Differences in profile variation within the same beach reached maximum values of 200 m^3/m in volume (Mt. Clérigo beach in September 2008; Fig. 4.4), or 100 m in width

(Amoreira beach in September 2008; Fig. 4.4). The non-uniform beach response is evident in the mobility and envelopes of change for each profile (Fig. 4.5). Alongshore ranges for both envelope and mobility in Amoreira beach are similar for profiles north and centre, while for profile south both indexes are approximately 50 m^3/m smaller in both positive (accretion) or negative variation (erosion), indicating lower range of variation. Mt. Clérigo beach evidences also alongshore variations in profile variability, with the centre profile presenting a wider mobility.

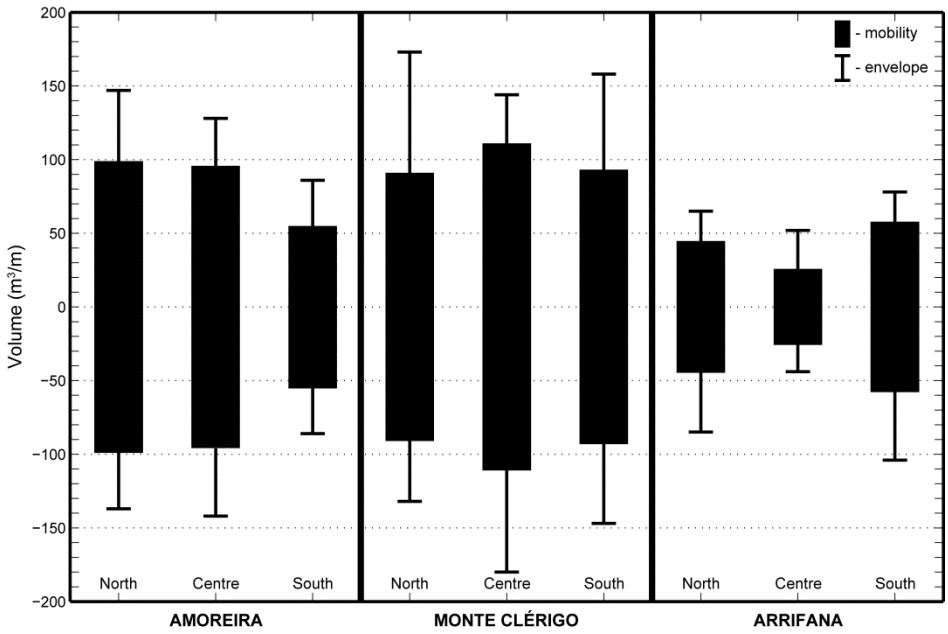

Figure 4.5 Profile volumetric mobility and envelope

Considering absolute ranges of profile envelope at Mt. Clérigo, all profiles present envelopes around 300 m^3/m, but the envelope of profile centre presents lower values, indicating higher erosion. Profile mobility and envelopes at Arrifana beach also show distinct alongshore variations. Profiles south and north present approximately twice the profile centre mobility, and change envelopes are significantly wider, implying that profile centre is less variable than the profiles at both ends of the beach. It is important to note that the magnitude of change in terms of average mobility and

envelope is similar between Amoreira and Mt. Clérigo, and both are approximately twice the average values for Arrifana.

Profile behaviour was also marked by diverse association between profiles at each embayment, as confirmed by correlation of temporal changes of volume and width for individual profiles within each beach (Table 4.1). Significant correlation was found between Amoreira north and centre profiles, for both volume ($R = 0.86$, $\rho < 0.01$) and width ($R = 0.82$, $\rho \leq 0.01$), while profile south was uncorrelated to any other profile in terms of beach width. For Mt. Clérigo there is a slightly higher agreement between profiles south and centre, despite all profiles being well correlated in both volume and width ($R \geq 0.76$, $\rho < 0.05$). At Arrifana higher correlation is found between profiles at each end of the beach, where profiles north and south present the highest correlation for beach volume ($R = 0.96$, $\rho < 0.01$), despite being 400 m apart.

Table 4.1 Correlation coefficients for beach profile volume and width variation

Profile name	**AMN**	**AMC**	**AMS**
AMN		0.82 *	0.29 ***
AMC	0.86 *		0.41 ***
AMS	0.51 **	0.75 *	
Profile name	**MCN**	**MCC**	**MCS**
MCN		0.91 *	0.81 *
MCC	0.89 **		0.95 *
MCS	0.76 **	0.92 **	
Profile name	**ARN**	**ARC**	**ARS**
ARN		0.67 *	0.82 *
ARC	0.73 *		0.68 *
ARS	0.96 *	0.75 *	

* statistically significant for $\rho < 0.01$
** statistically significant for $\rho < 0.05$
*** statistically not significant
Note: Correlation for profile volume at the left side (no shading) and correlation for profile width at the right side (in light grey shading)

4.5 DISCUSSION AND CONCLUSION

Seasonality in the wave forcing drives a seasonal cycle in beach change, particularly in swell-dominated beaches (Quartel *et al.*, 2008), and was notable in the three beaches during the first year of monitoring, despite the occurrence of an extreme single storm in January 2008. Nevertheless, over the two-year period of monitoring, the temporal variation at the three embayed beaches suggests that the seasonal winter erosion/summer accretion pattern of morphological change is not the dominant signal in the data. The occurrence of a storm group in January-February 2009 created the most conspicuous change, highlighting the importance of storm groups as drivers of morphological change. Storm clustering over weekly to monthly timeframes has been shown to produce highly significant erosion on exposed sandy beaches of western Portugal (Ferreira, 2005), eastern Australia (Thom, 1974) and the US Pacific northwest coast (Ruggiero *et al.*, 2005). Such extreme event grouping, by inducing severe erosion may require recovery periods of several years, promoting interannual variability that is noticeable in the beach and volume time series for Amoreira and Mt. Clérigo beaches.

Despite a similar general evolution pattern, differences between beaches have also been observed, and these are mostly the result of geomorphologic constrains specific to individual beaches, as embayed coastlines are prone to site-specific storm responses (Cooper *et al.*, 2004). Higher envelopes of shoreline change are expected for inlet-associated embayed beaches in comparison to headland-embayment systems in high-energy dissipative environments (Cooper *et al.*, 2007; O'Connor *et al.*, 2007). At Amoreira, the existence of a tidal stream that migrates and meanders across the intertidal beach influences shoreline variation, resulting in a more varied behaviour of beach width compared to the other two beaches. This higher shoreline variability within the embayment, however, is not matched by high volumetric variability. This suggests

that sediment exchanges between the intertidal and subaerial beach affect the shoreline position but not the overall sediment volume. Local geomorphologic constraints are also responsible for lower magnitude volume and width changes at Arrifana beach. Diffraction around the prominent northern headland and refraction on the gentle shoreface significantly reduce breaking wave heights from the dominant north-westerly waves, leading to lower energy wave conditions compared to Amoreira and Mt. Clérigo. Because of lower waves and higher confinement of Arrifana embayment, storm impacts are likely to be less severe. This is confirmed by the lower mobility and envelopes of change, as well as by the ability of the beach to regain its sediment volume and width by the end of 2009 summer, in contrast to Amoreira and Mt. Clérigo, which experienced net erosion of > 100 m^3/m and shoreline retreat of ~ 50 m.

Embayed high-energy dissipative beaches exposed to modally energetic swell are considered to be attuned to high-energy conditions and, therefore, require extreme events to cause significant morphological change (Cooper *et al.*, 2004). Despite H_{so} reached a maximum of 8 m during the January 2008 storm, the short duration of the event and its occurrence during neap tides, led to only moderate erosion (within what is assumed to be the seasonal variation). The response to the January-February 2009 storm group was, however, much more significant even though maximum H_{so} was significantly lower, not even reaching 7 m. As erosion on high-energy dissipative beaches is not directly related to the incident storm waves, but with the lower frequency motions generated in the inner surf zone (Russell, 1993), the duration of the storm events and their occurrence during periods of elevated water levels during spring high tide or significant surges, seem to be more important in determining beach response. When storm waves persist for long periods of time, as in the January-February 2009 storm group, infragravity motions, with their dominant offshore directed sediment

transport (Russell, 1993), provide conditions for continued sediment erosion, leading to the extreme erosion observed in all beaches. Such extreme erosion on Amoreira and Mt. Clérigo beaches had, however, no effect in the dunes and was restricted to the beach and nearshore. The ability of dissipative embayed coastlines to accommodate increasingly high waves, due to energy dissipation on progressively wider surf zones (Cooper *et al.*, 2004), implies that most of the waves that reach the backshore are already not competent for inducing significant morphological change, as observed in Mt. Clérigo and Amoreira. At the same level, the infragravity motions that convey the energy of the storm waves to the inner surf zone and beach, creating pulses of offshore sediment transport (Russell, 1993), are not active beyond the foreshore and therefore are unable to impact the backshore and dune. This has implications for the long-term behaviour of dissipative embayed coastlines, as even extreme events, if followed by moderate conditions that enable beach recovery, may not have long lasting effects on the coastline behaviour.

Variations in magnitude (but not overall pattern) of change were observed in each embayment. Embayment topography, particularly the presence of rocky headlands, significantly impacts morphodynamics of embayed beaches (Short, 1999). During high wave conditions the topographical influence of headlands on the surf zone dynamics is increased, inducing longshore gradients and forcing the development of cellular circulation (Short, 1985). Under these conditions, megarips develop and become the major mechanism of surf-zone circulation (Short, 1985; 1999), creating conditions for alongshore variation in beach response (Eliot and Clarke, 1982). Observations of surf-zone conditions during high waves on the three beaches, along with the measurement of profile change immediately after storms, confirmed the presence of megarips and quantified their impact on beach morphological change. Large rip channels connected to

deep feeder channels along the intertidal beach were observed on the centre of Amoreira and Mt. Clérigo embayments, while at Arrifana two megarips developed at both extremities of the beach. Profile erosion was always higher in the profiles fronting megarips or intersected by feeder channels, as evidenced in Arrifana. Similarity in behaviour of profiles north and south for Arrifana beach, for both volume and width (Table 4.1), supports the hypothesis that megarips are responsible for alongshore variability in profile and shoreline change in embayed beaches (Eliot and Clarke, 1982). The development of a megarip in the centre of Mt. Clérigo embayment is also associated with higher profile mobility (Fig. 4.5). Similarly, increased variability was observed in profiles centre and north in Amoreira beach, as the wide megarip developed in the centre of the beach migrated towards the northern section.

Extreme erosion on high-energy dissipative embayed beaches (as experienced during storm groups) appears to be associated with the development of cellular circulation with megarips persisting for extended periods of time. Because megarips tend to occupy topographically fixed positions on the beach, they induce variations in morphological change even along small beaches. High temporal and spatial variability in high-energy embayed beaches can, therefore, be expected, with significant deviations from the seasonal signal and alongshore non-uniform responses.

4.6 ACKNOWLEDGEMENTS

This work is a contribution to BAYBEACH project, funded by FCT under contract PTDC/CTE-GEX/66893/2006. Carlos Loureiro was also supported by FCT, grant SFRH/BD/27878/2006. We gratefully acknowledge the help of everyone involved in the fieldwork. Hydrodynamic data from Sines was provided by Instituto Hidrográfico. WANA wave data was kindly supplied by Puertos del Estado.

4.7 REFERENCES

Almeida, L.P., Ferreira, Ó. and Pacheco, A., 2011. Thresholds for morphological changes on an exposed sandy beach as a function of wave height. *Earth Surface Processes and Landforms* 36, 523-532.

Cooper, J.A.G., Jackson, D.W.T., Navas, F., McKenna, J. and Malvarez, G., 2004. Identifying storm impacts on and embayed, high-energy coastline: examples from western Ireland. *Marine Geology* 210, 261-280.

Cooper, J.A.G., McKenna, J., Jackson, D.W.T., O'Connor, M., 2007. Mesoscale coastal behaviour related to morphological self-adjustment. *Geology*, 35, 187-190.

Costa, M. and Esteves, R., 2010. Clima de agitação marítima na costa oeste de Portugal Continental", Proceedings of XI Jornadas Técnicas de Engenharia Naval – O Sector Marítimo Português. Edições Salamadra, Lisboa, Portugal. pp. 413-426.

Costa, M., Silva, R. and Vitorino, J., 2001. Contribuição para o estudo do clima de agitação marítima na costa Portuguesa. Proceedings 2as Jornadas de Engenharia Costeira e Portuária. AIPCN, Aveiro, Portugal. (20 p. CD-ROM).

Dolan, R., Hayden, B. and Heywood, J., 1978. A new photogrammetric method for determining shoreline erosion. *Coastal Engineering* 2, 21-39.

Eliot, I.G. and Clarke, D.J., 1982. Seasonal and biennial fluctuation in subaerial beach sediment volume on Warilla beach, New South Wales. *Marine Geology* 48, 89-103.

Farris, A.S. and List, J.H., 2007. Shoreline change as a proxy for subaerial beach volume change. *Journal of Coastal Research* 23, 740-748.

Fox, W.T. and Davis, R.A., 1978. Seasonal variation in beach erosion and sedimentation on the Oregon coast. *Geological Society of America Bulletin* 89, 1541-1549.

Ferreira, Ó., 2005. Storm groups versus extreme single storms: Predicted erosion and management consequences. *Journal of Coastal Research* SI42, 221-227.

Gama, C., Dias, J.M.A., Ferreira, Ó. and Taborda, R., 1994. Analysis of storm surge in Portugal, between June 1986 and May 1988. Proceedings of Littoral'94. EUROCOAST, Lisboa, Portugal. pp. 381-387.

Hansen, J.E. and Barnard, P.L., 2010. Sub-weekly to interannual variability of a high-energy shoreline. *Coastal Engineering* 57, 959-972.

Hayes, M.O. and Boothroyd, J.C., 1969. Storms as modifying agents in the coastal environment. *Beach and Nearshore Sediments and Processes,* SEPM Reprint Series Number 12, 25-39.

Jackson, D.W.T, Cooper, J.A.G and del Rio, L., 2005. Geological control of beach morphodynamic state. *Marine Geology* 216, 297-314.

Lahoz, M.G. and Albiach, J.C.C., 2005. Wave forecasting at the Spanish coasts. *Journal of Atmospheric & Ocean Science* 10, 389-405.

MacMahan, J.H., Thornton, E.B. and Reniers, A.J.H.M., 2006. Rip current review. *Coastal Engineering* 53, 191-208.

Morton, I.D., Bowers, J. and Mould, G., 1997. Estimating return period wave heights and wind speeds using a seasonal point process model. *Coastal Engineering* 31, 305-326.

Nordstrom, K.F., 1980. Cyclic and seasonal beach response: a comparison of Oceanside and bayside beaches. *Physical Geography* 1, 177-196.

O'Connor, M., Cooper, J.A.G, Jackson, D.W.T., 2007. Morphological behaviour of headland-embayment and inlet-associated beaches, Northwest Ireland. *Journal of Coastal Research* SI 50, 626-630.

Pita, C. and Santos, J.A., 1989. Análise dos temporais da costa oeste de Portugal Continental. Report NATO PO-WAVES 1/89-A, IH/LNEC, Lisboa, Portugal.

Quartel, S., Kroon, A. and Ruessink, B.G., 2008. Seasonal accretion and erosion patterns of a microtidal sandy beach. *Marine Geology* 250, 19-33.

Ruggiero, P., Kaminsky, G.M., Gelfenbaum, G. and Voigt, B., 2005. Seasonal to interannual morphodynamics along a high-energy dissipative littoral cell. *Journal of Coastal Research* 21, 553-578.

Russell, P.E., 1993. Mechanisms for beach erosion during storms. *Continental Shelf Research* 13, 1243-1265.

Short, A.D., 1985. Rip-Current Type, Spacing and Persistence, Narrabeen Beach, Australia. *Marine Geology* 65, 47-71.

Short, A.D., 1999. *Handbook of Beach and Shoreface Morphodynamics*. John Wiley & Sons, Chichester, 379 p.

Thom, B.G., 1974. Coastal erosion in Eastern Australia. *Search* 5, 198-209.

Wright, L.D., Guza, R.T. and Short, A.D., 1982. Dynamics of a high-energy dissipative surf zone. *Marine Geology* 45, 41-62.

Wright, L.D. and Short, A.D., 1984. Morphodynamic variability of surf zones and beaches - a synthesis. *Marine Geology* 56, 93-118.

CHAPTER 5

Extreme erosion in high-energy embayed beaches: influence of megarips and storm grouping

Loureiro, C., Ferreira, Ó., Cooper, J.A.G., 2012. Extreme erosion in high-energy embayed beaches: influence of megarips and storm grouping. *Geomorphology* 139-140, 155-171.

ABSTRACT

Megarips have long been recognised as an important, yet poorly documented, mechanism of beach erosion on high-energy embayed beaches. The persistence and cumulative effect of megarips during storm groups, are described from three embayed beaches (Arrifana, Mt. Clérigo and Amoreira) exposed to high-energy wave conditions in the mesotidal, bedrock-dominated southwestern coast of Portugal. Morphological changes, determined by topographic monitoring and supplemented by interpretation of digital imagery over two years, revealed the development of storm-induced megarips, which exerted a major influence on beach erosion. Differences in megarip influence within and between beaches are related to embayment geometry and orientation, which significantly influence the nearshore wave field. Rip location is topographically controlled, being determined by alongshore variations in breaking wave height and obliquity, along with interaction of wave-driven circulation patterns and embayment nearshore topography. Moderate beach sand loss during individual storms was linked to the development of megarips with associated rip-neck and feeder channels. Extreme erosion, however, occurred when megarips and feeder channels persisted during successive storms, promoting continued erosion and seaward sediment export. Observations show that once initiated, megarip channels persist for several months and continue to act as conduits for offshore sediment transport under non-storm conditions. The maintenance of such rip circulation systems, driven by morphodynamic feedback, reduces beach recovery ability until the rip-neck and feeder channels are infilled.

KEYWORDS: embayed beaches; megarips; storm groups; beach morphology; wave modeling; Portugal.

5.1 INTRODUCTION

Severe erosion on embayed beaches has long been associated with the occurrence of large-scale topographically controlled rip currents, or megarips (Short, 1985). Megarips occur when the embayment topography, particularly around headlands, alters surf zone dynamics during high waves, inducing persistent longshore gradients and the development of cellular circulation (Short and Masselink, 1999). Due to high offshore flow velocities and the seaward extent of megarips (beyond the surf zone), sediment is removed from the beach and transported seaward, to the lower shoreface or even the inner shelf (Short, 1985; Short and Masselink, 1999; Short, 2010).

The influence of embayed beach configuration in the location and dynamics of large scale rip currents was presented early in the rip current literature by McKenzie (1958). However, recent advances in understanding of rip current flow kinematics and morphological coupling have been based on rip channelled beaches on open coastlines, rather than topographic rips and megarips (MacMahan *et al.*, 2006, 2010). Apart from the first records of megarip flow on the nearshore by Evans *et al.* (2000) and Coutts-Smith (2004), no other measurements of megarip flow have yet been made in the beach or surf zone. The highly dynamic and energetic conditions associated with the occurrence of megarips make instrument deployment hazardous, and have constrained

attempts to measure megarip dynamics. Nevertheless, megarips have been associated with extreme beach and even foredune erosion during major storm events along high-energy embayed coastlines (*e.g.* Thom, 1974; Short and Hesp, 1982), and offshore sediment transport from beaches (*e.g.* Coutts-Smith, 2004; Smith *et al.*, 2010).

On unconstrained sandy beaches, severe erosion is traditionally associated with extreme single storms. However, the occurrence of storm groups has become a focus of renewed attention, since the combined erosion of successive storms can be similar or even higher than a single storm of higher magnitude (Lee *et al.*, 1998; Ferreira, 2005, 2006; Callaghan *et al.*, 2008). High-energy embayed beaches exposed to energetic swell and storms are considered to be attuned to high-energy conditions and, therefore, require extreme events to cause significant morphological change (Cooper *et al.*, 2004). However, the morphological impacts of such extreme events on embayed beaches, particularly storm groups, remain little studied, except for the early report of Thom (1974). Consequently, the cumulative effects of successive high-energy events on morphodynamic responses in embayed beaches (*e.g.* beach rotation, megarip development and headland sand bypassing) are still poorly understood.

This paper presents observations of morphological change, obtained during frequent surveys on three sandy embayed beaches in the southwestern coast of Portugal, exposed to high-energy wave conditions in a mesotidal environment. Wave data were obtained for an offshore location and propagated to the nearshore, using numerical wave modelling, in order to investigate the morphological response to wave forcing. Previous work (Loureiro *et al.*, 2011) has indicated that the general pattern of seasonal change along the study sites is disturbed by storm-group action, which induces dramatic beach erosion, and that beach response is not uniform alongshore.

The overall aim of this paper is to examine the role of megarips and storm grouping in the extreme erosion observed in embayed beaches exposed to high-energy wave conditions. The specific objectives are to: (*i*) quantify the volumetric and morphological beach response to wave forcing, particularly focusing on the impact of storm groups and the development of rip current systems; (*ii*) analyse the conditions for megarip development on the three beaches based on morphodynamic behaviour parameters and numerical wave modelling; (*iii*) evaluate the role of storm grouping on the persistence and enhanced action of megarips and (*iv*) discuss their impacts on extreme erosion and recovery ability of embayed beaches.

5.2 ENVIRONMENTAL SETTING

Along the bedrock-dominated southwestern coast of Portugal, beaches occur generally in embayments associated with small streams or in coastal re-entrants within the Carboniferous shale and greywacke cliffs. The coast is directly exposed to the North Atlantic swell, experiencing mean offshore significant wave heights (H_{so}) between 1.5 and 2 m, and peak periods (T_p) between 9 and 13 s, predominantly from northwest to westerly directions (θ) (Fig. 1) (Costa *et al.*, 2001; Costa and Esteves, 2010). Energetic wave conditions are relatively frequent, with H_{so} exceeding 3 m 10% of the time (Costa *et al.*, 2001). Storms along the western Portuguese coast are associated with $H_{so} \geq 5$ m (Pita and Santos, 1989), and are generally caused by frontal systems connected with high to mid-latitude depressions crossing the North Atlantic (Costa *et al.*, 2001). Storm groups occur frequently on the west coast of Portugal, once every year for a group of two storms and once every four years for a group of three storms (Ferreira, 2005). Storm groups may also be associated with the landfall of frontal systems. Their

occurrence is related to a southerly position of the Azores High Pressure System, which allows successive depressions to follow a more southerly path and impact directly on the Portuguese coast. Individual storms with high waves usually last an average of two days, but occasionally they can persist for more than five days (Costa *et al.*, 2001; Costa and Esteves, 2010).

Tides along the south-western coast of Portugal are semidiurnal and mesotidal, with maximum spring tidal range of 3.6 m and maximum tidal elevation about 2 m above mean sea level (MSL).

Field surveys were conducted in Arrifana, Mt. Clérigo and Amoreira beaches (Fig. 5.1), the former two are directly exposed to the dominant north-westerly waves while Arrifana roughly faces west and is partially protected by a prominent northern headland. All three beaches are composed of well-sorted, medium sand and, being exposed to a high-energy wave climate, are modally dissipative or intermediate skewed to dissipative in state. Arrifana is a swash-aligned beach, completely enclosed by up to 100 m-high cliffs, and separated from them by coarse gravel and boulders deposit. The subaerial beach is narrow, rarely presenting a well defined berm, while the intertidal area is wide and flat and frequently featureless. A wide and flat intertidal area also characterises Mt. Clérigo, yet the subaerial beach is wide and backed by partly vegetated dunes in the south and centre, while the northern sector is narrow and backed By 50 m-high cliffs. Amoreira beach is wide and backed by an extensive dune field. This embayment contains a bay-barrier estuary, with a small tidal stream. The beach has a persistent low tide terrace that is occasionally crossed by a migrating tidal channel. This creates a ridge and runnel-like morphology and produces a recurring planform rotation of Amoreira beach that is driven by the interaction of fluvial discharge and oceanographic forcing (Freire *et al.*, 2011).

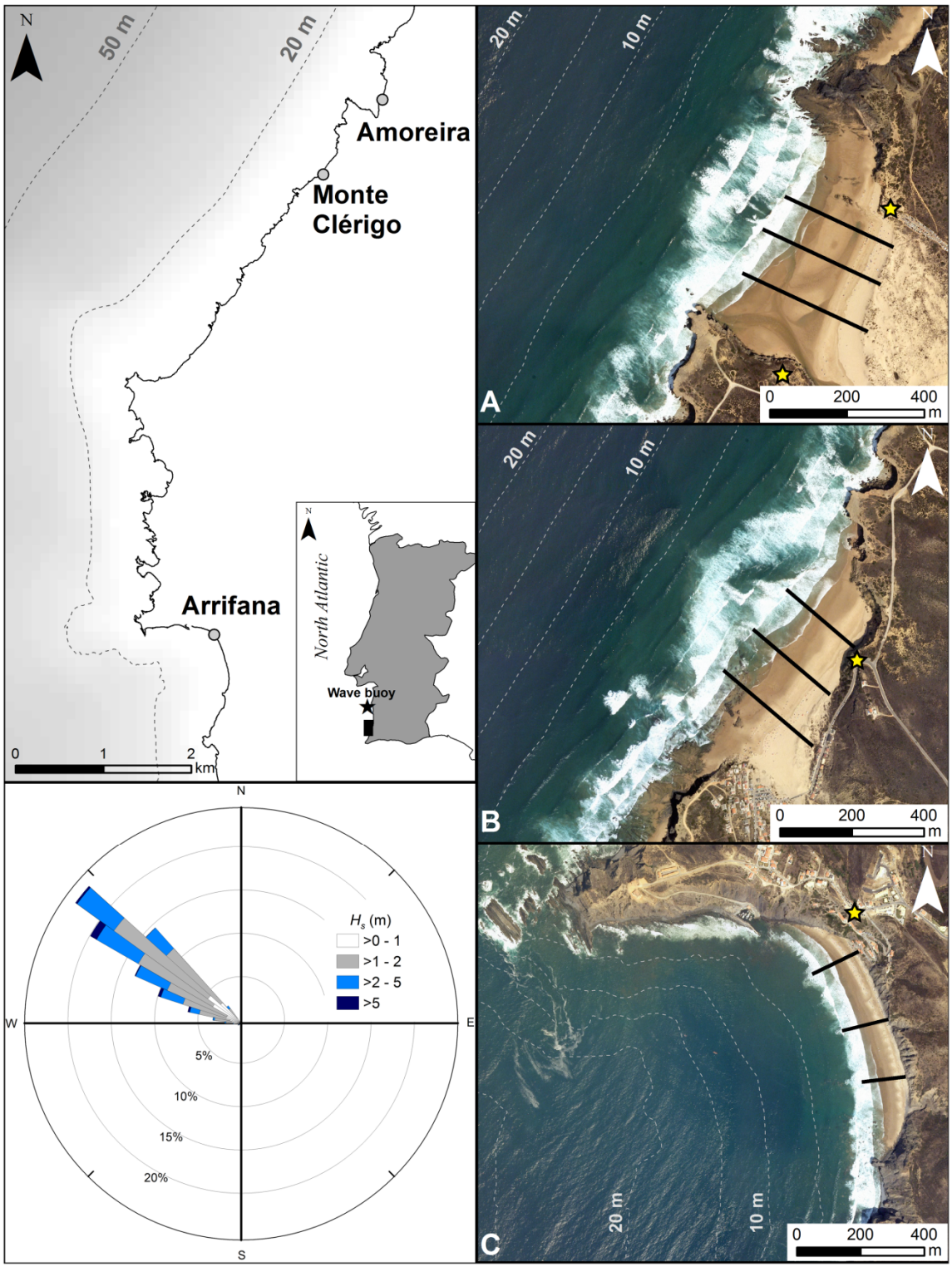

Figure 5.1 Geographical location of the study sites. Aerial view of Amoreira (A), Monte Clérigo (B) and Arrifana (C) embayments with indication of beach profiles location (black lines) and positions for image acquisition (stars). Bathymetry is given in metres below mean sea level (MSL). The wave rose was computed from Sines wave buoy data (black star in inset of location image), from September 2007 to September 2009.

5.3 METHODS

5.3.1 Beach and nearshore morphology

Morphological surveys were performed on Arrifana, Mt. Clérigo and Amoreira beaches along cross-shore beach profiles over a two year period, between September 2007 and September 2009. Surveys were undertaken regularly every two months, and were complemented by event-driven surveys carried out immediately after storms and 15 to 30 days later to monitor beach recovery, totalling 20 surveys completed on each beach over the two year period. Three profiles representative of the different beach sectors and with alongshore profile spacing between 200 and 100 m (Fig. 5.1), were monitored on each beach using a Trimble RTK-GNSS (Real Time Kinematic Global Navigation Satellite System). Surveys were always performed at low tide, preferentially during spring tides, and extended from the frontal dune or cliff base to waning depths, at least up to the mean low water spring level (MLWS), 1.4 m below mean sea level (MSL), or further seaward.

Volumetric change was computed for each profile (in m^3 per unit metre of beach length) by integrating the beach profile above the MLWS level. Recognition of a nodal point at approximately the MLWS level, separating berm and subtidal terrace changes on an exposed beach in Southern Portugal by Almeida *et al.* (2011), suggests a vertical morphodynamic separation of the profile at this level and, therefore, renders it as an appropriate lower level for beach volume calculation. Net gain or loss of sediment over the MLWS level is then considered an indicator of cross-shore exchange of sediment between (*i*) the subaerial and intertidal beach and (*ii*) the subtidal beach. Detailed topo-bathymetric surveys of the all three beaches and nearshore areas were performed in September 2008, during a period of general beach accretion, using a boat-mounted

single beam echosounder, RTK-GNSS positioning and tidal correction. Survey lines, spaced at 100 to 150 m intervals, extended seaward from the beach between 1 and 2 km, reaching depths of approximately 30 m below MSL. Prior to grid interpolation, raw survey data was smoothed using a moving average with a 50 m window, considered suitable to resolve nearshore sandbars at the study area. After smoothing, the bathymetric grids were produced using a locally adapted spline interpolation, which retained the general smoothness of the nearshore area, but also allowed for sharp changes along submerged rocky outcrops to be represented.

5.3.2 Rip and feeder configuration

Recent studies of rip systems at mesocale (months to years) have been based in visual identification of rip channels, mostly using video imaging techniques (*e.g.* Ranasinghe *et al.*, 2004; Holman *et al.*, 2006; Turner *et al.*, 2007; Orzech *et al.*, 2010; Gallop *et al.*, 2011). However, on the majority of cases, these are subjective methods based on manual visual analysis (Gallop *et al.*, 2011), and have been particularly noted to be of limited use in energetic conditions, when megarips develop (Short, 1985), as large waves break across the entire surf zone, hampering the identification of rip channels (Orzech *et al.*, 2010). Repeated bathymetric surveys have been also used to characterise rip morphology, but only during short-term field experiments covering restricted areas (*e.g.* MacMahan *et al.*, 2005) due to the logistical difficulties involved in monitoring the surf zone and nearshore in dynamic and energetic environments where rip currents develop (Brander *et al.*, 2001).

In the present work, a combined analysis of visual evidence and morphological patterns, synthesised in Fig. 5.2, is used to identify rip-neck and feeder channels and assess their interaction with beach profiles, in an attempt to overcome the shortcomings

identified above. Shallow nearshore bars and rip channels along the shoreline and surf zone are relatively easy to identify visually (Holman *et al.*, 2006; Thornton *et al.*, 2007; Turner *et al.*, 2007). Increased turbulence due to wave–current interactions, gaps in the breaking line, streaks of darker water and foam patches seaward of the breakers are distinctive features that make rip identification straightforward (Aagaard and Masselink, 1999). Instantaneous snapshot images were obtained during field surveys with a standard digital camera from high-ground fixed positions in each embayment, located in Fig. 5.1. Due to the narrow field of view of the camera used, several images were obtained sequentially with significant overlap and, when possible, mosaiced automatically using AutoStitch© (Brown and Lowe, 2007) to produce panoramic images of the entire embayments. The images were always acquired during low tide as the morphological expression of rip and feeder channels is amplified at this tidal stage (Brander, 1999). These were then used to identify rip and feeder channels and their locations relative to surveyed sections of the beach. Visual signatures of rip systems around the lower intertidal and shallow subtidal areas were characterized in accordance with a subjective boundary description, similar to the approach used by Brander *et al.* (2001). Fundamentally, incised channels and areas of reduced wave breaking were characterised as rip systems (Turner *et al.*, 2007), while areas of intense wave breaking are associated with bars or shoals (Thornton *et al.*, 2007). Rip systems were further divided into feeder and rip-neck channels according to the orientation of the channels. Feeder channels are generally incised alongshore or slightly obliquely, while rip-neck channels are distinctively cross-shore oriented, although not necessarily perpendicular to the shoreline or wave approach.

Besides the visual interpretation, rip-neck and feeder channel influence on profile morphology was analysed according to patterns of morphological relief

described by Brander and Cowell (2003). Rip-neck channel morphology exhibits sharply inflected slopes, with abrupt deepening (Fig. 5.2), that gradually become shallower in the offshore direction (Brander and Short, 2000; Brander and Cowell, 2003). Moreover, the bottom of rip-neck channels frequently contains coarse mega-ripples (Cook, 1970) that reflect the intense sediment transport. Feeders are morphologically distinguishable by being generally alongshore-oriented (some obliquity may be present), and also because the cross-shore profile along a feeder channel generally exhibits a marked trough followed seaward by bar morphology (Fig. 5.2) (Brander and Short, 2000; Brander and Cowell, 2003; Bruneau *et al.*, 2009).

Further indications of rip-neck and feeder channels were recorded during the surveys, performed at low tide when rip flows are higher due to tidal modulation (Brander and Short, 2000; MacMahan *et al.*, 2006). Distinctive and strong longshore and offshore flows that could be felt while undertaking topographic surveys further enhanced the recognition of feeder and rip-neck influence whenever the profiles were immediately adjacent to such channels (within a distance of approximately 20 m).

Following the analysis of visual evidence and morphological patterns, along with the auxiliary indications of nearshore flows, rip-neck and feeder interaction with beach topographic profiles was classified according to three situations outlined in Fig. 5.2: *a*) profile intersected by, or immediately fronting, a rip-neck channel; *b*) profile intersected or immediately adjacent to a feeder channel; and *c*) profile without immediate influence of rip-neck or feeder channel. Although surveys were not performed during high-energy events but immediately after, the megarips and associated feeder channels remain as distinctive features for a significant time, as strong rip flows persist even under subsequent moderate waves (Short, 1985) and significant time is needed for morphological readjustment (McKenzie, 1958). This is particularly

noticeable for rips that are topographically controlled by headlands (Gallop *et al.*, 2011).

Profile and rip interaction / Parameters	Profile intersected or immediately adjacent to rip-neck channel	Profile intersected or immediately adjacent to feeder channel	Profile without influence of rip-neck or feeder channels
Morphologic relief - descrition	- sharply inflected slope - abrupt deepening - cross-shore incision	- intertidal trough - bar seaward of trough - alongshore incision	- linear to concave slope - smooth deepening - no channel incision
Morphologic relief - cross-shore intertidal profile with (below) and without (above) terrace	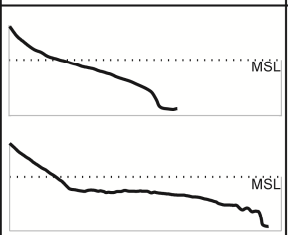	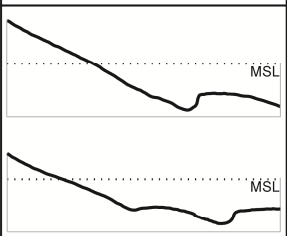	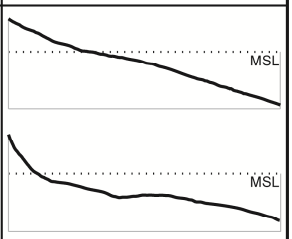
Visual signature - description	- cross-shore orientation - gaps in breaking line - foam seaward of breakers	- alongshore orientation - streaks of darker water - breaking in the bar seaward of trough	- along and cross-shore uniformity - homogenous bores - regular breaking line
Visual signature - photography			
Boundary diagram	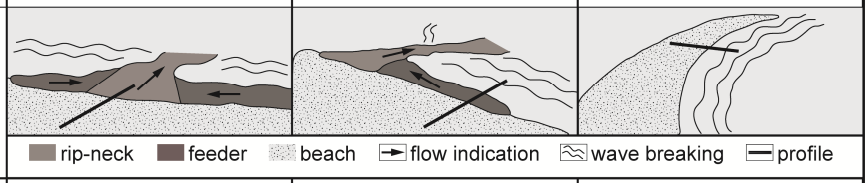		
Flow direction	- offshore directed	- alongshore directed	- onshore directed

Figure 5.2 Synthesis of morphological features and graphical signatures used for classification of beach profiles and rip systems interaction. Flow arrows in the boundary diagram are not scaled to velocity.

5.3.3 Offshore wave data

Offshore wave data were recorded by a Datawell directional wave buoy located at Sines (Fig. 5.3), 65 km north of the study areas in a mean water depth of 97 m. The data, composed of significant wave height, peak period and peak wave direction, were

obtained from Instituto Hidrográfico. Gaps in the measured wave record (~20% of the total record) were filled using modelled data from WANA network deepwater grid point 1044052 (Fig. 5.3) (Lahoz and Albiach, 2005), since significant correlation was obtained for H_{so} ($\rho \leq 0.001$, $n = 6137$, $R = 0.88$) and T_p ($\rho \leq 0.001$, $n = 6137$, $R = 0.61$). Correlation analysis was also performed for the several WANA grid points along the south-western coast of Portugal to evaluate if waves at Sines were representative of the deepwater conditions further south, in locations closer to the study area (Fig. 5.3). The analysis provided highly significant correlation between all WANA grid points for both H_{so} and T_p ($\rho \leq 0.001$, $n = 8276$, $R \geq 0.92$), suggesting close similarity of wave conditions along the south-western Portuguese coast.

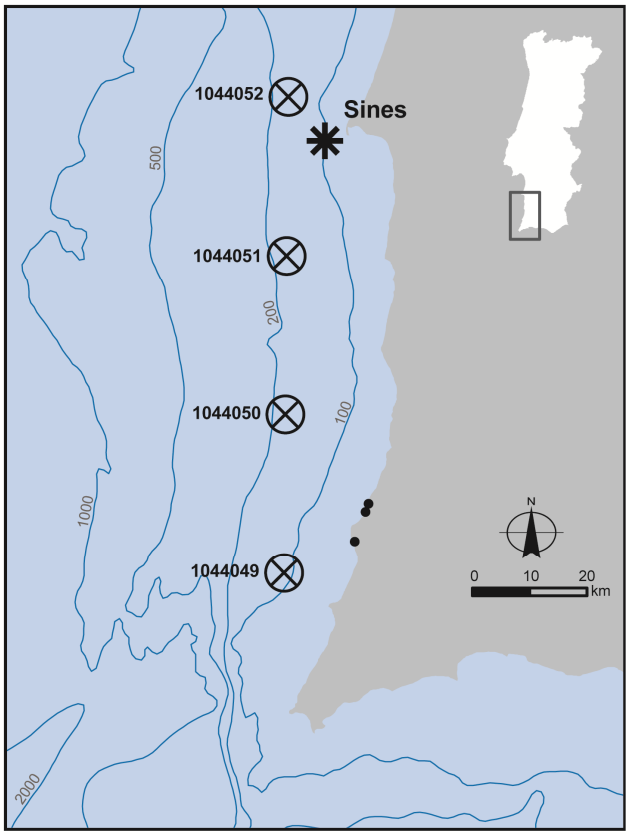

Figure 5.3 Location of Sines directional wave buoy (asterisk) and WANA grid points (crossed circles). Study sites are indicated by black dots and bathymetry is given in metres below MSL

5.3.4 Nearshore wave propagation

Numerical wave modelling with SWAN (Simulating WAves Nearshore; Booij *et al.*, 1999) was used to explore nearshore wave conditions for moderate and high-energy events. SWAN is a Eulerian, phase averaged, third-generation wave model that simulates the refractive propagation and evolution of the wave spectrum, and has been shown to accurately reproduce the nearshore wave field over complex bathymetries (*e.g.* Long and Özkan-Haller, 2005; Gorrel *et al.*, 2011).

SWAN was run in stationary mode, i.e. time is removed from the formulations and waves are assumed to propagate instantaneously across the modelling domain, using a nested scheme composed of three regular grids (Fig. 5.4). Grid resolutions of 100, 20 and 10 m were chosen for the large, medium and smaller grids, respectively. Model predictions were initialized on the three open boundaries of the larger grid with the parametric input from the wave buoy time series, using a JONSWAP spectral shape to represent the wave field. Input boundary conditions for the medium and small grids were determined from the computations over the large and medium grids, respectively. SWAN simulations accounted for non-linear triad wave-wave interactions, as they are rather important in shallow coastal areas (Booij *et al.*, 1999; Holthuijsen, 2007), for bottom friction dissipation using the default variable JONSWAP expression according to Hasselmann *et al.* (1973) and for breaking dissipation according to the default bore-based model of Battjes and Janssen (1978). A depth-induced wave breaking parameter (γ) of 0.78 was chosen, as this is a commonly accepted value of γ (Ranasinghe *et al.*, 2004), and was verified by dedicated tests on SWAN performance by Wood *et al.* (2001).

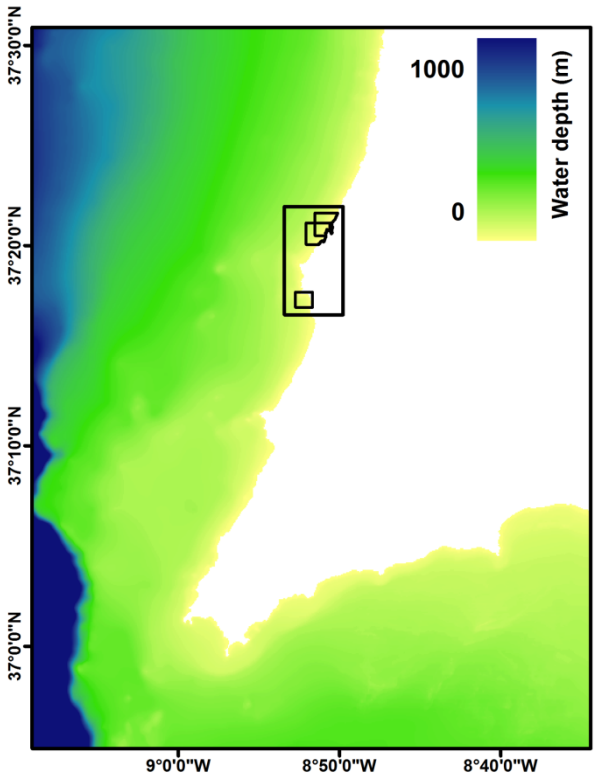

Figure 5.4 Nested grids used in SWAN runs. The small grids for each run are nested into a medium resolution grid encompassing the entire nearshore area of the study sites, which is then nested into a larger grid of the southwestern coast of Portugal (entire area of this figure), for which water depths below MSL are provided.

The nearshore wave field was computed for a range of offshore wave conditions, representing an increase from moderate to high-energy waves according to classes of 0.5 m from $H_{so} \geq 0.5$ m to $H_{so} \geq 7$ m. Taking into consideration the importance of storm events, different storm conditions were modelled independently. Average offshore conditions for a WNW, W and WSW storm were propagated into each embayment to investigate the combined effects of nearshore bathymetry and wave direction in the wave field using realistic conditions, while synthetic storms scenarios with constant H_{so} and T_p of 5 m and 15 s, respectively, but variable offshore wave directions (NW, W and SW) were used to isolate the effect of incoming wave direction. Mean conditions during the January-February 2009 storm group were also modelled

independently for each embayment. Breaking wave heights were obtained for 10 m bins alongshore for each embayment by determining the location where wave dissipation due to depth-induced breaking becomes significant, defined as the most offshore location where a value of 1% of depth-induced breaking is reached (Harley *et al.*, 2007).

5.3.5 Embayment scaling parameter (δ')

Circulation patterns on embayed beaches were analysed parametrically using the embayment scaling parameter (δ') of Short (1999), which relates the embayment configuration to the incident breaking wave conditions according to Eq. (5.1):

$$\delta' = S^2/100.C_l.H_b \quad (5.1)$$

where S is the embayment shoreline length, C_l is the embayment width (distance between headlands), and H_b is the breaking wave height. This empirical approximation was derived from unpublished work by Martens and collaborators on morphometric analysis of embayed beaches, and presented by Short (1996) and Short and Masselink (1999). The selection of this formula was based on the findings of Short (1999, 2010), who indicated that the degree of headland impact on surf zone circulation and, consequently, circulation type in embayed beaches can be predicted using δ'. When $\delta' > 19$, the impact of headlands is limited and normal surf zone circulation operates along the embayment, similar to what would be expected for unconstrained sandy beaches. As δ' ranges between 19 and 8, transitional circulation prevails with headlands increasingly influencing surf zone circulation. Rip currents increase in size and reduce in number and become progressively topographically-controlled. Fully cellular circulation develops when $\delta' < 8$, and topography controls the surf zone circulation, dominated by strong

longshore flows that feed on one to two megarips draining the entire embayment (Short, 1999, 2010). Following Short (1999, 2010), calculations of δ' were performed considering a typical surf zone gradient of 0.01 for each embayment. This is considered representative of dissipative environments such as those in this study. Values of H_b were obtained from alongshore averaged SWAN simulation results and the embayment configuration parameters S and C_l were obtained from GIS-based digital orthophotography analysis.

5.4 RESULTS

5.4.1 Wave conditions

High-energy events were concentrated between October and April, while during the remaining months wave conditions were less energetic, although H_{so} frequently exceeded 2 m (Fig. 5.5). Storm waves were mostly from WNW–NW directions, reflecting the storm climate of the southwestern coast of Portugal (82% of storms between 1988 and 2008 were from a WNW–NW direction (Costa and Esteves, 2010)). There were, however, two occasions when WSW storm waves impacted the coast (April 2008 and February 2009). This occurred for only a few hours, and was followed immediately by WNW waves that obliterated the effects of WSW storm waves on the beaches.

Grouping of high-energy events was frequent, even though the storm threshold ($H_{so} \geq 5$ m) was not reached in every single event (*e.g.* April 2008). If lower storm thresholds were considered, such as those proposed by Costa *et al.* (2001) ($H_{so} > 4.5$ m) or Costa and Esteves (2010) ($H_{so} \geq 3.5$ m for at least 12 hours with maximum H_{so} reaching 4.5 m), more high-energy events would be classified as storms and storm

groups. Nevertheless, the most significant events during the monitoring period (dark grey in Fig. 5.5) were a single storm in early January 2008, with H_{so} reaching 8 m and wave heights in excess of 5 m for 36 hours, and a group of 5 consecutive storms between mid January and early February 2009. This storm group, with storm peaks in the 16th, 20th and 25th January and 1st and 5th of February 2009, represented a period of continuously high waves for 22 days with maximum H_{so} of 6.7 m. Averaged over the entire storm group duration, H_{so} was 4.5 m and T_p 14.5 s from a west-northwesterly direction (300°).

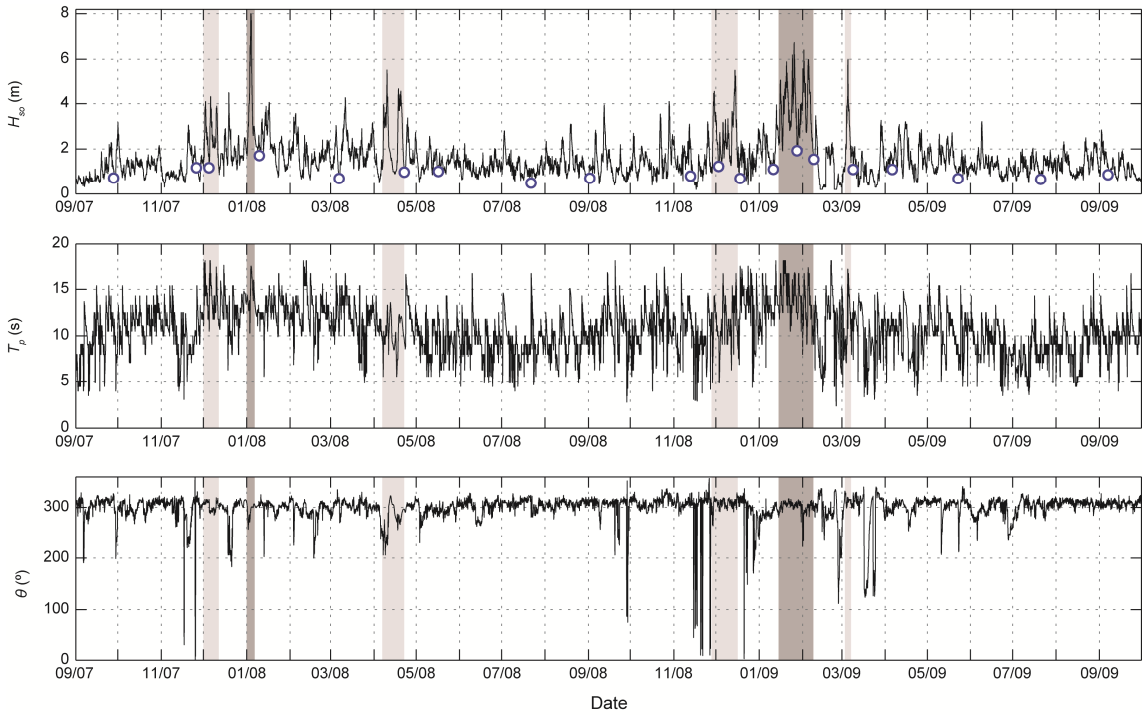

Figure 5.5 Time series of offshore significant wave height (H_{so}), peak period (T_p) and peak wave direction (θ) from September 2007 to September 2009. Circles in the top panel indicate timing of beach surveys. Shading highlights high-energy events (light grey) and extreme events (dark grey) during the monitoring period.

5.4.2 Morphological change

Time series of profile volume above MLWS level are presented in combination with the classification of rip system interaction with the cross-shore beach profiles for each embayment (Figs. 5.6 – 5.8).

5.4.2.1 Arrifana

At Arrifana erosion-dominated periods occurred during high waves, and were associated with the development of feeder and rip-neck channels intersecting or in the vicinity of the profiles (Fig. 5.6). From late November to early December 2007, following an increase in wave heights with grouping of high-energy events, average profile erosion of 27 m^3/m occurred, with the development of feeder channels adjacent to Arrifana north and south profiles. With the onset of the early January 2008 extreme storm, a further 62 m^3/m where eroded on average in Arrifana beach profiles by mid-January 2008. This was accompanied by the development of rip systems in the extremities of the beach, with feeder channels intersecting both the central and southern profiles (while a rip was present in the northern section of the beach, it was located more than 20 m north of the profile location). The storm-induced erosion was followed by gradual beach recovery, although without complete infilling of the rip systems. Alongshore migration of the southern rip-neck channel, which had already intersected the south profile by the time of the March 2008 survey, was associated with beach accretion, as this rip was already significantly infilled. The recovery process was interrupted in mid-April by a group of two storms, which reactivated the erosional conditions in the southern rip system and promoted the development of another rip system in the northern section of the beach. Significant recovery took place during the

following months at Arrifana beach, as the rip-neck and feeder channels become infilled, allowing onshore displacement of sand from the intertidal to the subaerial beach.

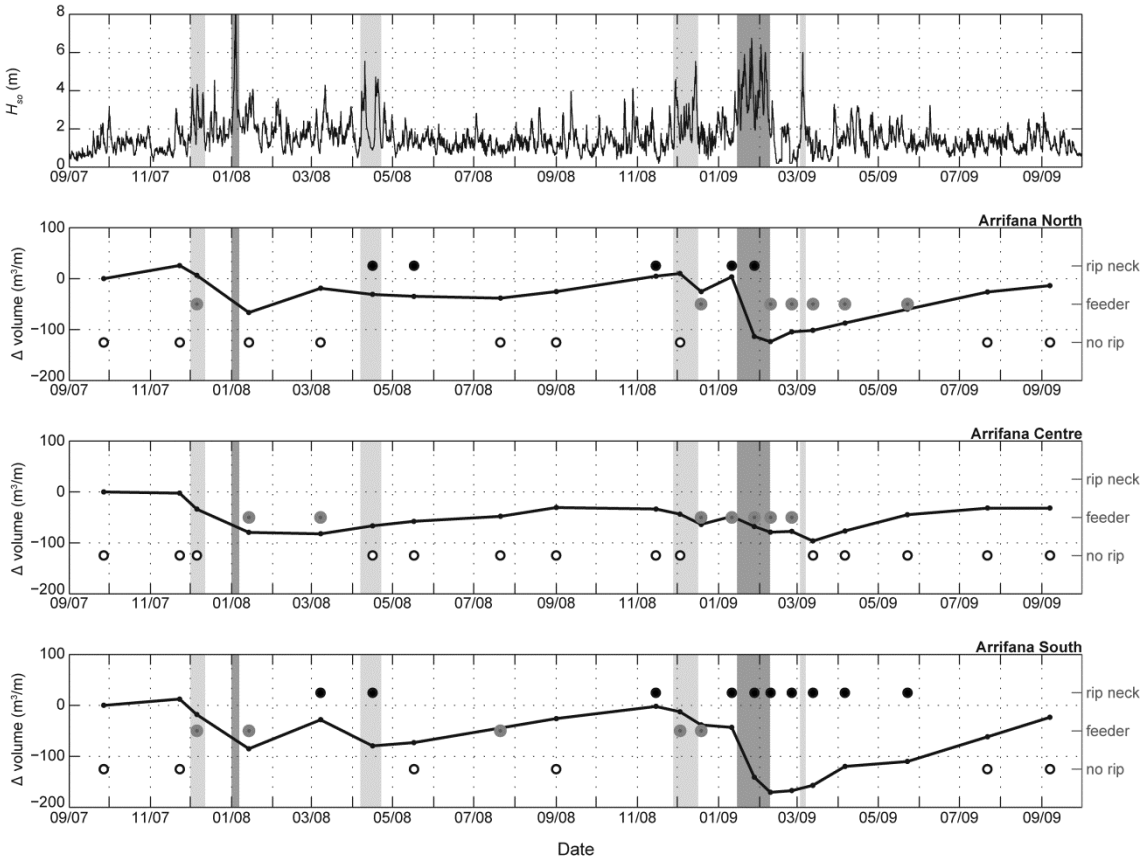

Figure 5.6 Time series of offshore significant wave height (H_{so}) (top panel) and cumulative volume changes for Arrifana beach profiles (black solid line in lower panels). Circles represent profile and rip interaction, with black, grey and hollow circles indicating the influence of rip-neck, feeder channel and no rip influence, respectively. Shaded bars highlight high-energy events.

Erosive conditions resumed by December 2008, with development of rip system circulation across the entire embayment. It was, however, with the onset of the January-February 2009 storm group that most abrupt changes occurred, with generalised erosion at Arrifana beach, particularly noticeable on the north and south profiles. Erosion of 117 m^3/m and 98 m^3/m in the north and south profiles, respectively, was associated with the development of rip-neck channels intersecting profile location, while at the central

profile the development of a feeder channel resulted in moderate erosion (20 m^3/m). Although all profiles at Arrifana recovered significantly during the 7 months following the January-February 2009 storm group (Fig. 5.6), it was mostly after the rip-neck and feeder channels become infilled under lower waves that volumetric change increased substantially.

5.4.2.2 Mt. Clérigo

During the first year of monitoring, beach profiles at Mt. Clérigo showed similar variation to that of Arrifana. Erosion dominated the period between late November 2007 and April 2008, followed by accretion until mid-November 2008 (Fig. 5.7). During the erosion dominated period, the lowest volumes attained in the northern and central profiles, in April and March 2008, respectively, were associated with the development of a large-scale rip system, whose rip-neck channel was initially located in the centre of the beach and then migrated northwards. Although no rip-neck or feeder channel could be identified adjacent to the southern profile (Fig. 5.7), erosion at Mt. Clérigo during the first year of monitoring reached its maximum in this profile with the removal of 122 m^3/m of sediment in relation to the initial profile volume. Between November 2008 and early April 2009, a second erosion-dominated period associated with high waves and storm grouping resulted in extreme erosion throughout the entire Mt. Clérigo embayment. Average erosion of 98m^3/m for Mt. Clérigo beach profiles marked the initial phase of this erosion-dominated period, which lasted until early January 2009. During this initial phase no rip-neck or feeder channels developed in the vicinity of the south profile, while feeder channels interacted with the centre and north profiles. The second phase of erosion between early January and early April 2009, occurred in close association with the January-February 2009 storm group (Fig. 5.7). On average, this

second phase led to a further 196 m^3/m of sand being removed from the profiles, with most of the erosion concentrated during the storm group (average erosion of 167 m^3/m between 11/01/2009 and 09/02/2009).

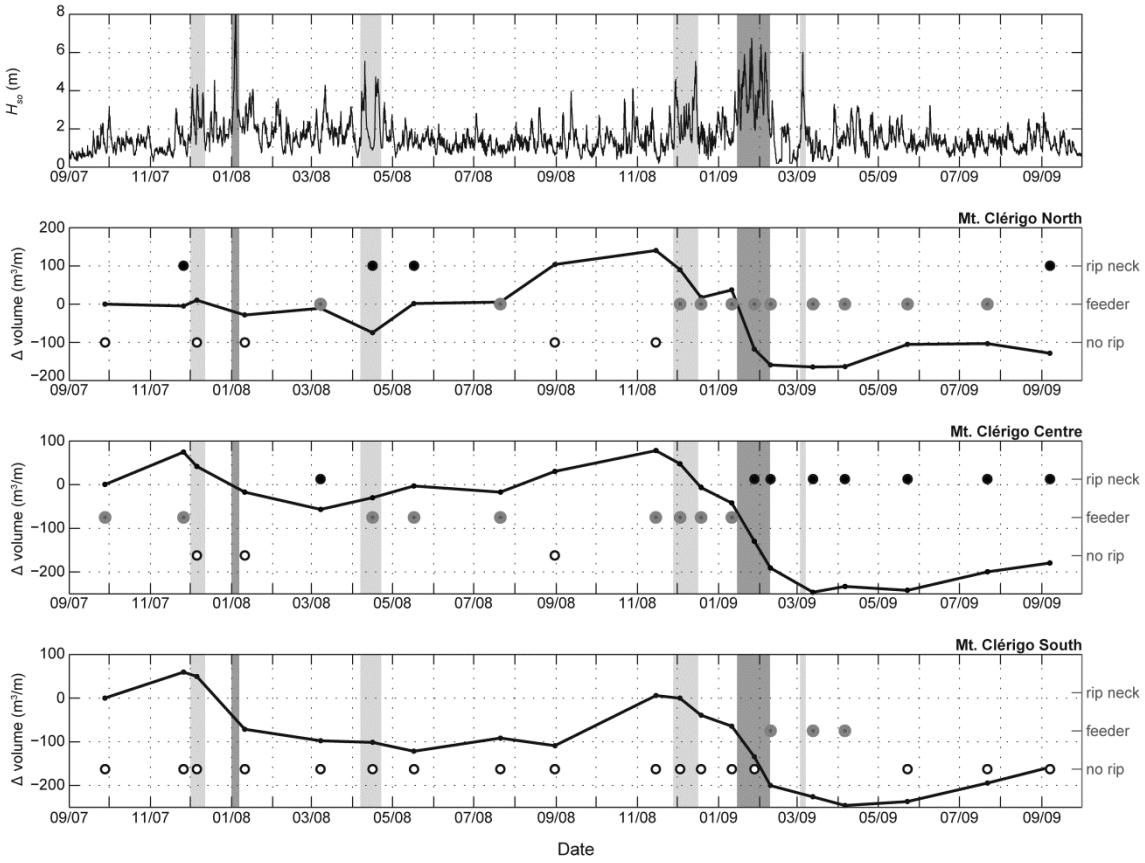

Figure 5.7 Time series of offshore significant wave height (H_{so}) (top panel) and cumulative volume changes for Mt. Clérigo beach profiles (black solid line in lower panels). Refer to Fig. 5.6 caption for description of symbols.

The extreme erosion during the storm group was accompanied by the development of a wide megarip in the centre of the beach, with a rip-neck channel intersecting the lower intertidal section of the central profile. Connected to it, feeder channels from both sides of the beach intersected the southern and northern profiles. Beach recovery was initiated in late April for all three profiles but even after 5 months the volume restored to the beach was significantly lower than what was removed

between November 2008 and early April 2009 (on average recovery only reached 21% of the eroded volume). Notably, during the recovery period, the central rip-neck channel and the northern feeder channel were still active, hindering significant recovery, while sediment accretion on the southern profile was only initiated after April 2009, once the feeder channel had been infilled (Fig. 5.7).

5.4.2.3 Amoreira

Beach profile response to high-energy events at Amoreira beach was variable during the first year of monitoring, although the association between rip-neck or feeder channels and erosion-dominated periods was still clearly recognised (Fig. 5.8). Significant erosion on central and southern profiles occurred immediately in response to December 2007 energetic waves group (three events with H_{so} around 4 m in 15 days), and the early January 2008 extreme storm. This later erosional event was accompanied by the development of a rip system with feeder channels interacting with the central and southern profiles. Eroded volumes reached 148 m^3/m in the southern profile and 110 m^3/m in the central profile, but only 13 m^3/m in the northern profile. However, following a northward displacement of the rip system in the subsequent months, 213 m^3/m of sand were removed from the north profile. Recovery from this erosive period took as much as 7 to 9 months, although it did not proceed linearly in the central and southern profiles, occurring subsequent to the infilling of rip-neck and feeder channels. Under the action of the January-February 2009 storm group, severe erosion occurred in the northern and central profiles (Fig. 5.8), while the south profile only experienced moderate erosion. Maximum erosion of 268 m^3/m was registered in the central profile, closely followed by the northern profile with an eroded volume of 243 m^3/m. During this storm group a wide megarip developed in the centre of the beach, with a rip-neck

channel intersecting the central profile. This was directly connected to a deep feeder channel in the northern section. Both features persisted for several months, hindering beach recovery in the northern and central profiles (Fig. 5.8).

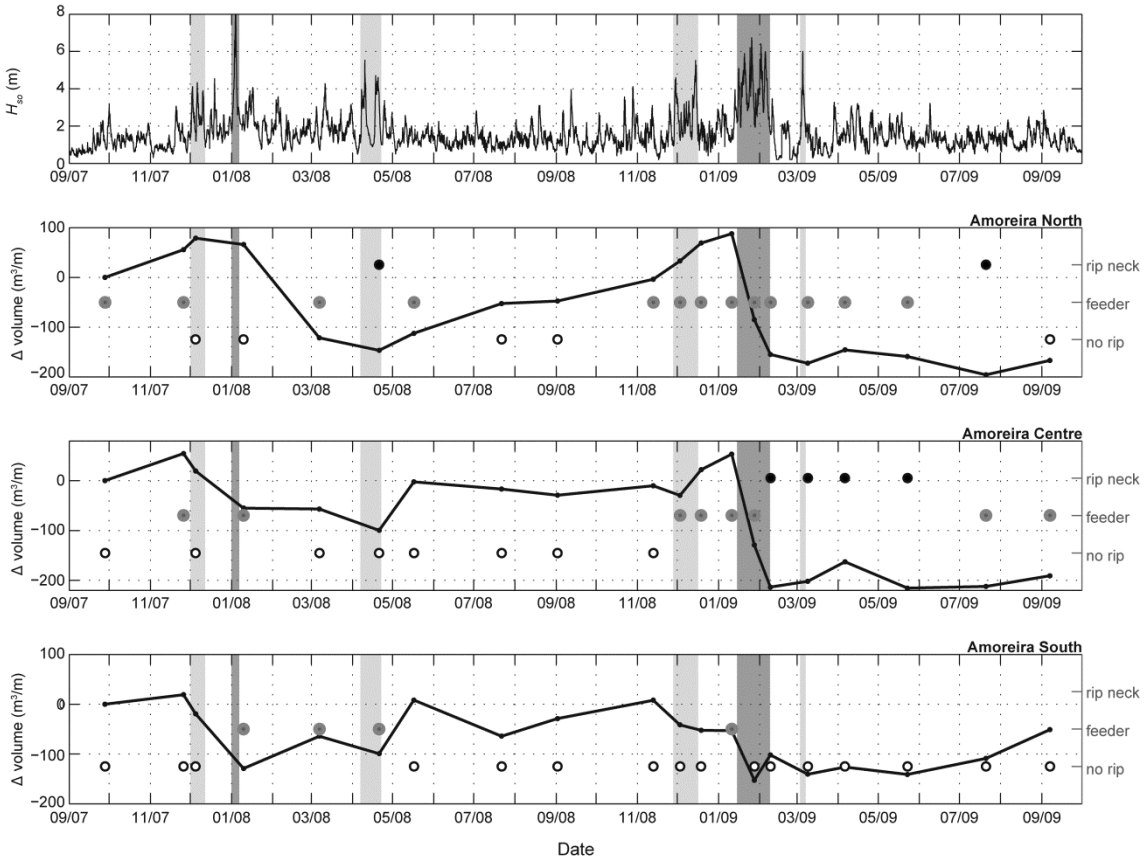

Figure 5.8 Time series of offshore significant wave height (H_{so}) (top panel) and cumulative volume changes for Amoreira beach profiles (black solid line in lower panels). Refer to Fig. 5.6 caption for description of symbols.

5.4.3 Nearshore wave modelling

In the absence of hydrodynamic measurements in the shoaling and surf zone of the three embayments studied, particularly during moderate and high-energy events that drive most significant morphological changes, numerical wave modelling was used for simulation of nearshore wave field. Breaking wave heights were obtained for increasing offshore wave conditions (Table 5.1), real and synthetic storms (Table 5.2 and Fig. 5.9),

and also for the average conditions during the January-February 2009 storm group (Fig. 5.10). Model results highlight the sensitivity of the alongshore variation in nearshore wave heights to the offshore bathymetry in Arrifana embayment, while Mt. Clérigo and Amoreira exhibit fairly uniform alongshore conditions. Modelled breaking wave heights indicate that for Mt. Clérigo and Amoreira beaches, which are directly exposed to the dominant north-westerly waves, alongshore variation in breaking wave height is almost negligible, as evidenced for standard deviation values below 0.1 in all simulations (Table 5.1).

Table 5.1 Mean offshore wave conditions used in model runs and corresponding alongshore averaged breaking wave heights ($H_{b\bar{y}}$) and standard deviation ($H_{b\sigma}$) for Arrifana, Mt. Clérigo and Amoreira embayments. Grey shading highlights modal conditions.

H_{so} Classes	Mean offshore conditions			Arrifana		Mt. Clérigo		Amoreira	
	H_{so} (m)	T_p (s)	θ (º)	$H_{b\bar{y}}$ (m)	$H_{b\sigma}$ (m)	$H_{b\bar{y}}$ (m)	$H_{b\sigma}$ (m)	$H_{b\bar{y}}$ (m)	$H_{b\ \sigma}$ (m)
0.5 – 1.0	0.81	9.4	297	0.55	0.08	0.87	0.04	0.82	0.09
1.0 – 1.5	1.26	10.1	300	0.88	0.12	1.43	0.04	1.37	0.09
1.5 – 2.0	1.73	11.2	302	1.03	0.14	1.66	0.05	1.62	0.08
2.0 – 2.5	2.22	12.0	301	1.47	0.20	2.38	0.04	2.33	0.08
2.5 – 3.0	2.75	12.6	299	1.94	0.27	3.08	0.02	3.05	0.03
3.0 – 3.5	3.21	12.9	299	2.20	0.31	3.48	0.02	3.45	0.03
3.5 – 4.0	3.76	13.5	297	2.38	0.35	3.74	0.03	3.71	0.03
4.0 – 4.5	4.26	14.2	297	2.57	0.36	4.00	0.03	3.97	0.03
4.5 – 5.0	4.73	14.2	294	2.82	0.42	4.35	0.03	4.32	0.03
5.0 – 5.5	5.23	14.6	294	3.18	0.48	4.88	0.03	4.86	0.03
5.5 – 6.0	5.75	15.2	296	3.74	0.59	5.75	0.04	5.73	0.04
6.0 – 6.5	6.25	15.3	298	4.03	0.67	6.25	0.04	6.23	0.05
6.5 – 7.0	6.63	15.7	297	4.39	0.77	6.80	0.05	6.79	0.05
> 7.0	7.82	17.1	298	4.62	0.85	7.23	0.05	7.22	0.06

On these two beaches, breaking wave height is, on average, equivalent to the offshore wave height, with most variation within a difference range of 10%. Conversely, Arrifana beach shows considerable alongshore variation and important

reductions in breaking wave height comparing to the offshore counterpart (Fig. 5.9 and Table 5.1). The northern section of the beach experiences breaker heights up to 3.5 m lower than the southern section, during the most extreme conditions when $H_{so} \geq 7$ m. This alongshore gradient, which increases concurrently to offshore wave height as evidenced by increasing standard deviation values (Table 5.1), is due to the sheltering effect of the prominent northern headland, which forces the diffraction of the dominant west-northwesterly waves. Wave diffraction, together with refraction and attenuation on a gentle shoreface (average slope of 1.1°), induces breaking wave heights on average 35% lower than the offshore wave height, but ranging between 60% and 20% lower on the northern and southern sectors, respectively.

The nearshore wave conditions during storms, both the observed and synthetic events (Figs. 5.9 and 5.10) reflect, in general, the alongshore gradients identified in Arrifana embayment, while highlighting higher sensitivity of Mt. Clérigo and Amoreira embayments to changes in incoming wave direction. For synthetic storms, where only wave direction has been modified, Arrifana embayment maintains significant alongshore gradients, but these are quite insensitive to the variation in wave direction, with the centre of the embayment exhibiting similar conditions for NW, W and SW storms (Fig. 5.9).

Considering both the real storms (Table 5.2) and synthetic storms, breaking wave conditions calculated for Mt. Clérigo and Amoreira embayments are similar, not only in height, but also alongshore uniformity (Figs. 5.9 and 5.10). In these two embayments offshore regular bathymetry precludes noticeable alongshore variations, but their orientation does enhance the attenuation of real WSW and synthetic SW stormy waves, with modelled breaking wave heights being reduced by up to 1.5 m.

Table 5.2 Characteristics of observed storms from different directions used for model runs. Values of H_{so}, T_p and θ are time averages for the duration of each event.

Storm	WNW	W	WSW
Start date	14/12/2008	01/02/2009	10/04/2008
Duration (hours)	15	32	5
H_{so} (m)	5.16	5.50	5.31
T_p (s)	13.8	13.6	11.9
θ (º from North)	309	275	241

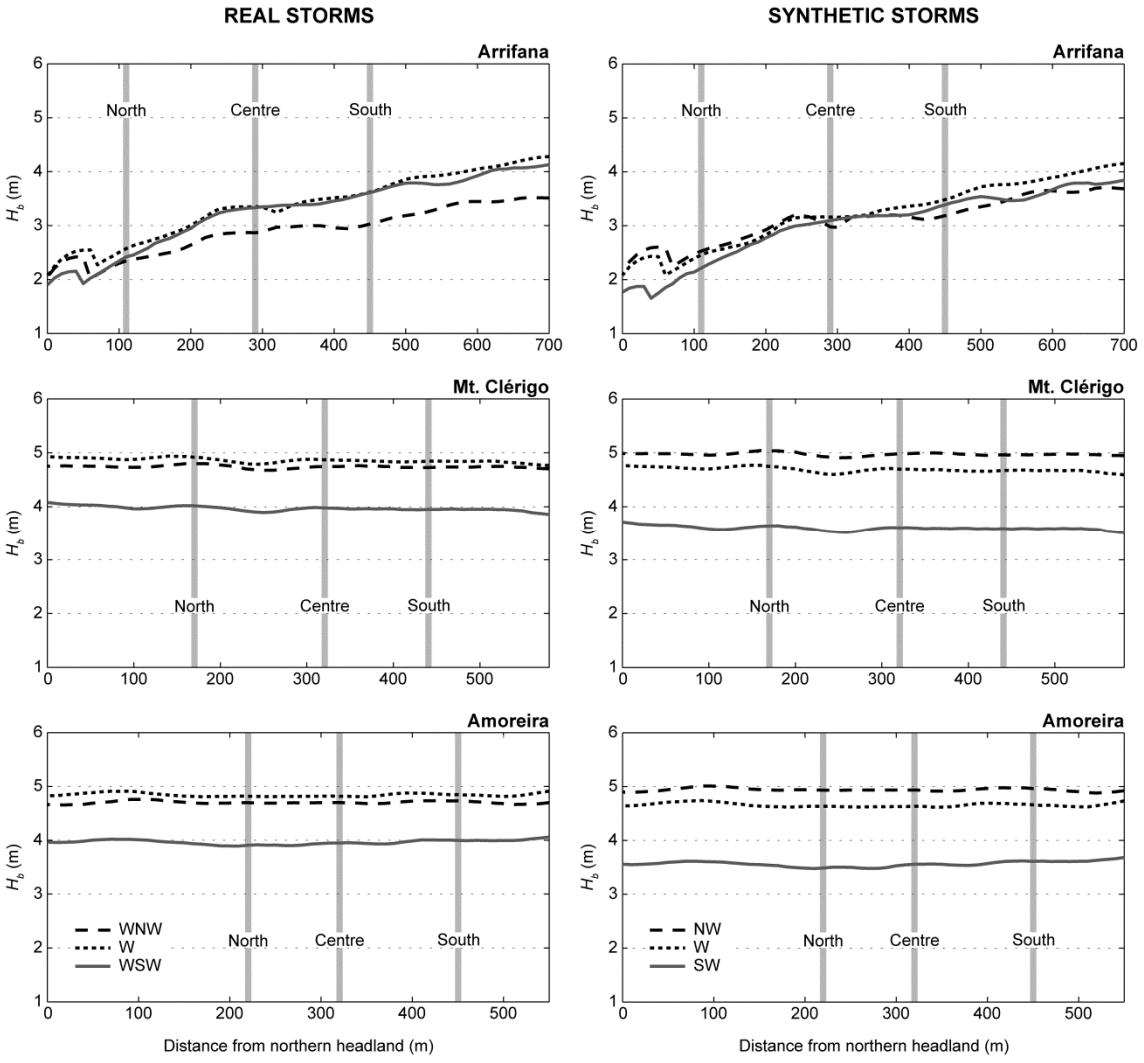

Figure 5.9 Alongshore variation in breaking wave height (H_b) for each embayment. Wave conditions were modelled for the storms identified in Table 5.2 (left panel) and for synthetic storms (right panel). Synthetic storms have constant offshore wave height (5 m) and peak period (15 s), but variable offshore wave directions of 315º (NW), 270º (W) and 225º (SW). Profile location is represented by grey lines.

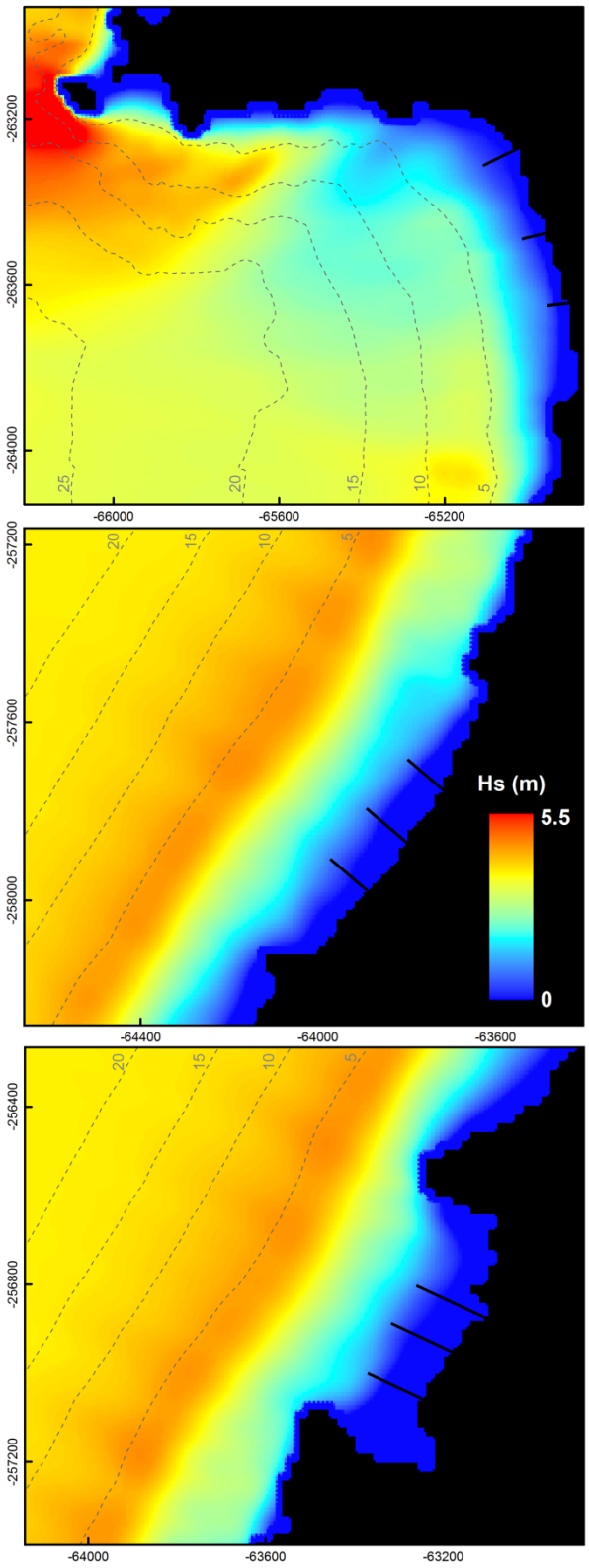

Figure 5.10 Modelled significant wave height (H_s) for the average conditions recorded during the January-February 2009 storm group (offshore boundary conditions: Hso – 4.5 m; Tp – 14.5 s; θ – 300º) at Arrifana (top panel), Mt. Clérigo (centre panel) and Amoreira (bottom panel). Depth contours (dotted lines) are in metres below MSL, and black lines indicate profile location.

5.4.4 Embayment circulation

Parametric analysis of embayment circulation was performed for the modal wave conditions and also for the range of modelled breaking wave heights presented in Table 5.1, using the formulation for the embayment scaling parameter (δ') described in Eq. (5.1). The computed values of δ' place Arrifana as an embayment modally subjected to normal circulation, owing to significant length and moderate breaking wave heights (Table 5.3). Computing δ' for the range of alongshore averaged modelled breaking wave heights in Arrifana, the wave-driven circulation becomes transitional as H_b approaches 2 m, and cellular circulation is established when H_b overcomes 3.5 m (Fig. 5.11).

Table 5.3 Geometric and morphodynamic characteristics of the embayments.

Parameters	Arrifana	Mt. Clérigo	Amoreira
Embayment shoreline length (m)	2050	950	820
Embayment width (m)	1340	780	570
Beachface slope (º)	2.2	2.0	1.3
Modal H_b (m)	1.03	1.66	1.62
Modal δ'	30	7	7

Mt. Clérigo and Amoreira embayments evidence similar wave conditions, as presented in the nearshore wave modelling (Section 5.4.3), and the geometric characteristics of these two embayments are also similar, as both have reduced widths and lengths. Therefore, the combination of small dimensions along with similar exposure to more energetic conditions renders both beaches modally cellular (Table 5.3). Transitional circulation is approached in both embayments when H_b reduces to values below 1.5 m (Fig. 5.11), while normal circulation occurs very infrequently (H_b <

0.5 m). Although a δ' value of 7 places Mt. Clérigo and Amoreira embayments in a modally cellular circulation type, such a value is very close to the threshold for transitional circulation (defined as $\delta' \geq 8$), implying that sustained conditions of cellular circulation in both embayments are only established once H_b exceeds 2 m (Fig. 5.11).

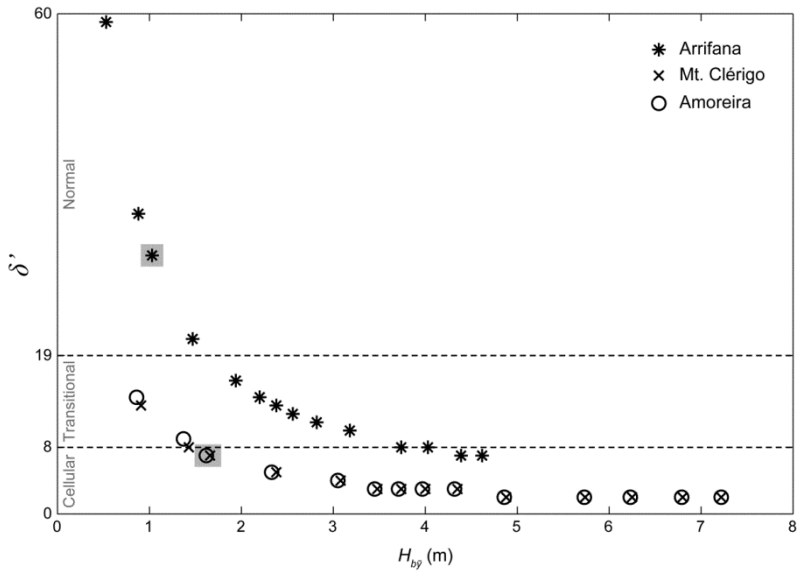

Figure 5.11 Embayment scaling parameter (δ') for different alongshore averaged breaking wave heights ($H_{b\bar{y}}$) in each embayment (refer to Table 5.1). Shading highlights modal conditions at each embayment.

5.5 DISCUSSION

5.5.1 Megarips or large rips?

The results presented in this study highlight the role of megarips in the periodic erosion of sand from high-energy embayed beaches, providing new insights into their cumulative action during and after storm groups. While significant progress has been made recently in the study of the hydrodynamics and morphodynamic coupling of rip systems, particularly by field experiments (*e.g.* Brander and Short, 2000; MacMahan *et al.*, 2005; Bruneau *et al.*, 2009; Austin *et al.*, 2010), such efforts have concentrated on

open coast rips. Conceptually, despite their large dimensions and association with moderate to high wave conditions, those are mainly large-scale accretionary rips associated with downstate transitions in intermediate beaches and are consequently quite different to topographic rips or megarips (Brander and Short, 2000; Short, 2007; MacMahan *et al.*, 2010). The rip systems described here differ from such large-scale accretion rips because they develop during high-energy events (Fig. 5.12), when the beaches would otherwise have transitioned upstate to dissipative conditions, characterized by the absence of rip circulation (Wright and Short, 1984). Their location and development is also controlled by embayment configuration, which places then conceptually as topographic rips, transitioning to megarips under high-energy conditions and dominating the circulation of entire embayments (Short, 2010).

The reduced dimension of the embayments studied, combined with exposure to an energetic wave climate, contributes to circulation types influenced by embayment topography almost permanently, as indicated by the embayment scaling parameter (δ'). Although conditions for transitional or cellular circulation may be maintained for most of the wave conditions encountered in Arrifana, Mt. Clérigo and Amoreira, the actual transition for megarip circulation only occurs during high waves. A breaking wave height (H_b) of 3 m was proposed by Short (1985, 2010) as a threshold for the transition to megarip circulation, considering that when H_b exceeds this value fully dissipative conditions would prevail (Wright and Short, 1984). While detailed validation of this threshold cannot be presented, analysis of the variation of δ' for increasing wave heights (Fig. 5.11) suggests that when H_b reaches 3.5 m conditions for cellular circulation are established for all embayments. The beaches studied are modally intermediate to dissipative in state, and observations confirm that as H_b increases to more than 3 m dissipative surf zones prevail, with megarips dominating the surf zone circulation in

Arrifana, Mt. Clérigo and Amoreira. When wave conditions decrease, these rip systems do not cease functioning. However, they maintain roughly the same position, not experiencing significant alongshore migration as observed for accretionary/erosional rips (*e.g.* Holman *et al.*, 2006; Turner *et al.*, 2007; Orzech *et al.*, 2010). This occurs because they remain topographically controlled, downgrading from megarips to large-scale topographic rips.



Figure 5.12 Panoramic mosaics of megarip circulation during storm and post-storm wave conditions for Arrifana. The upper panel presents the embayment under storm conditions, recorded on 05/02/2009 under 5.5 m WNW offshore waves. Arrows provide flow-behaviour indications of the megarips, and dashed lines indicate rip-head plumes. The intense wave breaking across the entire surf zone is reduced within the rip-neck channel due to wave–current interaction. Post-storm conditions, recorded on 09/02/2009, are shown in the lower panel. Dark patches and the absence of wave breaking on both beach extremities indicate the position of the feeder channels and deep rip-neck channels.

5.5.2 Megarip development

Temporal and spatial changes in wave breaking drive variations in wave set-up/down, producing pressure gradients that induce water flow from areas of high waves towards areas of low waves, where flow convergence creates a constrained jet-like flow that exits the surf zone as a rip current (Bowen, 1969; MacMahan *et al.*, 2006; Dalrymple *et al.*, 2011). Topographic rips and megarips share this same forcing mechanism, but while most rips are driven by longshore variations in wave height due to bathymetric variation generally associated with rhythmic shoals and channels in intermediate beaches (Aagaard and Masselink, 1999), and less frequently with wave–wave interactions (MacMahan *et al.*, 2006), topographic rips and megarips result from longshore variations in wave height due to attenuation and refraction around offshore topographic features like headlands and reefs (Short, 1985).

Alongshore variations in breaking wave height assessed using numerical wave modelling for Arrifana beach are consistent with the development of a megarip in the more protected northern sector (Fig. 5.13). The sheltering effect of the northern headland creates a geometric shadow, leading to an area of significantly lower breakers on the northern sector (Fig. 5.10), inducing an alongshore flow towards the northern headland. The position of this megarip endorses the suggestion that under extreme conditions with oblique incident waves, a wave setup-driven mechanism would be responsible for the development of a megarip in the protected end of an embayment (Coutts-Smith, 2004), similar to re-circulation cells present in the lee of groynes, as recently demonstrated by Pattiaratchi *et al.* (2009). Due to nearshore bathymetry and convergence of breaking waves with the circulation cell, the northern megarip is deflected obliquely towards the centre of the embayment, instead of flowing straight

offshore. It then develops an alongshore component, visible in the rip head plume (Fig. 5.12), restricting the seaward extent of the northern megarip.

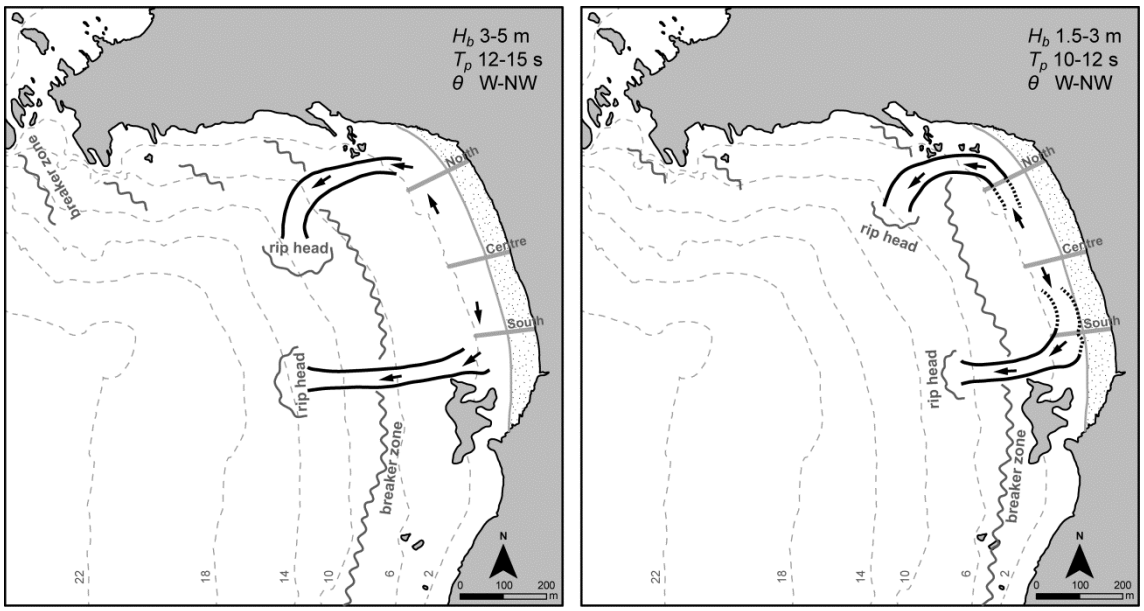

Figure 5.13 Schematic mapping of megarip circulations during storm (left panel) and post-storm conditions (right panel) for Arrifana embayment. Rip-neck channels (limited by solid black lines) are indicated for both storm and post storm conditions; while feeder channels (limited by dashed black line) are only clearly identifiable during post-storm conditions (refer to Fig. 5.12 for snapshot view). Arrows indicate flow direction only and are not scaled to velocity, and bathymetry is in metres below MSL.

Development of a second megarip in a southern location, adjacent to the southern profile at Arrifana beach, cannot be derived from modelled alongshore variations in breaker height alone. However, there is a tendency for megarip development adjacent to headlands (as a contour current) exposed to an obliquely incident wave field (Coutts-Smith, 2004; Short, 2010), just as a rip system develops in the up-drift side of a groyne or structure (Pattiaratchi *et al.*, 2009; Dalrymple *et al.*, 2011). Driven by oblique waves, an alongshore current runs parallel to the beach and is forced to turn seaward against the downdrift headland. Lateral positioning of the southern megarip at Arrifana supports this hypothesis, due to the occurrence of obliquely incident waves. Despite the reduced extension of the southern headland, the

beach is bounded by submerged rocky outcrops approximately 100 m southwards of profile south, which force the alongshore current to deflect offshore, forming the distinctive southern megarip (Fig. 5.13). A divergence zone, separating the alongshore currents feeding both the northern and southern megarips, is located in the centre of the embayment, as evidenced by the post-storm snapshot in Fig. 5.12. The location of a divergence zone in the alongshore currents is associated with changes in the alongshore gradient in wave height due to topographic sheltering (Pattiaratchi *et al.*, 2009). Breaking wave heights obtained from wave modelling confirm that the centre of Arrifana embayment evidences more constant wave conditions, with intermediate heights between the lower waves in the northern section and the higher waves in the southern section (Fig. 5.9).

Megarips have also been noted in the centre of longer embayments (>1–2 km), associated with shore normal incident waves (Short, 1985, 2010). Although Mt. Clérigo and Amoreira are significantly shorter than this (approximately 600 m), both beaches are normally exposed to the energetic north-westerly waves. During high-energy events, one megarip developed roughly on the centre of each embayment, occasionally extending to the northern sectors of both beaches (Figs. 5.14 and 5.15). The absence of noteworthy alongshore variation in modelled breaking wave height at Mt. Clérigo and Amoreira (Figs. 5.9 and 5.10), provide no immediate explanation for megarip development due to breaker gradients at these beaches. However, development of megarips in the centre of embayed beaches has been shown to occur during storms (Wright *et al.*, 1979; Short, 1985), and recent analytical modelling approaches by Silva *et al.* (2010) suggest development of cellular circulation with a rip developing in the centre of embayed beaches under normal incident waves. Such rip circulation is related to embayment geometry influencing the nearshore wave field, particularly breaker

height and wave obliquity at breaking, as suggested by Huntley *et al.* (1988) and confirmed numerically by Silva *et al.* (2010). While obtained for low to moderate wave conditions, the results of Silva *et al.* (2010) provide a hypothesis for the initial development of an embayment-scale rip circulation system. Under increasing wave heights this circulation system would transition into a megarip since, as suggested by the authors, once the circulation is established, wave height variation would only strengthen or weaken the current velocities without modifying the circulation patterns.

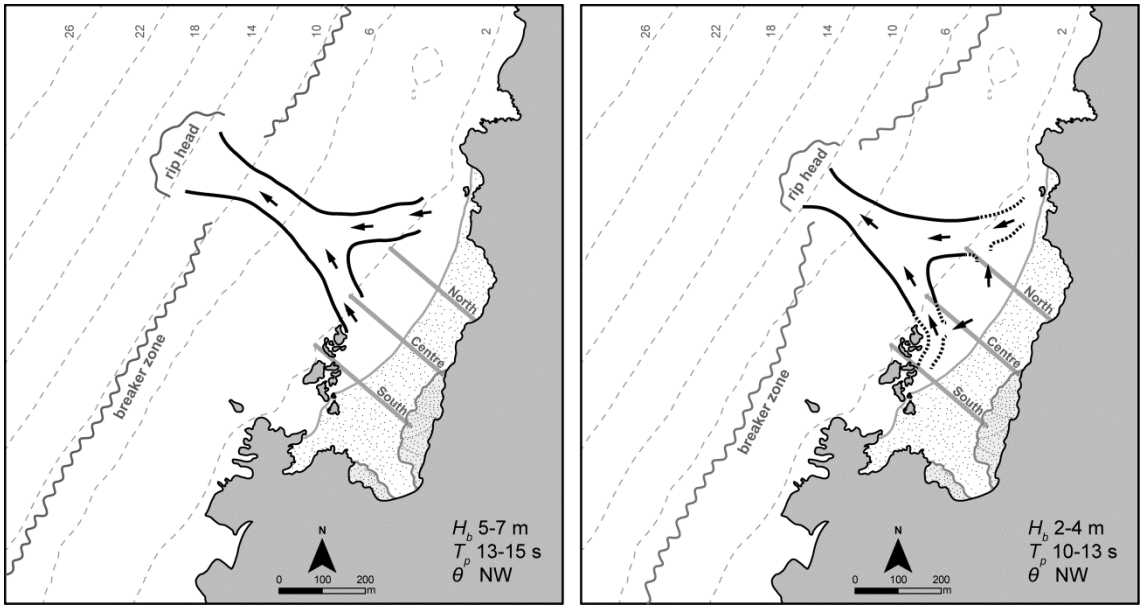

Figure 5.14 Schematic mapping of megarip circulations during storm (left panel) and post-storm conditions (right panel) for Mt. Clérigo embayment. Refer to Fig. 5.13 caption for description of symbols.

At Mt. Clérigo, nearshore topographic control is likely to also influence the development and location of a megarip in the centre of the embayment, as a rocky outcrop in the lower intertidal and subtidal zone extends obliquely from the south to the centre of the beach (Fig. 5.14). This outcrop provides a permanent barrier that forces longshore currents to flow seaward, as reported elsewhere by Davidson-Arnott (2010), scouring a channel that widens to a large megarip during high-energy events.

Apart from the Arrifana megarips, where conditions for alongshore variation in breaker height inducing pressure gradients are maintained due to topographic sheltering, no other megarip could be inferred from wave modelling results. All models of rip circulation are forced by alongshore variations in wave height (MacMahan *et al.*, 2006), and under homogeneous alongshore contours, as observed for Amoreira and M. Clérigo embayments, such variations are not expected to be significant. Nonetheless, as evidenced in previous studies, even small bathymetric irregularities can influence surf zone hydrodynamics, inducing wave gradient-driven rip circulations (Calvete *et al.*, 2007; MacMahan *et al.*, 2008; Dalrymple *et al.*, 2011).

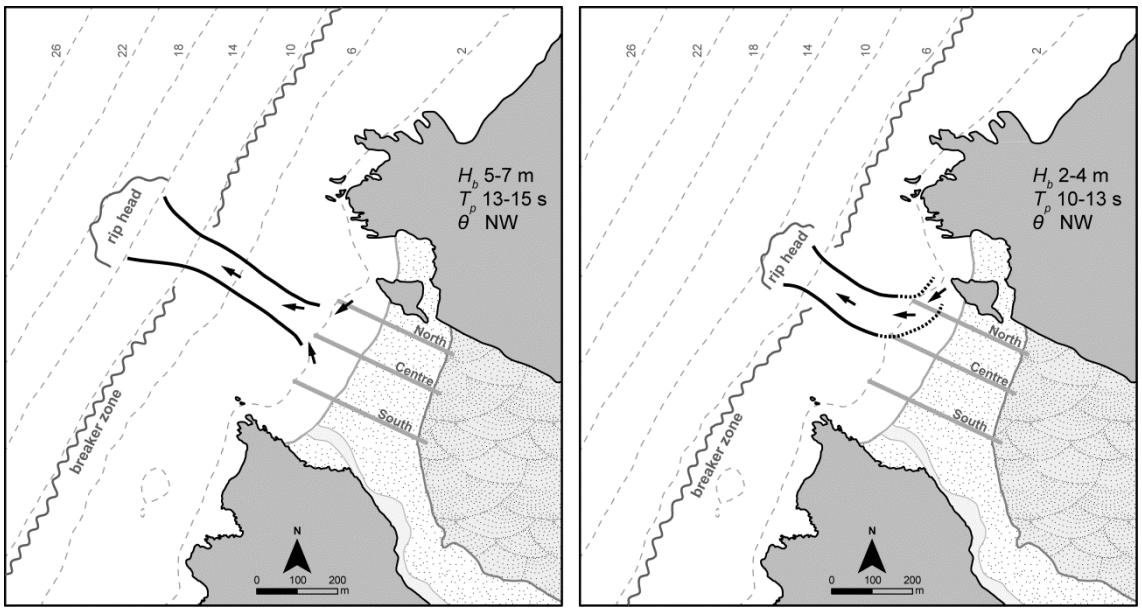

Figure 5.15 Schematic mapping of megarip circulations during storm (left panel) and post-storm conditions (right panel) for Amoreira embayment. Refer to Fig. 5.13 caption for description of symbols.

5.5.3 Enhanced erosion by megarips and storm grouping

Localised beach and dune erosion has been associated to the coupling between rhythmic cuspate shorelines and rip currents in long embayments (Thornton *et al.*, 2007). Along highly compartmentalized coastlines, with small and bedrock-bounded

embayed beaches, cellular circulation, and particularly megarips, has also been presented as a major mechanism of beach erosion (Short, 1985), while undertow has been found to be of reduced efficiency in cross-shore sediment transport (Dehouck *et al.*, 2009). Destructive effects and erosive hazards may be greatly enhanced by the action of megarips (Wright, 1981), especially because of their ability to transport sediment, flushing entire beach compartments through their wide and deep feeder systems and intense rip flows (Short, 1979; Wright, 1981). Most severe beach erosion occurs in the lee of megarips (Short, 1985), and for profiles at Arrifana south, Mt. Clérigo centre and Amoreira centre, where megarip development was more frequent, erosion was generally higher than in the remaining profiles. Profiles intersecting or adjacent to feeder channels draining to the main rip also experienced enhanced erosion, as evidenced in profiles Mt. Clérigo north and south and Amoreira north. In contrast, Amoreira southern and Arrifana central profiles exhibited lower variation, being also less regularly associated with either rip-neck or feeder channels (Figs. 5.6 and 5.8).

The coupling of rip-neck and feeder channels with enhanced erosion of Arrifana, Mt. Clérigo and Amoreira beach profiles is noticeable during individual high-energy events, although the relationship is not always immediate or linear since morphodynamic response is influenced by antecedent conditions, requiring an adjustment time (Wright and Short, 1984). Nevertheless, under the action of the January-February 2009 storm group the relationship is remarkable. Storm groups, or sequences of storms without significant recovery in between (Ferreira, 2006), have long been recognised as an important mechanism for extreme erosion of embayed beaches (Thom, 1974), driving dramatic shoreline retreat on erosion hotspots (Smith *et al.*, 2010), or triggering erosion-dominated periods of several years (Thom and Hall, 1991). Considering that the most significant beach cut on short embayed beaches is produced

by megarips (Wright, 1981), their maintenance during storm groups would be expected to produce extreme and continued erosion. Our results provide field evidence of this process. All profiles were influenced by megarips during the January-February 2009 storm group, either by rip-neck or feeder channels, inducing widespread beach erosion. Except for profiles Arrifana centre, located in a divergence zone where feeder channel influence was tangential, and Amoreira south where feeder influence was short-lived, all profiles were severely eroded. This storm group clearly demonstrated the spatial extent of megarips and confirmed their ability to dominate the circulation of entire embayments. Moreover, the persistence of megarip action during the storm group led to the development of large and deep rip-neck and feeder channels (Fig. 5.12), which required a significant post-storm period to be infilled. Rip currents remained active for a long period, as they were coupled to the underlying morphology, and caused continued erosion.

5.5.4 Implications for beach recovery

Seaward transport of sediment is greatly enhanced by megarips, which are considered to be responsible for sediment exchange between embayed beaches and the nearshore or even the inner-shelf (Short, 1985; Coutts-Smith, 2004). Sediment removed from the beach by megarips has been shown to be deposited at depths of 10 to 25 m (Coutts-Smith, 2004; Smith *et al.*, 2010), owing to seaward extensions of approximately 1.5 to 4 times the surf zone width (Coutts-Smith, 2004; Dalrymple *et al.*, 2011), or between 1 and 2 km (Short, 2010). Sand withdrawn from Arrifana, Mt. Clérigo and Amoreira beaches by megarips was presumably transported to depths between 10 to 15 m, based on schematic mapping (Figs. 5.13 - 5.15), and spread out on the lower shoreface, as observed elsewhere by Coutts-Smith (2004) and Smith *et al.* (2010),

resulting in net loss of sediment from beaches. There were, however, significant differences between the study beaches. These can be explained by differences in wave forcing, since increase in incident wave height is associated with higher rip current speeds (Pattiaratchi *et al.*, 2009; Dalrymple *et al.*, 2011), and also a higher offshore extent of megarips (Coutts-Smith, 2004). On Mt. Clérigo and Amoreira beaches, due to normal exposure to incident storm waves, which break without considerable attenuation driving either stronger or/and seaward extended megarip flows, a higher volume of sand was lost and apparently to greater depths, as evidenced by the inability of both beaches to recover in the following months. On Arrifana beach, where breaking wave heights are consistently lower, net volumetric loss was reduced, although severe erosion occurred during the January-February 2009 storm group.

During storm groups, sediment lost from the beach and the upper-shoreface is expected to be even greater than for single storm events (Cowell *et al.*, 1999), due to inability to reach a storm equilibrium profile during storm groups (Inman *et al.*, 1993) and continued conditions for megarip-driven erosion as a result of coastal disequilibrium (Smith *et al.*, 2010).While megarips developed during the first year of monitoring caused moderate erosion, even with the January 2008 extreme single storm, no significant net volumetric loss was observed. In contrast, erosion associated with the January-February 2009 storm group was significant, probably associated with substantial export of sediment to the nearshore, promoted by the long duration of the event.

Once formed, and being topographically forced, large rips can persist in the same location for extended periods (Short, 1985), evidencing a much longer lag-time in their response to changing wave conditions (Gallop *et al.*, 2011). Owing to positive morphodynamic feedback, alongshore gradients are maintained and eventually

enforced. Rip-neck and feeder channels continue then to flush and erode sediment, resulting in stable circulation patterns which have been observed to persist for several years in the case of rips controlled by headlands (Gallop *et al.*, 2011). Considerable time is then needed for readjustment after megarip-induced erosion (McKenzie, 1958), and complete recovery can require several years (Wright and Short, 1983). Since high-energy conditions were maintained throughout the January-February 2009 storm group, megarip circulation was continuously active for at least 22 days, creating large and deep channels. Consequently, rip-neck and feeder channel influence on beach profiles was not only intense but also persistent. Beach recovery has been significantly inhibited, except for Arrifana beach, and channel infilling has been occurring slowly, mostly due to onshore and lateral expansion of subtidal and lower intertidal shoals. Once the channels become infilled a faster recovery is expected, as evidenced in Arrifana beach. The enhanced ability of Arrifana beach to recover after the storm group suggests that sediment taken from the beach remained at shallower depths, within the constrained environment of the embayment, and was available for subsequent rip and feeder channel infilling allowing beach recovery, most likely because megarips at Arrifana were less intense and/or extensive.

5.6 CONCLUSION

Morphological change in three embayed beaches along the high-energy southwestern coast of Portugal was monitored over two years. During this period, profile erosion has been mostly related to the development of megarips and associated rip-neck and feeder channels. Differences within and between beaches were related to embayment geometry and orientation. On short beaches normally exposed to incident

storm waves (Mt. Clérigo and Amoreira), a single megarip developed in the centre of each embayment, while obliquely incident waves were associated with the development of two megarips in both extremities of Arrifana embayment, driven by marked alongshore gradients in breaking wave height and interaction with embayment boundaries.

On the three embayed beaches studied, moderate erosion was observed during individual storms, and more importantly, extreme erosion occurred when megarips persisted for several weeks during the action of a storm group. Net sediment loss on the more exposed Mt. Clérigo and Amoreira beaches suggests sand export to the lower shoreface, driven by the persistent action of megarips during the storm group. While megarips have long been recognised as an important mechanism of embayed beach erosion, their continued and enhanced action during storm groups has only now been demonstrated, providing a clear connection between megarips and storm groups in the extreme erosion of embayed beaches. This study also demonstrates that the maintenance of a rip circulation pattern after storms (or storm groups), enforced by morphodynamic feedback, reduces beach recovery ability until the rip-neck and feeder channels are infilled.

Comprehensive field measurements of megarips have yet to be accomplished (*e.g.* including measurements of surf zone hydrodynamics and nearshore bathymetric change driven by megarips), and this study does not fill such gap. However, by relating megarip influence to profile variation and analysing modelled nearshore wave data, along with parametric indications of megarip occurrence, the present work provides new insights into the conditions that drive megarip development and the role of megarips in the erosion and recovery of embayed beaches.

5.7 ACKNOWLEDGEMENTS

We gratefully acknowledge the help of everyone involved in the fieldwork data collection, especially at dawn during cold winter stormy days. Thanks also to Rui Taborda, Guillaume Dodet and Xavier Bertin for providing initial training with SWAN, and Derek Jackson for discussion of modelling aspects. Mara Nunes and Thomas Smyth suggested improvements to early versions of the manuscript. This work is a contribution to BAYBEACH project (Evolution and Management of Embayed Beaches in Contrasting Environments) funded by FCT under contract PTDC/CTE-GEX/66893/2006. Carlos Loureiro was supported by FCT, grant reference SFRH/BD/27878/2006. Hydrodynamic data from Sines buoy were provided by Instituto Hidrográfico. Modelled WANA wave data were kindly supplied by Puertos del Estado.

5.8 REFERENCES

Aagaard, T. and Masselink, G., 1999. The surf zone. In: Short, A.D. (Ed.), *Handbook of Beach and Shoreface Morphodynamics*. John Wiley & Sons, Chichester, pp. 71–118.

Almeida, L.P., Ferreira, Ó., Pacheco, A., 2011. Thresholds for morphological changes on an exposed sandy beach as a function of wave height. *Earth Surface Processes and Landforms* 36, 523–532.

Austin, M., Scott, T., Brown, J., Brown, J., MacMahan, J., Masselink, G., Russel, P., 2010. Temporal observations of rip current circulation on a macro-tidal beach. *Continental Shelf Research* 30, 1149–1165.

Battjes, J.A. and Janssen, J.P.F.M., 1978. Energy loss and set-up due to breaking of random waves. Proceedings of the 16th International Conference on Coastal Engineering. ASCE, New York, USA, pp. 569–587.

Booij, N., Ris, R.C., Holthuijsen, L.H., 1999. A third-generation wave model for coastal regions - 1. Model description and validation. *Journal of Geophysical Research* 104 (C4), 7649–7666.

Bowen, A.J., 1969. Rip currents. 1. Theoretical investigations. *Journal of Geophysical Research* 74, 5467–5478.

Brander, R.W., 1999. Field observations on the morphodynamic evolution of a low energy rip current system. *Marine Geology* 157, 199–217.

Brander, R.W. and Cowell, P.J., 2003. A trend-surface technique for discrimination of surfzone morphology: rip current channels. *Earth Surface Processes and Landforms* 28, 905–918.

Brander, R.W. and Short, A.D., 2000. Morphodynamics of a large-scale rip current system at Muriwai Beach, New Zealand. *Marine Geology* 165, 27–39.

Brander, R.W., Cowell, P.J., Short, A.D., 2001. Morphometric approaches to describing rip current behaviour. *Journal of Coastal Research* SI 34, 128–137.

Brown, M. and Lowe, D., 2007. Automatic panoramic image stitching using invariant features. *International Journal of Computer Vision* 74, 59–73.

Bruneau, N., Castelle, B., Bonneton, P., Pedreros, R., Almar, R., Bonneton, N., Bretle, P., Parisot, J.P., Sénéchal, N., 2009. Field observations of an evolving rip current on a meso-macrotidal well-developed inner bar and rip morphology. *Continental Shelf Research* 29, 1650–1662.

Callaghan, D.P., Nielsen, P., Short, A.D., Ranashinge, R., 2008. Statistical simulation of wave climate and extreme beach erosion. *Coastal Engineering* 55, 375–390.

Calvete, D., Coco, G., Falqués, A., Dodd, N., 2007. (Un)predictability in rip channel systems. *Geophysical Research Letters* 34, L05605.

Cook, D.O., 1970. Occurence and geologic work of rip currents off southern California. *Marine Geology* 9, 173–186.

Cooper, J.A.G., Jackson, D.W.T., Navas, F., McKenna, J., Malvarez, G., 2004. Identifying storm impacts on an embayed, high-energy coastline: examples from western Ireland. *Marine Geology* 210, 261–280.

Costa, M. and Esteves, R., 2010. Clima de agitação marítima na costa oeste de Portugal Continental. Proceedings of XI Jornadas Técnicas de Engenharia Naval — O Sector Marítimo Português. Edições Salamandra, Lisboa, Portugal, pp. 413–426.

Costa, M., Silva, R., Vitorino, J., 2001. Contribuição para o estudo do clima de agitação marítima na costa Portuguesa. Proceedings of 2as Jornadas de Engenharia Costeira e Portuária. AIPCN, Aveiro, Portugal (20 pp. CD-ROM).

Coutts-Smith, A., 2004. The significance of mega-rips along an embayed coastline. Ph.D. Thesis, University of Sydney, Australia.

Cowell, P.J., Hanslow, D.J., Meleo, J.F., 1999. The shoreface. In: Short, A.D. (Ed.), *Handbook of Beach and Shoreface Morphodynamics*. John Wiley & Sons, Chichester, pp. 39–71.

Dalrymple, R.A., MacMahan, J.H., Reniers, A.J.H.M., Nelko, V., 2011. Rip currents. *Annual Review of Fluid Mechanics* 43, 551–581.

Davidson-Arnott, R., 2010. *Introduction to Coastal Processes and Geomorphology*. Cambridge University Press, Cambridge. 442 p.

Dehouck, A., Dupuis, H., Sénéchal, N., 2009. Pocket beach hydrodynamics: the example of four macrotidal beaches, Brittany, France. *Marine Geology* 266, 1–17.

Evans, P., Hanslow, D., Coutts-Smith, A., You, Z., 2000. Nearshore-inner shelf sediment exchange on the NSW central coast. Proceedings of the 27th International Conference on Coastal Engineering. ASCE, Sydney, Australia, pp. 3151–3164.

Ferreira, Ó., 2005. Storm groups versus extreme single storms: predicted erosion and management consequences. *Journal of Coastal Research* SI 42, 221–227.

Ferreira, Ó., 2006. The role of storm groups in the erosion of sandy coasts. *Earth Surface Processes and Landforms* 31, 1058–1060.

Freire, P., Taborda, R., Bertin, X., Guerreiro, M., Fortunato, A.B., Silva, A.M., Andrade, C., Oliveira, A., Antunes, C., Freitas, M.C., Nahon, A., Rodrigues, M., Bruneau, N., 2011. Medium-term morphodynamic evolution of a small coastal inlet. *Journal of Coastal Research* SI 64, 666–670.

Gallop, S.L., Bryan, K.R., Coco, G., Stephens, S.A., 2011. Storm-driven changes in rip channel patterns on an embayed beach. *Geomorphology* 127, 179–188.

Gorrel, L., Raubenheimer, B., Elgar, A., Guza, R.T., 2011. SWAN predictions of waves observed in shallow water offshore of complex bathymetry. *Coastal Engineering* 58, 510–516.

Harley, M.D., Turner, I.L., Morris, B.D., Short, A.D., Ranasinghe, R., 2007. Nearshore wave climate and localised erosion during high wave events — SE Australia. Proceedings of the 18th Australasian Coastal and Ocean Engineering Conference. IEAust, Melbourne, Australia (No. 89 CD-ROM).

Hasselmann, K., Barnett, T.P., Bows, E., Carlson, H., Cartwright, D.E., Enke, K., Ewing, J.A., Gienapp, H., Hasselmann, D.E., Kruseman, P., Meerburg, A., Müller, P., Olbers, D.J., Richter, K., Sell, W., Walden, H., 1973. Measurements of wind–wave growth and swell decay during the Joint North Sea Wave Project

(JONSWAP). *Ergänzungsheft zur Deutschen Hydrographischen Zeitschrift* A8 (12), 1–95.

Holman, R., Symonds, G., Thornton, E.B., Ranasinghe, R., 2006. Rip spacing and persistence on and embayed beach. *Journal of Geophysical Research* 111, C01006.

Holthuijsen, L.H., 2007. *Waves in Oceanic and Coastal Waters*. Cambridge University Press, Cambridge. 387 p.

Huntley, D.A., Hendry, M.D., Jaines, J., Greenidge, B., 1988. Waves and rip currents on a Caribbean pocket beach, Jamaica. *Journal of Coastal Research* 4, 69–79.

Inman, D.L., Elwany, M.H.S., Jenkins, S.A., 1993. Shorerise and bar-berm profiles on ocean beaches. *Journal of Geophysical Research* 98 (C10), 18181–18199.

Lahoz, M.G. and Albiach, J.C.C., 2005. Wave forecasting at the Spanish coasts. *Journal of Atmospheric & Ocean Science* 10, 389–405.

Lee, G.H., Nicholls, R.J., Birkemeier, W.A., 1998. Storm-driven variability of the beach and nearshore profile at Duck, North Carolina, USA, 1981–1991. *Marine Geology* 148, 163–177.

Long, J.W. and Özkan-Haller, H.T., 2005. Offshore controls on nearshore rip currents. *Journal of Geophysical Research* 110 (C12), C12007.

Loureiro, C., Ferreira, Ó., Cooper, J.A.G., 2011. Morphologic change and morphodynamics at high-energy embayed beaches in southwestern Portugal. Proceedings of Coastal Sediments 2011, vol. 2. World Scientific Publishing, Singapore, pp. 1375–1389.

MacMahan, J.H., Thornton, E.B., Stanton, T.P., Reniers, A.J.H.M., 2005. RIPEX: observations of a rip current system. *Marine Geology* 218, 113–134.

MacMahan, J.H., Thornton, E.B., Reniers, A.J.H.M., 2006. Rip current review. *Coastal Engineering* 53, 191–208.

MacMahan, J.H., Thornton, E.B., Reniers, A.J.H.M., Stanton, T.P., Symonds, G., 2008. Low-energy rip currents associated with small bathymetric variations. *Marine Geology* 255, 156–164.

MacMahan, J.H., Brown, J., Brown, J., Thornton, E., Reniers, A., Stanton, T., Henriquez, M., Gallagher, E., Morrison, J., Austin, M.J., Scott, T.M., Sénéchal, N., 2010.Mean Lagrangian flow behaviour on an open coast rip-channeled beach: a new perspective. *Marine Geology* 268, 1–15.

McKenzie, P., 1958. Rip-current systems. *Journal of Geology* 66, 103–113.

Orzech, M.D., Thornton, E.B., MacMahan, J.H., O'Reilly, W.C., Stanton, T.P., 2010. Alongshore rip channel migration and sediment transport. *Marine Geology* 271, 278–291.

Pattiaratchi, C., Olsson, D., Hetzel, Y., Lowe, R., 2009. Wave-driven circulation patterns in the lee of groynes. *Continental Shelf Research* 29, 1961–1974.

Pita, C. and Santos, J.A., 1989. Análise dos temporais da costa oeste de Portugal Continental, Report NATO PO-WAVES 1/89-A. IH/LNEC, Lisboa, Portugal.

Ranasinghe, R., Symonds, G., Black, K., Holman, R., 2004.Morphodynamics of intermediate beaches: a video imaging and numerical modelling study. *Coastal Engineering* 51, 629–655.

Short, A.D., 1979. Three dimensional beach-stage model. *Journal of Geology* 87, 553–571.

Short, A.D., 1985. Rip-current type, spacing and persistence, Narrabeen Beach, Australia. *Marine Geology* 65, 47–71.

Short, A.D., 1996. The role of wave height, period, slope, tide range and embaymentisation in beach classifications: a review. *Revista Chilena de Historia Natural* 69, 589–604.

Short, A.D. (Ed.), 1999. *Handbook of Beach and Shoreface Morphodynamics*. John Wiley & Sons, Chichester. 379 p.

Short, A.D., 2007. Australian rip systems: friend or foe? *Journal of Coastal Research* SI 50, 7–11.

Short, A.D., 2010. Role of geological inheritance in Australian beach morphodynamics. *Coastal Engineering* 57, 92–97.

Short, A.D. and Hesp, P.A., 1982. Wave, beach and dune interaction in Southeastern Australia. *Marine Geology* 48, 259–284.

Short, A.D. and Masselink, G., 1999. Embayed and structurally controlled beaches. In: Short, A.D. (Ed.), *Handbook of Beach and Shoreface Morphodynamics*. John Wiley & Sons, Chichester, pp. 230–249.

Silva, R., Baquerizo, A., Losada, M.A., Mendonza, E., 2010. Hydrodynamics of a headland-bay beach — nearshore current circulation. *Coastal Engineering* 57, 160–175.

Smith, A.M., Mather, A.A., Bundy, S.C., Cooper, J.A.G., Guastella, L.A., Ramsay, P.J., Theron, A., 2010. Contrasting styles of swell-driven coastal erosion: examples from KwaZulu-Natal, South Africa. *Geological Magazine* 147, 940–953.

Thom, B.G., 1974. Coastal erosion in Eastern Australia. *Search* 5, 198–209.

Thom, B.G. and Hall, W., 1991. Behaviour of beach profiles during accretion and erosion dominated periods. *Earth Surface Processes and Landforms* 16, 113–127.

Thornton, E.B., MacMahan, J., Sallenger, A.H., 2007. Rip currents, mega-cusps and eroding dunes. *Marine Geology* 240, 151–167.

Turner, I.L., Whyte, D., Ruessink, B.G., Ranasinghe, R., 2007. Observations of rip spacing, persistence and mobility at a long, straight coastline. *Marine Geology* 236, 209–221.

Wood, D.J., Muttray, M., Oumeraci, H., 2001. The SWAN model used to study wave evolution in a flume. *Ocean Engineering* 28, 805–823

Wright, L.D., 1981. Beach cut in relation to surf zone morphodynamics. Proceedings of the 17th International Conference on Coastal Engineering. ASCE, Sydney, Australia, pp. 978–996.

Wright, L.D. and Short, A.D., 1983. Morphodynamics of beaches and surf zones in Australia. In: Komar, P.D. (Ed.), *CRC Handbook of Coastal Processes and Erosion*. CRC Press, Boca Raton, Florida, pp. 35–64.

Wright, L.D. and Short, A.D., 1984. Morphodynamic variability of surf zones and beaches - a synthesis. *Marine Geology* 56, 93–118.

Wright, L.D., Thom, B.G., Chappell, J., 1979. Morphodynamic variability of high-energy beaches. Proceedings of the 16th International Conference on Coastal Engineering. ASCE, Hamburg, Germany, pp. 1180–1194.

CHAPTER 6

General conclusions

Aiming to define the medium-term morphodynamic variability of embayed beaches in contrasting geomorphological settings, this study approaches embayed beach morphodynamics from a broader, embayment-wide scale, towards a focused, process-oriented scale. Across these scales of analyse, a unifying notion, that geological control significantly influences embayed beach morphodynamic behaviour, has been hypothesized and confirmed through exploration of data obtained from a two-year monitoring program conducted at six embayments in the southwestern Portuguese coastline. While much work remains to be done for a more complete understanding of embayed beach morphodynamics, the results and conclusions presented in the main chapters of this thesis provide new insights and innovative techniques for embayed beach morphodynamic investigation.

Parametric approaches to beach morphodynamic state were found to have limited applicability at an embayment-wide scale, as the fundamental role of geological control in coastal embayments is not embodied in widely used parametric approaches. Parametric beach state determined using averaged wave, tide and sediment variables was comparatively assessed with an innovative probabilistic analysis, implemented using a Bayesian network model, which considered the entire wave, tide and sediment distributions observed at the study embayments. Both approaches revealed inconsistencies with the observed beach state determined using a novel hierarchical

field-based classification of beach state. These inconsistencies were found to result primarily from an inadequacy of current approaches to differentiating beach state types in embayed beaches, particularly within the intermediate domain in geologically constrained settings. A thorough identification of geologically controlled beach types has yet to be accomplished and further research is required for a wider assessment of the effects of geological control on beach morphodynamic type. While parametric classification based on the dimensionless fall velocity was found useful in distinguishing the extremes in the reflective to dissipative continuum in wave-dominated environments, even within mesotidal conditions and geologically controlled settings, intermediate beach types could not be meaningfully distinguished. Dimensionless parameters should therefore be used only as elementary descriptors of embayed beach state for differentiating between the three major beach types (reflective-intermediate-dissipative), with additional beach type differentiation being developed on regional scales according to observations of embayed beach behaviour. Approaching beach morphodynamic state classification within a probabilistic framework, as proposed here, offers an alternative reasoning that is likely to benefit from the integration of additional variables, not necessarily parametric ones, for which Bayesian networks are particularly suited. Further research is required to test this hypothesis, yet this should always be based upon the notion that parametric values are elementary descriptors of beach morphodynamics and that in embayed beaches geological control constrains morphological variability and, consequently, is likely to modify beach morphodynamic state.

Morphological variability in embayed beaches was found to be fundamentally constrained by the presence of geological boundaries, which promoted diverse spatial and temporal variability patterns within the six embayments analysed. Decomposition

of morphological change using empirical orthogonal functions and correlation analysis demonstrated the presence of localized responses produced by lateral and vertical boundary interference with embayment morphodynamics. These include beach rotation phenomena, topographically-controlled rip circulation and reduced profile fluctuation. Despite the importance of such mechanisms in determining alongshore non-uniform embayment response, the primary mode of morphological variability, which represented 67% to 94% of the variance in the six embayments, is a cross-shore component correlated at the 99% confidence level with the normalized wave power for most sites.

This novel relationship stresses the importance of combined parameterization of wave and tide forcing in process-response relations between hydrodynamics and morphological change for mesotidal coastal environments. More research is, however, necessary to further evaluate the applicability of the normalized wave power in a beach morphodynamic context. A spatial decoupling in cross- and longshore responses was accompanied by a temporal decoupling in response times, and these were found to increase for higher constrained conditions (from 1 day in exposed embayments to 1 week or more in more sheltered sites). Higher survey frequency, eventually using video monitoring techniques, would allow refining the forcing-response relations and improve determination of embayment response times. A preliminary conceptual framework for describing boundary effects in embayed beaches is presented, suggesting that decreasing sediment abundance and substrate depth intensify vertical boundary effects, while higher indentation and wave obliquity enhance the effects of lateral boundaries. Further research is required to evaluate this scheme and extend it to a measurable framework. In that context, determining the thickness of sediment cover required for unconstrained profile fluctuation, although possibly a site- and profile-type specific

variable is a research topic yet to be explored, and one of particular significance for geologically controlled settings.

While results clearly demonstrate that geological control impacts the morphological variability in all six embayments studied, west coast embayments, exposed to high-energy wave conditions and presenting higher accommodation spaces and sediment volumes, presented increased temporal and spatial variability. Being located in a swell-dominated environment with markedly seasonal wave climate, changes in beach morphology displayed a general seasonal pattern. This seasonal pattern was, however, supplanted by an episodic component driven by the occurrence of a storm group composed by 5 individual storms, producing marked interannual variability. The multi-storm event produced dramatic beach erosion, which was, however, restricted to foreshore and nearshore areas, as dunes were unaffected. This has implications for the long-term behaviour of high-energy embayments, as even extreme events may not have lasting impacts on the overall embayment evolution. Further research on embayed beach morphological change during storms is, nonetheless, still required, given the site-specificity of embayment response to high-energy conditions. Moreover, morphological change in high-energy embayed beaches displayed significant spatial variations within each embayment. Alongshore non-uniform patterns of beach change were investigated and related to megarip development, as their topographically-controlled location was directly related to the variability observed within embayments.

A detailed analysis of storm-induced megarip development and impact in alongshore non-uniform embayed beach erosion is presented. In order to relate megarip influence to morphologic variation, a classification framework of rip-current discrimination, based on the morphological and visual expression of rip and feeder-channel configuration, was proposed. Moderate beach erosion during individual storms

in high-energy embayments was linked to the development of megarips with associated rip-neck and feeder channels, while extreme erosion occurred when megarips persisted during successive storm events, promoting continued erosion and seaward sediment export.

Megarip channels were found to persist for several months and continued to act as conduits for offshore sediment transport under non-storm conditions, reducing beach recovery ability. Megarip location is topographically-controlled, and a combination of visual analysis and numerical modelling allowed to elucidate that megarip development was determined by alongshore variations in breaking wave height and obliquity, along with interaction of wave-driven circulation patterns and embayment nearshore topography. Megarips are still a largely unreported mechanism of embayed beach erosion, and despite the new insights provided here into the conditions that drive megarips development and the role of megarips in the erosion and recovery of embayed beaches much work remains. Comprehensive beach and nearshore morphologic monitoring during storm events, along with hydrodynamic field measurements during storms in embayed beaches are particularly required. Nearshore circulation in embayed settings is complex, yet further research is fundamental for improved understating of embayed beach morphodynamics.

While the primary aim of this thesis is to improve the scientific knowledge of embayed beach morphodynamics, there are implications for the management and beach use safety of embayed beaches within the findings presented here. Studying embayed beaches within contrasting environments allowed to identify a wide variability in morphological mechanisms and responses. These are likely to be even more diverse if more embayments have been considered. This urges caution when defining management interventions, such as nourishment or stabilization, for embayed beaches if

a proper monitoring program has not been executed before. Identifying if an embayed beach is likely to exhibit beach rotation, or if megarips develop during storms, will unquestionably need to be considered for proper embayed beach management. Furthermore, an improved understating of rip current and megarip circulation and morphological coupling is paramount for improving beach use and safety, as rip currents are amongst the primary hazards for beach swimmers. Given the topographically-controlled nature of most rip circulation cells within embayments, studies detailing their positions and general functioning are likely to significantly improve the safety of beachgoers.